Development of a sixth generation model for the NW European Shelf (DCSM-FM 0.5nm)

Development of a sixth generation model for the NW European Shelf (DCSM-FM 0.5nm)

Model setup, calibration and validation

Firmijn Zijl
Julien Groenenboom

11203715-004

Deltares

Title
Development of a sixth generation model for the NW European Shelf (DCSM-FM 0.5nm)

Client	Project	Attribute	Pages
RWS-WVL	11203715-004	11203715-004-ZKS-0003	112

Keywords
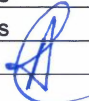D-HYDRO, D-Flow Flexible Mesh, North Sea, NW European Continental Shelf, sixth-generation

Summary
Upon request of Rijkswaterstaat (RWS) Deltares has developed a sixth-generation hydrodynamic model of the Northwest European Shelf. Specifically, this model covers the North Sea and adjacent shallow seas and estuaries in the Netherlands, such as the Wadden Sea, the Ems-Dollard estuary, the Western Scheldt and the Eastern Scheldt. The development of this model (DCSM-FM) is part of a more comprehensive project in which sixth-generation models are developed for all waters managed and maintained by RWS. An important difference with the previous fifth generation models is the use of the D-HYDRO Suite, the new software framework for modelling free surface flows, which was first released in 2015 and allows for the use of unstructured grids.

While the previous generation models for the same area were specifically aimed at an optimal representation of water levels for operational forecasting under daily and storm surge conditions, for the sixth-generation model(s) the scope is wider. This model should also be suitable to use for e.g. water quality and ecology studies, oil spill modelling, search and rescue and to provide three-dimensional (3D) boundary conditions (including temperature and salinity) for detailed models of e.g. the Haringvliet and Rhine-Meuse Delta (RMM).

The above applications pose a wide range and sometimes mutually exclusive demands on a model. Therefore, two horizontal schematizations were proposed:
1   DCSM-FM 0.5nm: a relatively coarse schematization (minimum grid size of 800-900 m in Dutch waters), primarily aimed at ensemble-based probability forecasting, but also forming a sound basis for a future three-dimensional model development including temperature and salinity as state parameters.
2   DCSM-FM 100m: a relatively fine schematization with a minimum resolution of ~100 m in some Dutch waters (such as the Wadden Sea) to be used for accurate (operational) water level forecasting. This model will be a based on the model in item 1a, but with refinement where required.

The present report deals with the development of the relatively coarse two-dimensional DCSM-FM model (DCSM-FM 0.5nm).

Version	Date	Author	Initials	Review	Initials	Approval	Initials
	dec. 2017	Firmijn Zijl		Martin Verlaan		Frank Hoozemans	
	Dec. 2018	Firmijn Zijl		Martin Verlaan		Frank Hoozemans	
v1.0	Dec. 2019	Firmijn Zijl		Martin Verlaan		Toon Segeren	

Status
final

Contents

1 Introduction

1.1 Background

Rijkswaterstaat (RWS) has requested Deltares to develop a sixth-generation hydrodynamic model of the Northwest European Shelf. Specifically, this model should cover the North Sea and adjacent shallow seas and estuaries in the Netherlands, such as the Wadden Sea, the Ems-Dollard estuary, the Western Scheldt and the Eastern Scheldt.

The development of this model is part of a more comprehensive project in which sixth-generation models are developed for all waters maintained by RWS. An important difference with the previous fifth generation models is the use of the D-HYDRO Suite, the new software framework for modelling free surface flows, which was first released in 2015 and allows for the use of unstructured grids. Eventually, all fifth generation models will be replaced with a sixth generation equivalent.

The existing fifth generation models for the NW European Shelf and North Sea (DCSMv6 and DCSMv6-ZUNOv4, see Zijl (2013)) were depth-averaged models, specifically aiming at an optimal representation of water levels for operational forecasting under daily and storm surge conditions. For the sixth-generation model(s) the scope is wider; the model should also be suitable to use for e.g. water quality and ecology studies, oil spill modelling, search and rescue and to provide three-dimensional (3D) boundary conditions (including temperature and salinity) for detailed models of e.g. the Haringvliet and Rhine-Meuse Delta (RMM).

The above applications pose a wide range and sometimes mutually exclusive demands on a model. This is because both the relative importance of representing certain phenomena as well as the allowed computational time varies per application. Since the demands are impossible to meet with one model, two horizontal schematizations (resulting in 3 models) were proposed:

1. DCSM-FM 0.5nm: a relatively coarse schematization (minimum grid size of 800-900 m in Dutch waters). The corresponding computational time makes it possible to use for the following models:
    a. a 3D transport model, including temperature and salinity as state variables
    b. A 2D tide-surge model that is fast enough used to produce probability forecasts with a 2 – 10 day lead-time. These forecasts will be based on meteorology of the ECMWF Ensemble Prediction System (EPS) and will replace the fourth-generation model DCSMv5 that is currently used for this application.
2. DCSM-FM 100m: a relatively fine schematization with a minimum resolution of ~100 m in some Dutch waters (such as the Wadden Sea) to be used for accurate (operational) water level forecasting. This model will be a based on the schematization in item 1, but with refinement where required.

The present report deals with the development of the relatively coarse two-dimensional DCSM-FM 0.5nm model primarily aimed at ensemble forecasting (item 1b above), but also forming a sound basis for a future 3D model development. For reference purposes, this version of the model will also be referred to as dflowfm2d-noordzee_0_5nm-j17_6-v1.

To ensure that all sixth-generation models are compatible, the guidelines with generic technical and functional specifications as specified in (Spruyt et al. 2017) were used during the setup of this model.

1.2 Guide to this report

The next chapters describe the setup of DCSM-FM 0.5nm (Chapter 2). Chapter 3 describes the tide gauge data that is used to calibrate and validate the model, while in Chapter 4 and Chapter 5 the calibration and the validation are presented. The report ends with conclusions and recommendation in Chapter 6.

Development of a sixth generation model for the NW European Shelf (DCSM-FM 0.5nm)

2 Model setup

2.1 Network

2.1.1 Network coverage, horizontal extent

The model network of DCSM-FM covers the northwest European continental shelf, specifically the area between 15° W to 13° E and 43° N to 64° N (e.g. Figure 2.1). This means that the open boundary locations are the same as in the fifth generation model DCSMv6 (Zijl et al., 2013). An extension of the model domain was considered as this might have a beneficial impact on the surge representation, since a larger part of the surge signal is then generated inside the model by means of wind stress and atmospheric pressure gradients. Consequently, a smaller part has to enter the domain through an approximated surge boundary condition based on air pressure alone. Even though tests computations showed an improvement during the highest storm surge events, this was considered too limited to justify the additional computations cost of an extended domain. The results of these test computations are described in Appendix A.

2.1.2 Grid size

The computational grid of the previous generation WAQUA-DCSMv6 model has rectangular cells with a uniform resolution. One of the advantages of D-HYDRO Flexible Mesh above WAQUA is the enhanced possibility to better match resolution with relevant local spatial scales. In Zijl et al. (2016) a test is reported where, starting from a grid with uniform resolution, the deep areas off the shelf were refined by a factor of up to 4 x 4. The advantage of coarsening in deep areas in particular is twofold: Firstly, it reduces the number of cells in areas where local spatial scales allow it and secondly it eases the numerical time step restriction. The combination of both lead to a reduction in computational time with a factor ~4, while – crucially - maintaining accuracy. On the other hand, in shallow areas, resolution plays an important role in accurately representing tide and surge, including its enhanced non-linear interaction (Zijl, 2016a).

Given the above considerations, the DCSM-FM network was designed to have a resolution that increases with decreasing water depth. The starting point was a network with a uniform cell size of 1/10° in east-west direction and 1/15°. This course network was refined in three steps with a factor of 2 by 2. The areas of refinement were specified with smooth polygons that were approximately aligned with the 800 m, 200m, 50 m and 12.5 m isobaths (i.e., lines with equal depth). Areas with different resolution are connected with triangles. The choice of isobaths ensures that the cell size scales with the square root of the depth, resulting in relatively limited variations of wave Courant number within the model domain.

Other considerations in positioning the refinements were the number of cells between transitions (at least a few). Also, it was ensured that all coastlines, except very small islands, were covered by a few rows of the highest resolution cells. This implies that in areas with steep coasts the transition to the highest resolution takes place in deeper water. Another exception was made for the southern North Sea, where the area of highest resolution was expanded. This was done to ensure that the highly variable features in the bathymetry can properly be represented on the network. Furthermore, it ensures that the areas where steep salinity gradients can be expected are within the area with the highest resolution.

The resulting network is shown in Figure 2.1 and has approximately 630,000 cells with a variable resolution. The largest cells (shown in yellow) have a size of 1/10° in east-west

direction and 1/15° in north-south direction, which corresponds to about 4 x 4 nautical miles (nm) or 4.9-8.1 km by 7.4 km, depending on the latitude. The smallest cells (shown in red) have a size of 2/3' in east-west direction and 1/2' in north-south direction. This corresponds to about 0.5 nm x 0.5 nm or 840 m x 930 m in the vicinity of the Dutch waters.

The network is specified in geographical coordinates (WGS84).
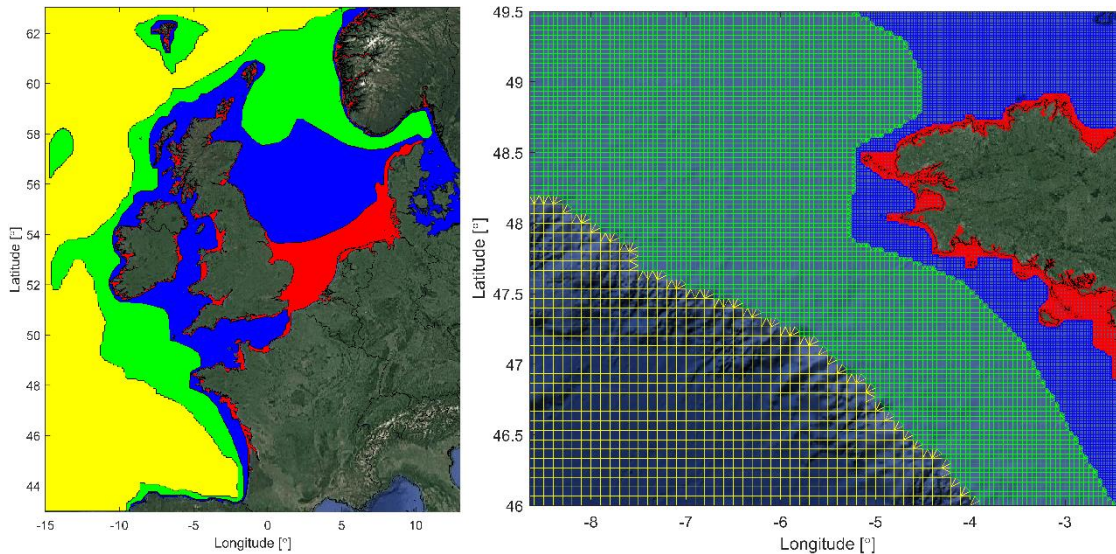
Figure 2.1   Overview (left) and detail (right) of the DCSM-FM model network with the colours indicating the grid size (yellow: ~4 nm; green: ~2 nm; blue: ~1nm; red: ~0.5 nm).

2.2   Network optimization

The computational time step used is automatically limited by D-HYDRO Flexible Mesh based on a Courant criterium. This means that parts of the network with a combination of small flow links and high velocities are most likely to restrict the time step and consequently increase the computational time. Figure 2.2 displays an example of the maximum occurring flow velocity during an arbitrary neap-spring cycle in colour, whereas the black dots indicate the locations of computational cells that are responsible for limiting the time step at least once during this period.

From the example in Figure 2.2 it also becomes clear that the time step restricting cells are located in areas with high flow velocities and mostly at the triangles used for the transition in resolution. These triangles have flow links (the connection of two circumcentres) that are shorter than in the highest resolution rectangles on one of its sides.

To allow for a larger time step and consequently a faster computation, the grid was improved at the locations of the restricting cells. By extending the refinement of the grid more offshore, the transition of the two resolution is moved outside of the region of high flow velocities. Even though this measure slightly increases the amount of computational cells, since the time step is no longer automatically limited there the net effect is a decrease in computational time (see paragraph 2.9.9).

After a few repetitions of manually changing the transition of resolution to eliminate restricting cells and therewith improving the computation time, all restricting cells on the transition of resolution were resolved (see right of Figure 2.2). The remaining restricting cells are located

between in the Pentland Firth (see Figure 2.3). These restricting cells are not on the transition of resolution but are within the area covered by the higher resolution rectangles. This means that removing these restrictions is not possible with the above described method.

Another way to eliminate the restricting cells in this region would be to locally coarsen the grid. However, since an accurate schematization of this narrow area is deemed to be important for a correct representation of tide propagation towards the North Sea, it was decided to retain the highest resolution cells there. The potential improvement in computational time would at maximum be a few percent.
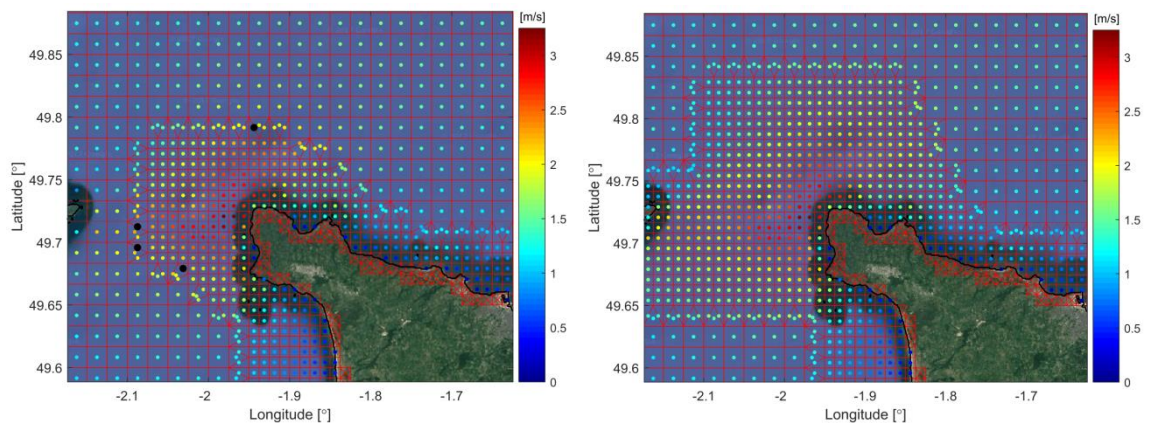
Figure 2.2   Maximum flow velocities in flow element center during a neap-spring cycle near the Normandy coast. The black line displays the sea-land boundary and the permanently dry cells are indicated by red crosses. The black dots represent computational cells that are limiting the time step (left: before optimization; right: after optimization)
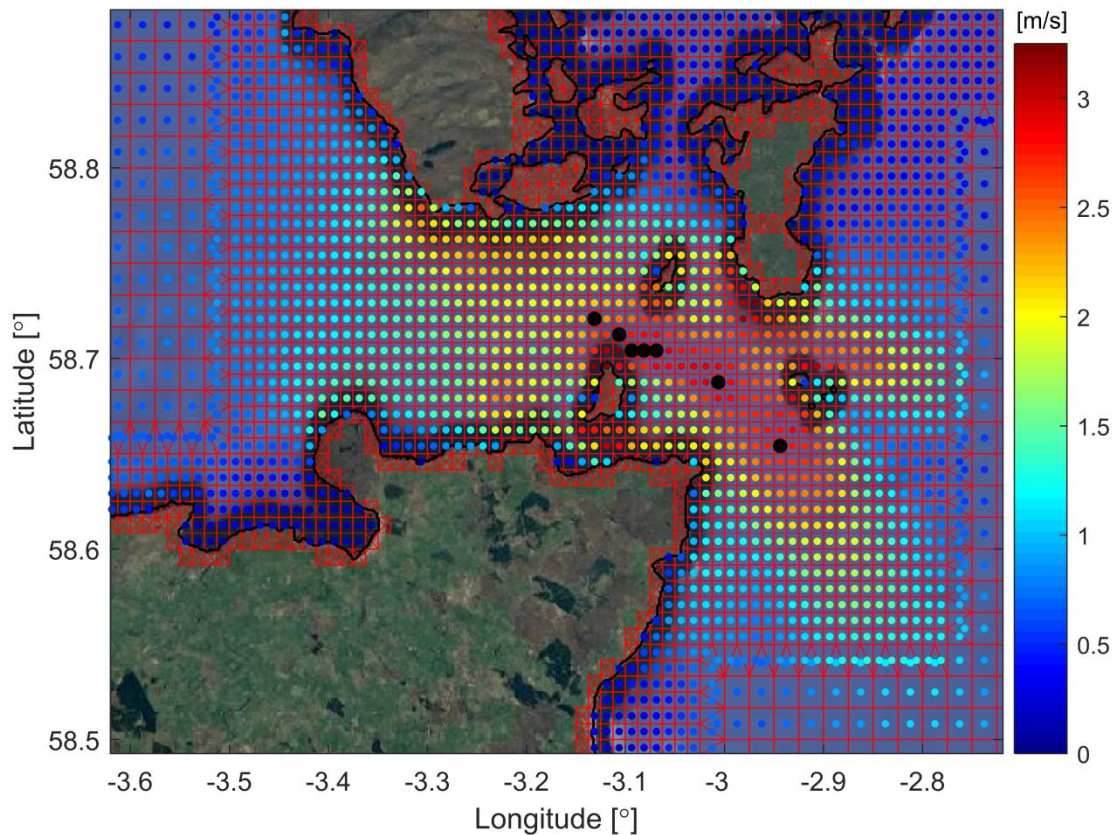
Figure 2.3   Maximum flow velocities in flow element center during a neap-spring cycle in the Pentland Firth. The black line displays the sea-land boundary and the permanently dry cells are indicated by red crosses. The black dots represent computational cells that are limiting the time step.

2.3   Land-sea boundary, dry points and thin dams

After the local refinement of the network, the cells that covered land were removed from the computational domain. The first step was to interpolate the EMODnet bathymetric data to the grid and to delete all cells that do not have EMODnet data in its vicinity. Subsequently, a land-sea boundary obtained from the World Vector Shoreline (https://shoreline.noaa.gov/) was used to distinguish between land and water. All cells that, according to this land-sea boundary, were covered by more than 40% land were made inactive by specifying so-called *dry points*. The creation of these dry points was done automatically by a MATLAB-script. Figure 2.4 shows an overview of the resulting computational domain in the southwestern part of the Netherlands. The black line indicates the land-sea boundary and the red crosses within the grid illustrate the dry points.
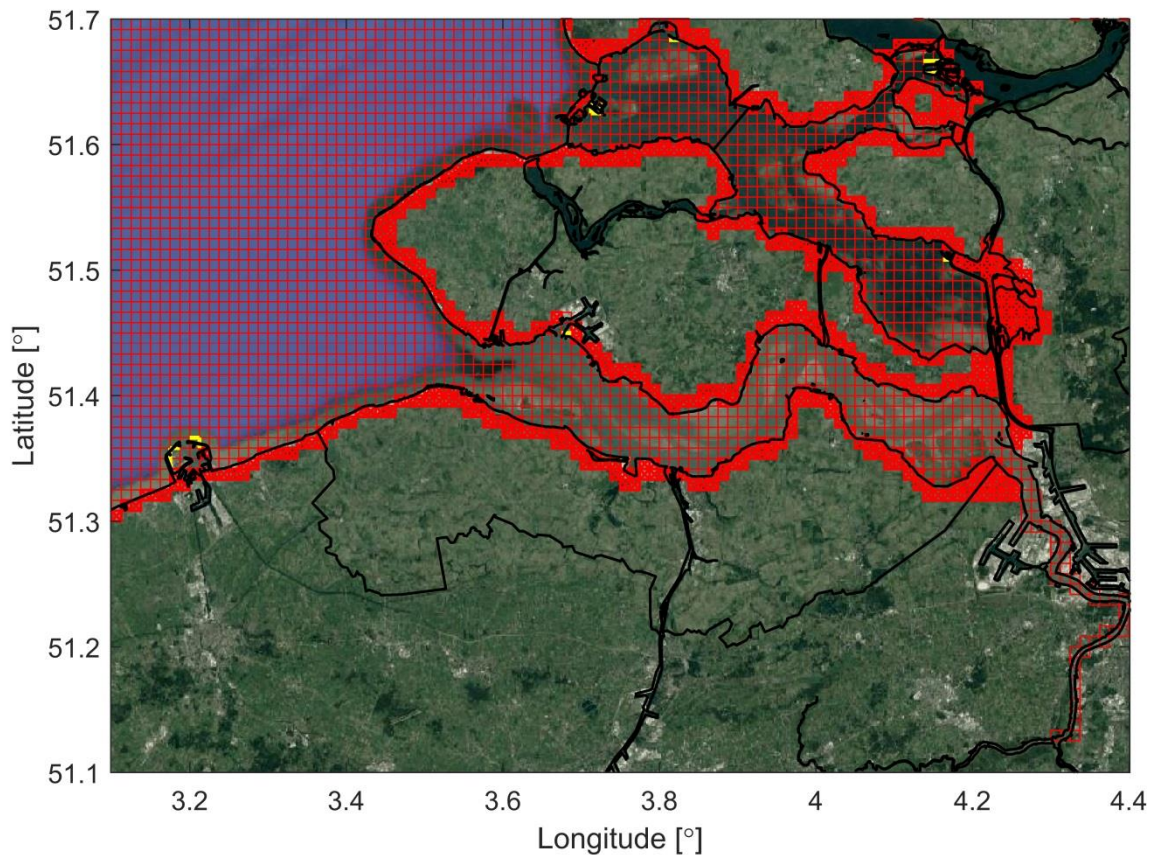
Figure 2.4   Overview of the computational grid (red), land-sea boundary (black), dry points (red crosses) and thin dams (yellow) in the Southwest Delta.

After this automated creation of a first set of dry points, a lot of manual work was necessary to get to the final version of the model geometry. During visual inspection of the shorelines dry cells were added or removed where necessary. In addition, features that are relatively small compared to the area of a cell, are captured in the model schematisation by specifying so-called *thin dams*. These thin dams prohibit flow exchange through cell edges. The thick, yellow lines in Figure 2.5 illustrate how the entrance to the Humber Estuary (in which tide gauge station Immingham is located) and the breakwaters of the port of Ijmuiden are represented by thin dams.
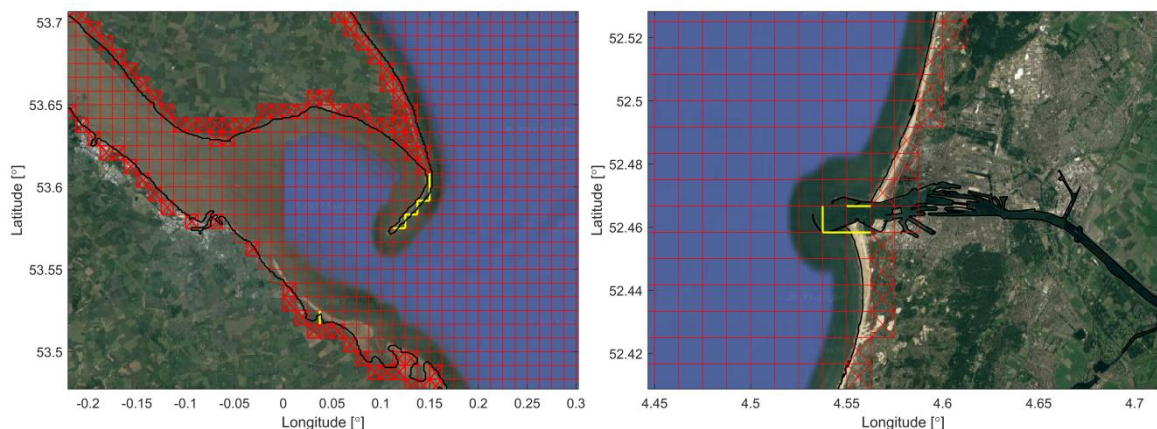
Figure 2.5   Overview of the computational grid (red), land-sea boundary (black), dry points (red crosses) and thin dams (yellow) in the Humber Estuary (left) and around the harbour of Ijmuiden (right).

Another example of manual adjustments is at the Scheldt river (entrance to the port of Antwerp). There, the river was too thin to be retained in the automated dry point creation. At some location in the river a dry point was added since the threshold of 40% land was exceeded and this resulted in blockage of the upstream river. The dry point was removed to allow for a tidal flow up to the upstream part of the model domain. Even larger bodies of water were excluded from the model in a couple of fjords in Norway. Some fjords consist of very small inlets that are connected to relatively large upstream basins. Also, these erroneously created dry points were removed from the model schematisation. The resulting geometry near one of the many fjords in Norway is shown in Figure 2.6.
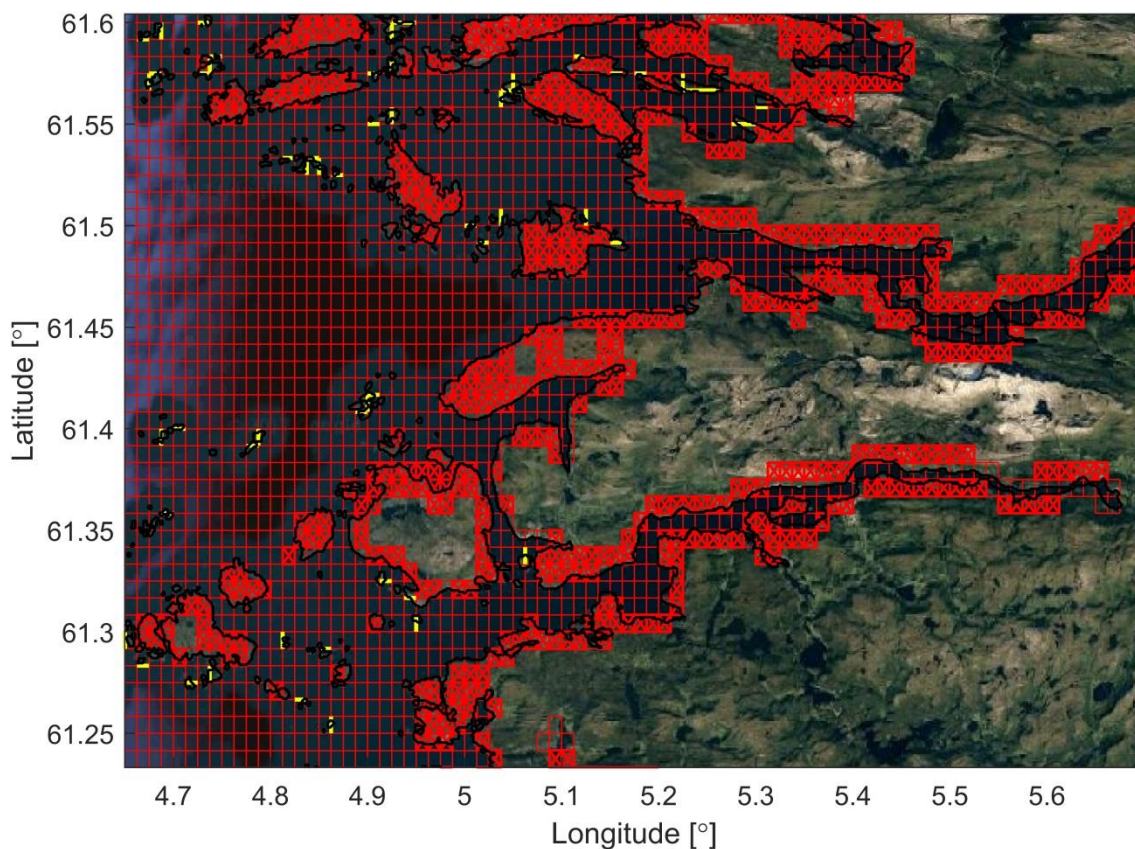
Figure 2.6   Overview of the computational grid (red), land-sea boundary (black), dry points (red crosses) and thin dams (yellow) in Norway.

In order to simulate the correct effect of estuaries on the hydrodynamics, not only certain automatically created dry points had to be removed but also additional grid cells were added to the model domain. Since the removal of grid cells was based on the availability of EMODnet data in the vicinity of the grid cell, some estuaries were not included in the model domain as no bathymetry data was available at these locations. Based on the land-sea boundary and Google Earth, the computational grid at the largest and most important estuaries that were not automatically incorporated in the model domain were manually added.

2.4   Bathymetry

The DCSM-FM model bathymetry has been derived from a gridded bathymetric dataset (October 2016 version) from the European Marine Observation and Data Network (EMODnet;

EMODnet Bathymetry Consortium, 2016), a consortium of organisations assembling European marine data, metadata and data products from diverse sources. The data are compounded from selected bathymetric survey data sets (single and multi-beam surveys) and composite DTMs, while gaps with no data coverage are completed by integrating the GEBCO 30'' gridded bathymetry.

The resolution of the gridded EMODnet dataset is 1/8' x 1/8' (approx. 160 x 230 m). Since the number of data points was too large to directly interpolate to the DCSM-FM network, it was first split into four parts which were then interpolated consecutively. For interpolation, the average of the surrounding data points was used, within a search radius equal to the cell size.

LAT-MSL realization
The EMODnet bathymetry data (October 2016 version) is only provided relative to Lowest Astronomical Tide (LAT). To make these data applicable for DCSM-FM, we have converted to the Mean Sea Level (MSL) vertical reference plane. The LAT-MSL relation was derived from a 19-year tide-only simulation (calendar years 2005 to 2023) with the previous generation DCSMv6. The long duration is required to capture an entire 18.6-year nodal cycle. The LAT-MSL relation was initially determined by taking the difference between the mean water level and the lowest occurring water level in the above-mentioned period.

As an example, the resulting LAT-MSL relation in the Dutch Wadden Sea is depicted in Figure 2.7. Just outside the Wadden Sea, a gradual change in LAT-value is found. However, in the Wadden Sea abrupt transitions in the MSL-LAT realization occur. This is due to temporary drying during low water in large parts of these intertidal areas. Consequently, LAT is not properly defined in these areas. To improve the LAT realization, the LAT-values in grid cells were the difference between LAT and the minimum depth of the surrounding depth points was less than 1 m, were deleted from the data set. Subsequently, the missing values are replaced by the closest remaining LAT-value. Figure 2.8 shows the resulting improved MSL-LAT realization in the Dutch Wadden Sea. The final MSL-LAT realization is also shown in Figure 2.9 for the entire model domain.
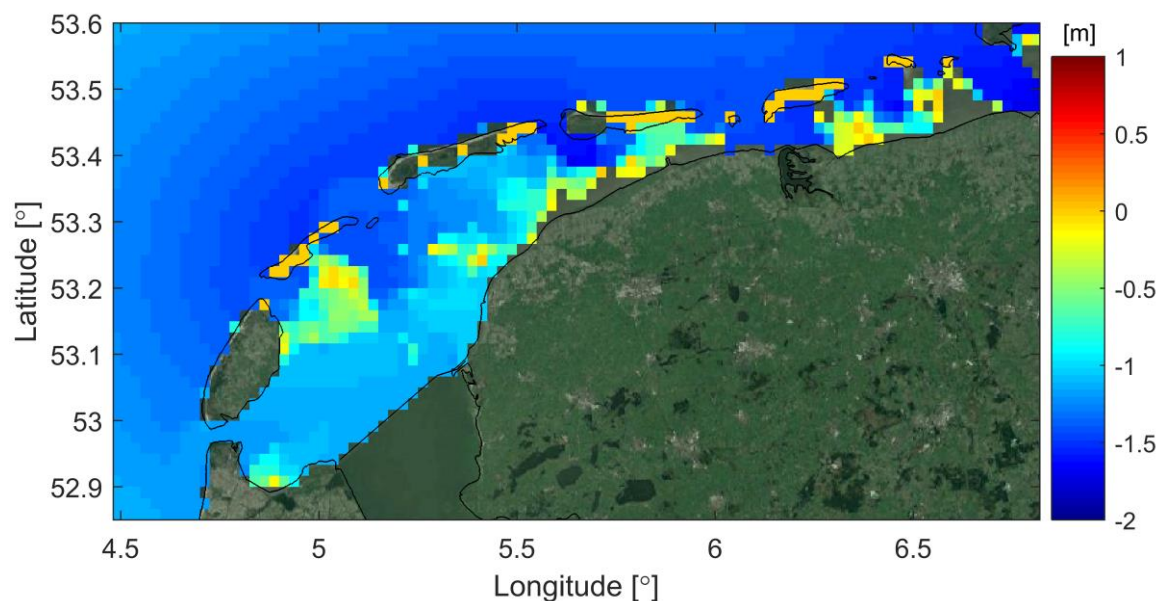
Figure 2.7   Initial MSL-LAT realization in the Dutch Wadden Sea
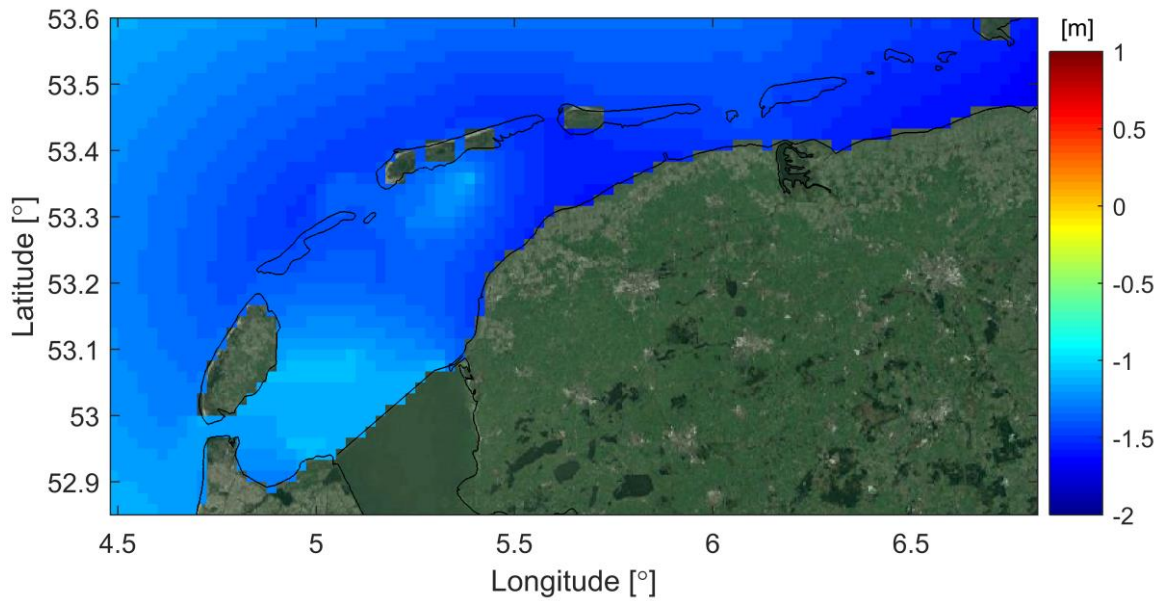
Figure 2.8   Final MSL-LAT realization in the Dutch Wadden Sea
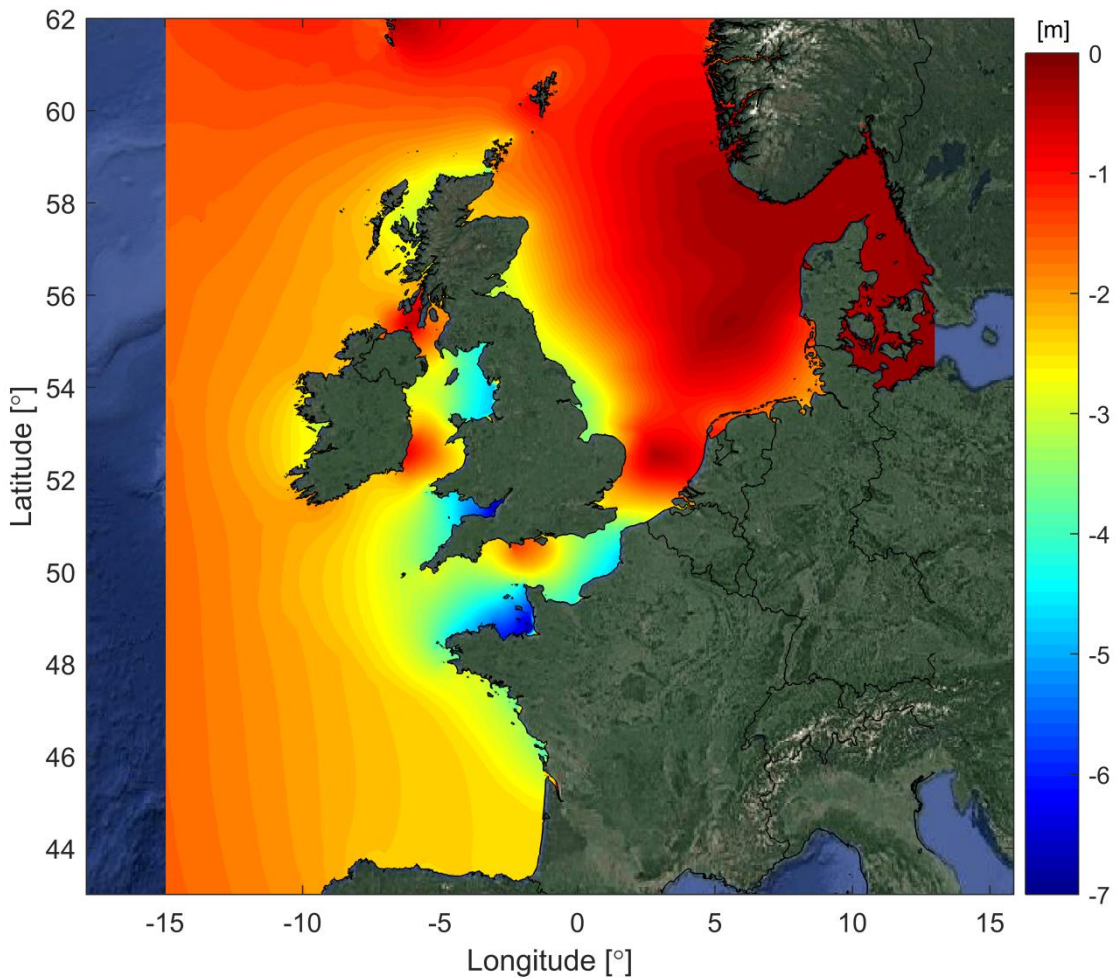
Figure 2.9   Overview of the final LAT-MSL realization used.

Baseline bathymetry

For large parts of the Dutch waters there is also Baseline[1] bathymetry data available. First, these data have been compared in the Wadden Sea with the EMODnet bathymetry (see Figure 2.10). Red (blue) indicates bed levels where Baseline data is higher (lower) than the EMODnet data. Note that the Baseline bathymetry is referenced to NAP, while for the comparison the EMODnet data was referenced to MSL. While differences are generally smaller than a few decimetres, along the channels larger differences occur.

Besides comparing the data, multiple tests have been done assessing the impact on water levels. When generating a model bathymetry using the Baseline software, triangulation is used to derive the depths at the net nodes. With this method, the combination of the relatively coarse network and high-resolution underlying bathymetry samples results in a poor representation of the channels in the Wadden Sea: deep and shallow points alternate, also in the direction of the channel. Further tests where the Baseline samples are used, but the interpolation onto the network is done in D-Flow FM by means of grid cell averaging, result in a visually more realistic model bathymetry. Crucially, this method also results in better water levels in the Wadden Sea, especially during low waters. Since it is expected that this improvement will also be retained after calibration, it was decided to use the latter method for generating the model bathymetry in Dutch waters.
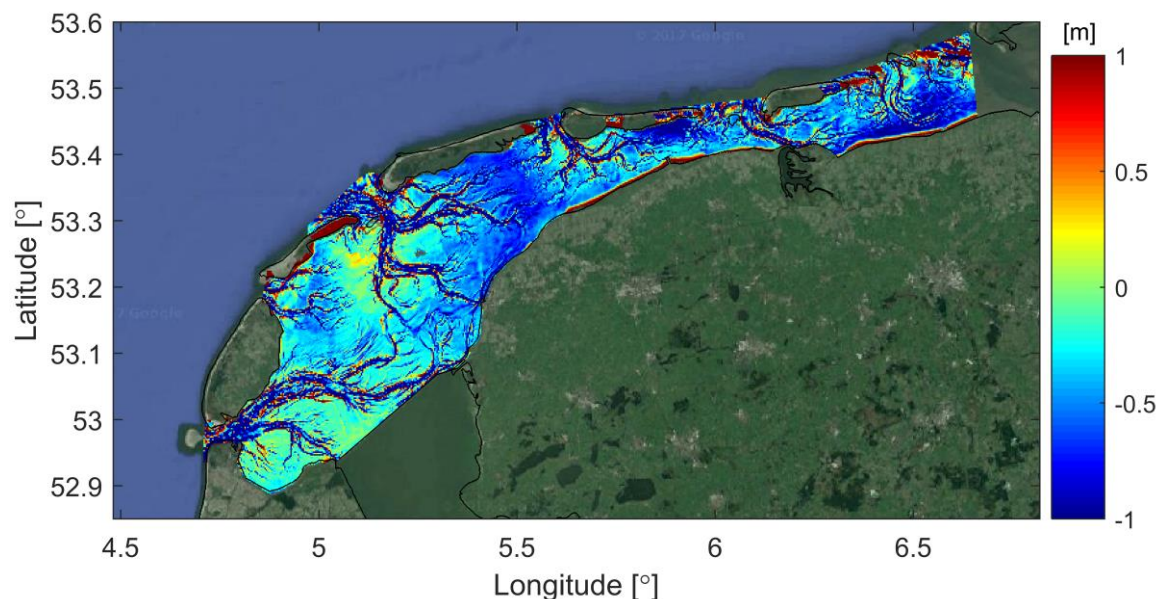
Figure 2.10 Baseline bathymetry (rel. to NAP) minus EMODnet bathymetry (rel. to MSL) in the Dutch Wadden Sea.

Bathymetry interpolation procedure

The bed levels in the model are based on bathymetry samples that are specified in the external forcing file. The z-coordinate in the net nodes is calculated by the D-Flow FM software in the following procedure:

1) The EMODnet data (divided into 4 parts because the files are too large for the software) is projected on the net nodes by grid cell averaging (operand: overwrite) with a relative search cell size of 1.

2) The same data is used again with a grid cell averaging operation, but with a relative search cell size of 2. The information is only added to the nodes where no bathymetry

---

[1] . *Baseline is an ArcGIS plugin from RWS, which is used by RWS to manage their geographical data for their numerical models.*

information was available yet (operand: append). Using this approach, the few net nodes that are just outside the coverage of the EMODnet data will also get a value at the net nodes.

3) The samples containing the above described MSL-LAT realization are projected on the grid by triangulation and subsequently added to the previously specified values (operand: +). Now, the model bathymetry is relative to MSL instead of LAT.

4) Next, the bathymetry in net nodes where Baseline bathymetry samples are available are overwritten by the grid cell averaged value (operand: overwrite, relative search cell size of 1).

5) In the upstream part of the Western Scheldt the main channel was artificially blocked. This obstruction has been corrected in the model bathymetry, using a polygon within which a constant value is prescribed.

6) In some locations the lower water levels where erroneously affected by the local bathymetry. This can result in artificial drying during low waters (lower plot Figure 2.11), but also when this is not the case the impact can be noticeable (upper plot Figure 2.11). Where this cannot be resolved by moving the station location by one or two cells, the local bathymetry has been adjusted by prescribing an adjusted depth in the immediate area. These manual steps were only performed in foreign stations where a solution was possible with the adjustment of only a few cells.

7) All net nodes that are still missing a z-coordinate are assigned the value prescribed with the keyword *Bedlevuni*, in this case 5m.
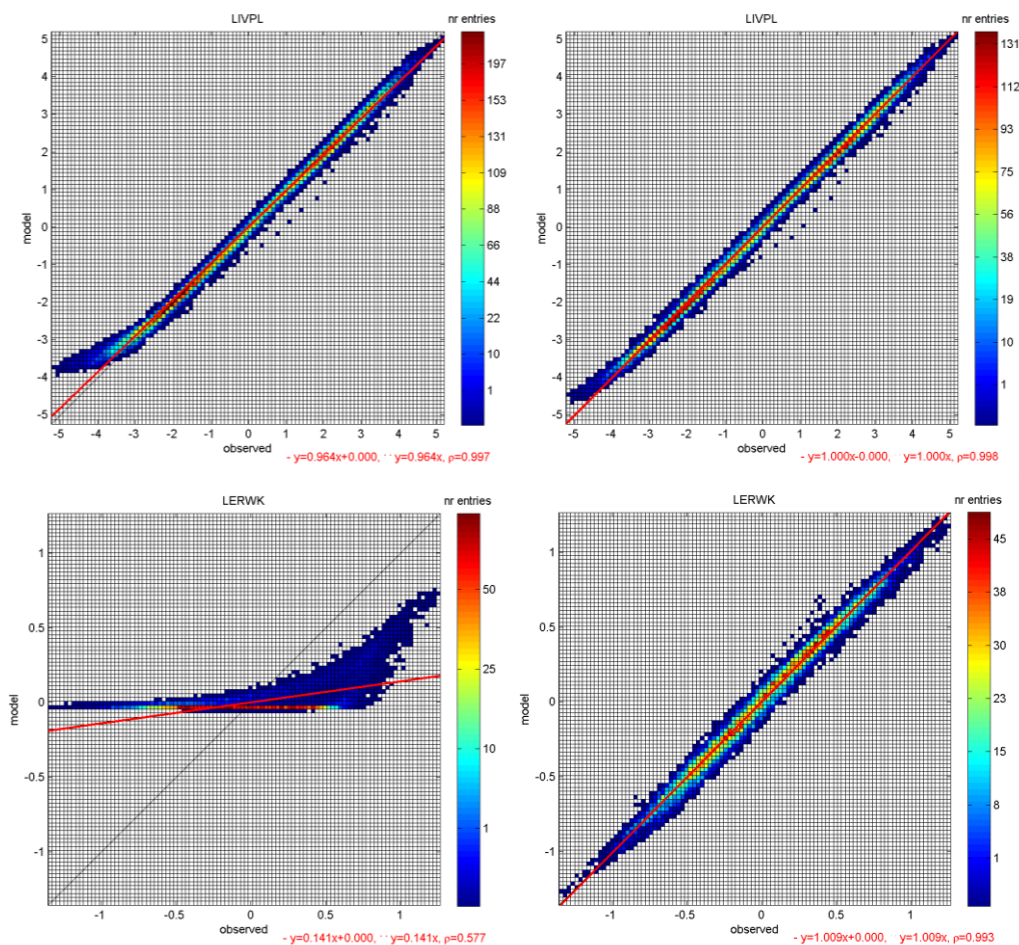
Figure 2.11 Scatter plots of the measured (horizontal) and modelled (vertical) water level before (left) and after (right) manual adjustment of the local bathymetry (upper plot: Liverpool; lower plot: Lerwick)

The model bathymetry is provided on the net nodes. Depths at the middle of the cell edges (the velocity points) are set to be determined as the mean value of the depth at the adjacent nodes. Depths at the location of the cell face (the water level points) are specified to be determined as the minimum of the depth in the surrounding cell edges. These bathymetry interpolations options are prescribed by setting *bedlevtype=3*.

An overview of the resulting DCSM-FM model bathymetry is presented in Figure 2.12. This shows that depths of more than 2000 m occur in the northern parts of the model domain, with depths exceeding 5000 m in the south-western part. The North Sea is much shallower with depths rarely exceeding 100m in the central and southern part (Figure 2.13). In Figure 2.14 a detail of the DCSM-FM model bathymetry is shown focussing on the southern North Sea. In the southern North Sea depths are generally less than 50 m.
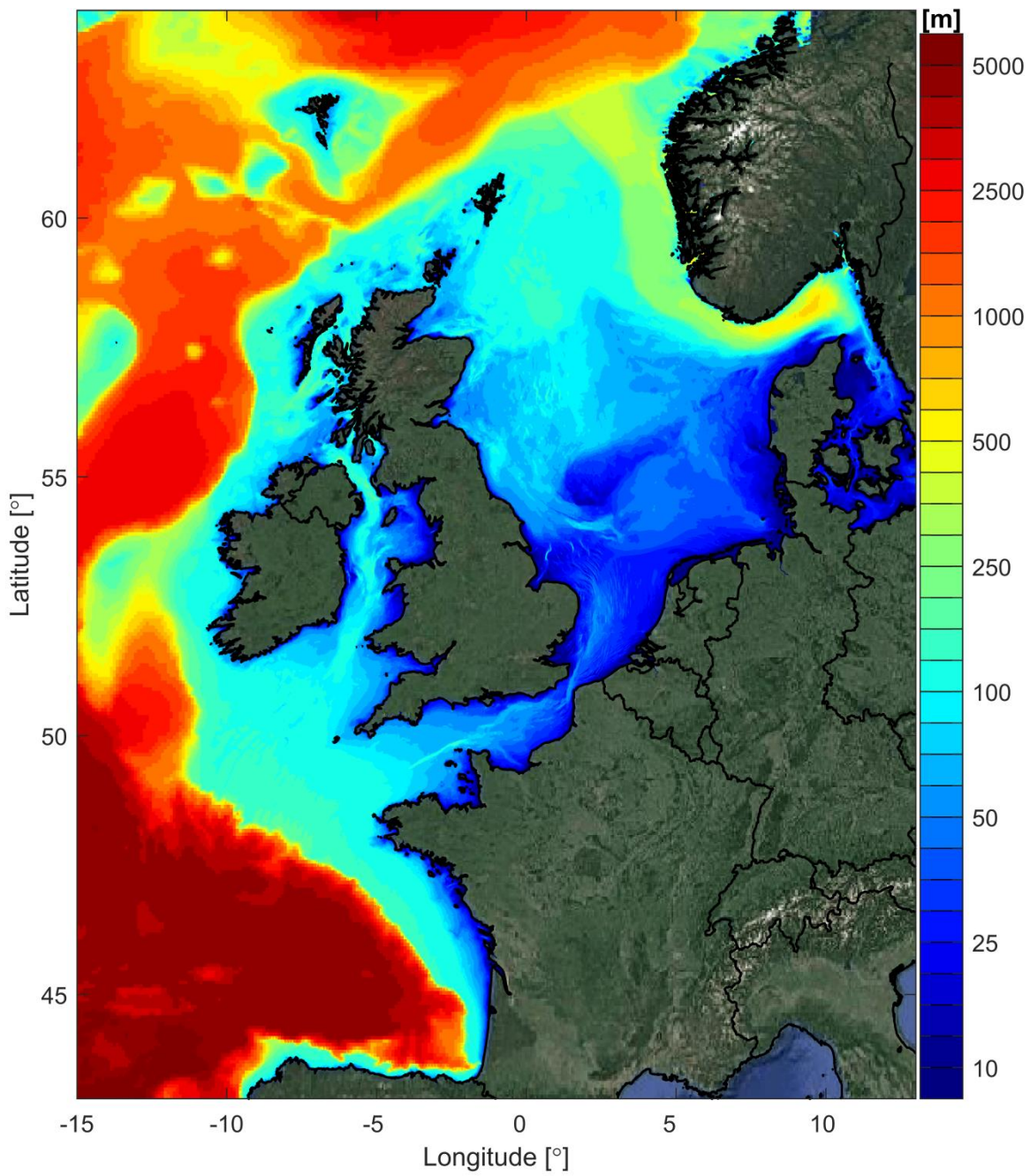
Figure 2.12 Overview of the DCSM-FM model bathymetry (depths relative to MSL).
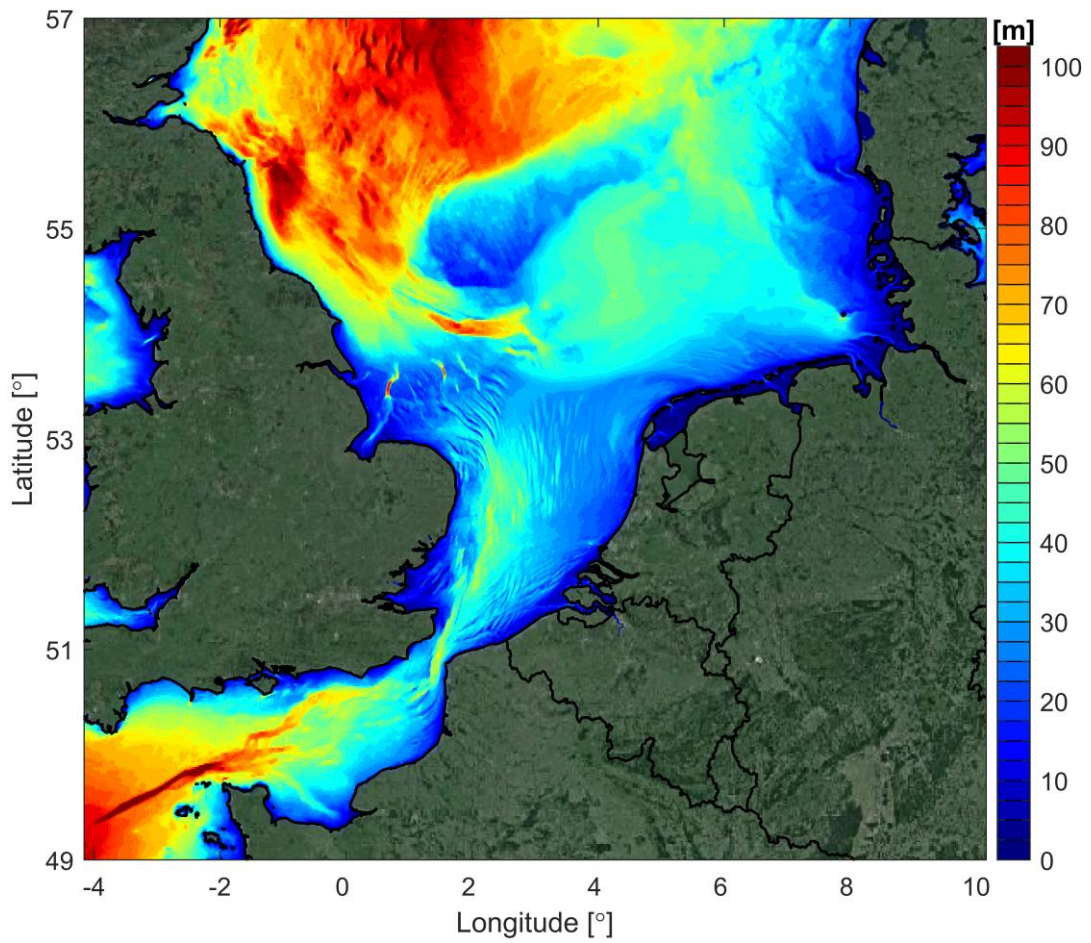
Figure 2.13 DCSM-FM model bathymetry in the central and southern North Sea (depths relative to MSL).
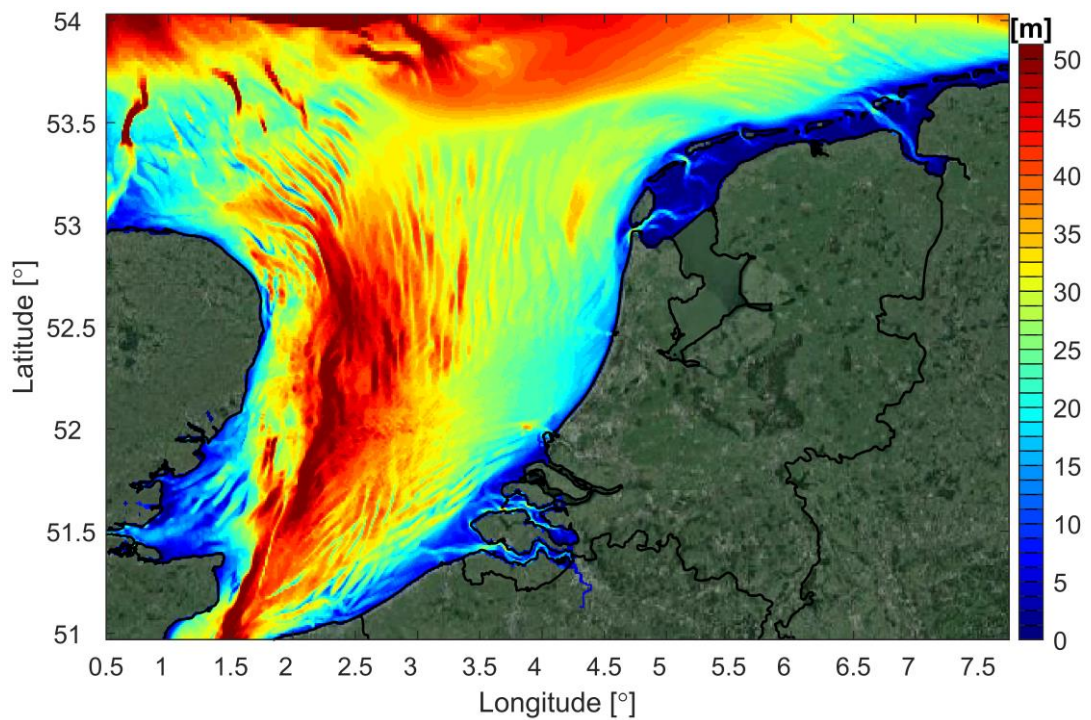
Figure 2.14 DCSM-FM model bathymetry in the southern North Sea (depths relative to MSL).
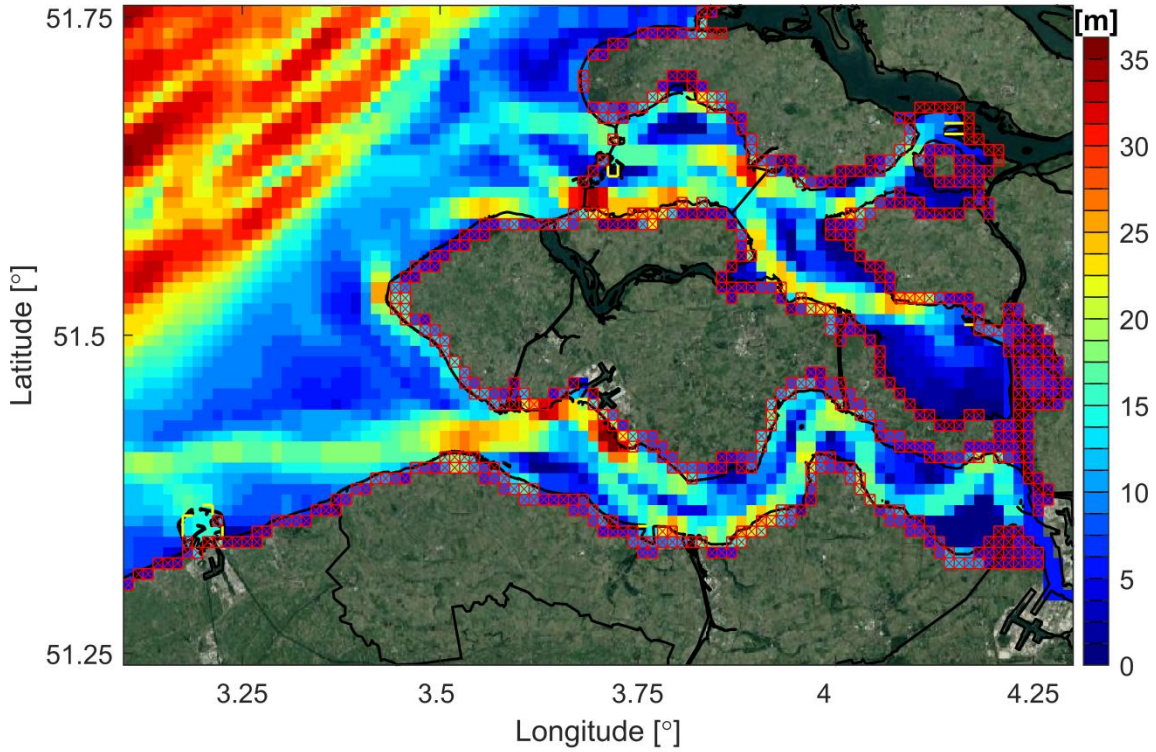
Figure 2.15 DCSM-FM model bathymetry in the South-western Delta (depths relative to MSL; permanently dry cells indicated with red crosses).
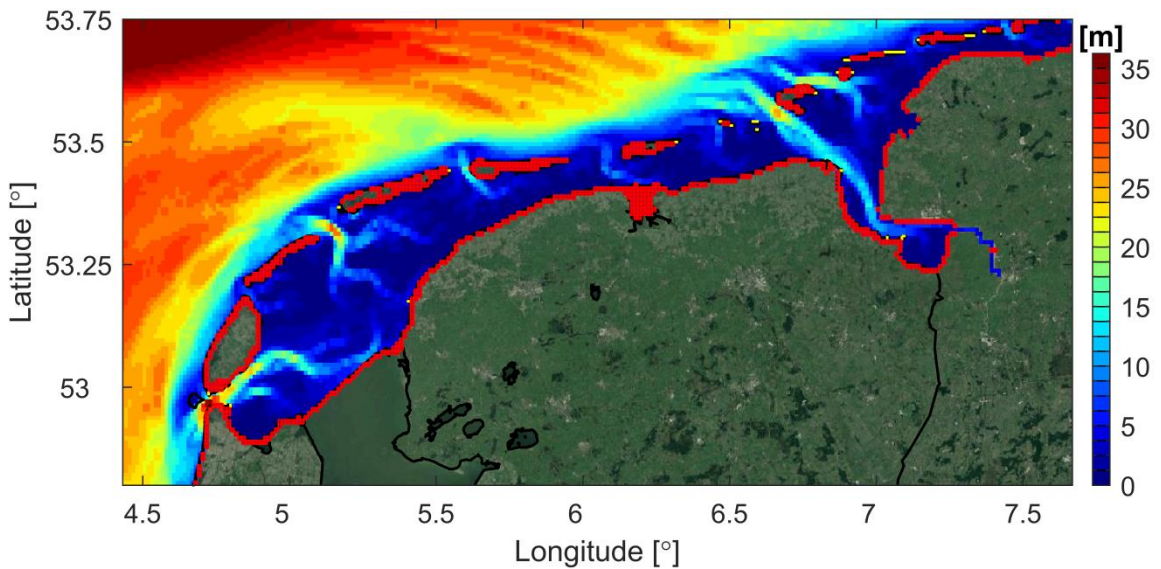
Figure 2.16 DCSM-FM model bathymetry in the Wadden Sea and Ems-Dollard (depths relative to MSL; permanently dry cells indicated with red crosses).

2.5 Bottom roughness

To account for the effect of bottom friction, a uniform Manning roughness coefficient of 0.028 s/m$^{1/3}$ was initially applied. During the model calibration (see Chapter 4) this value was adjusted to obtain optimal water level representation. The resulting roughness fields are presented in Figure 2.17 and Figure 2.18. The minimum and maximum bottom roughness values applied are 0.012 s/m$^{1/3}$ and 0.050 s/m$^{1/3}$.
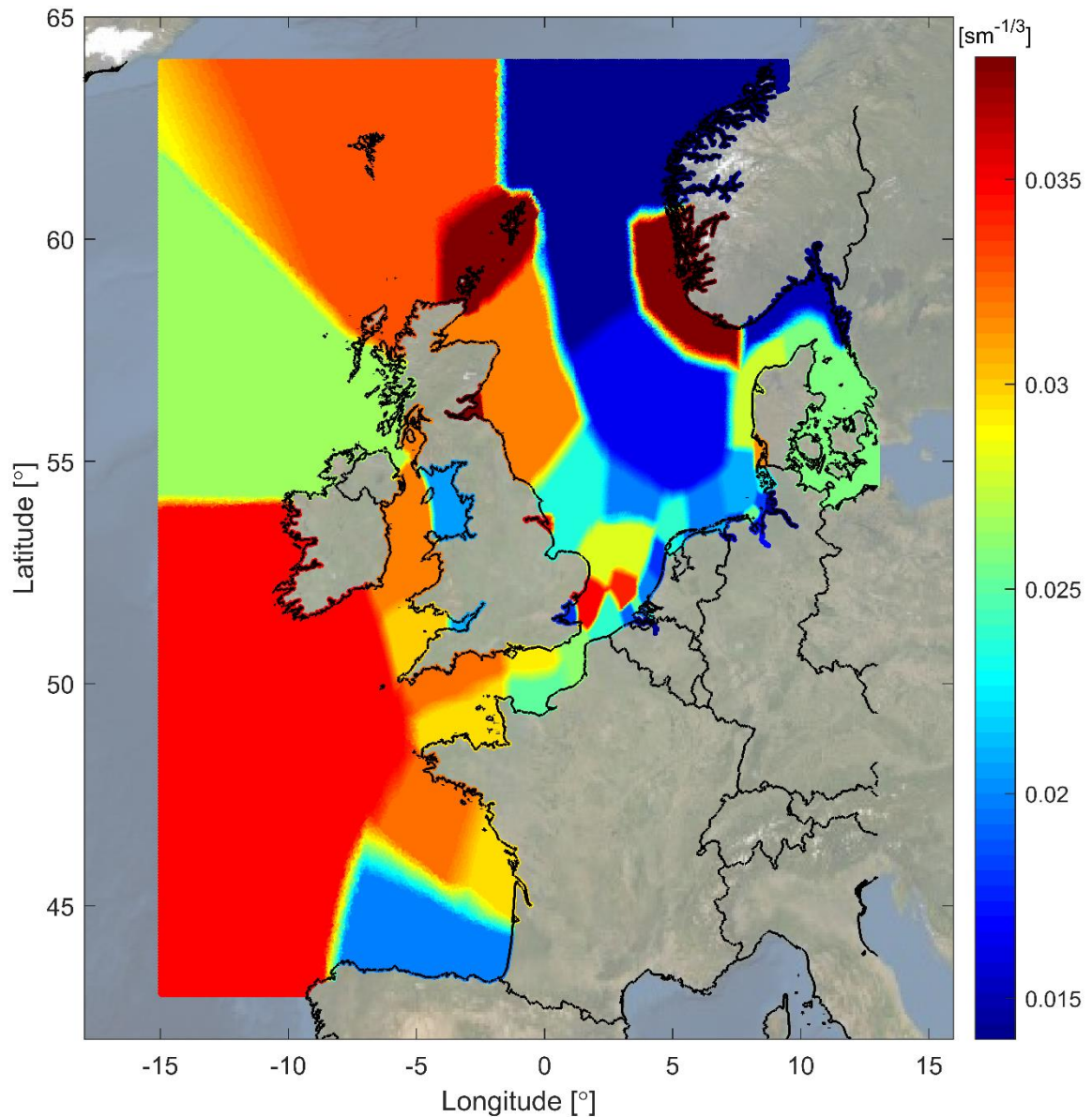
Figure 2.17 Overview of the (preliminary) space-varying Manning bottom roughness field of DCSM-FM.
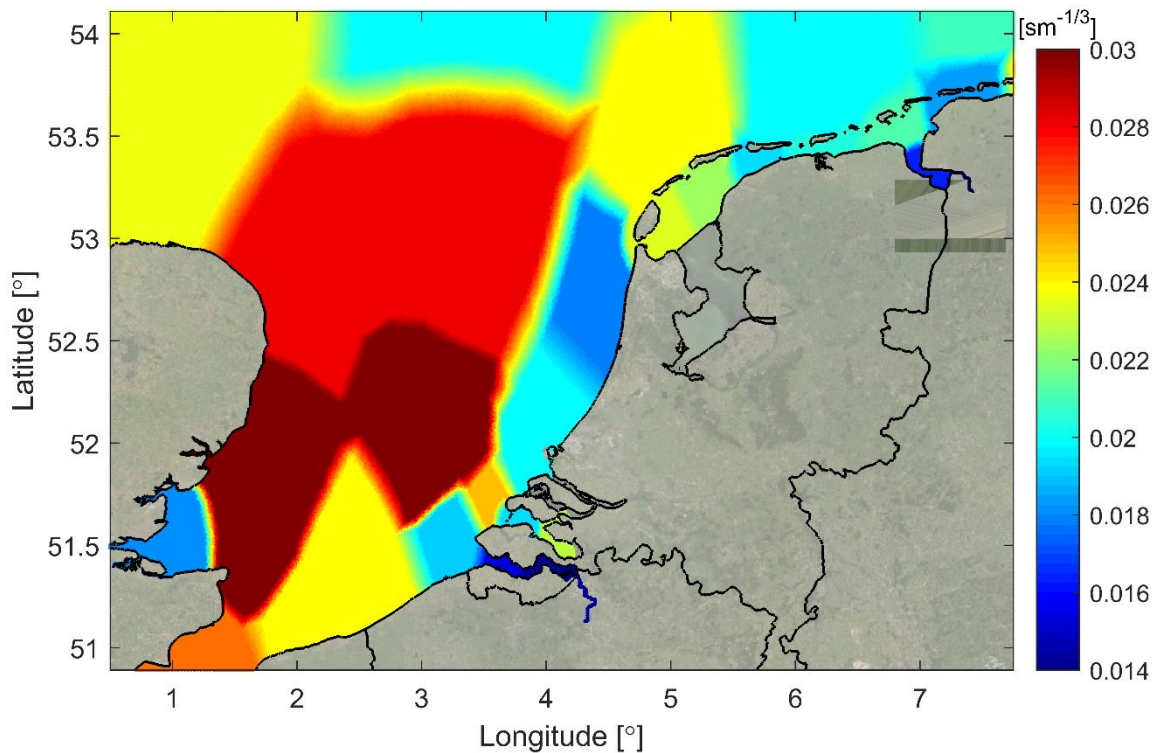
Figure 2.18 Detail of (preliminary) space-varying Manning bottom roughness field of DCSM-FM in Dutch waters.

2.6 Open boundary conditions

At the northern, western and southern sides of the model domain, open water level boundaries are defined. Water levels are specified at 209 different locations along those boundaries. In between these locations the imposed water levels are interpolated linearly.

Tide

At the northern, western and southern sides of the model domain, open water level boundaries are defined. The tidal water levels at the open boundaries are derived by harmonic expansion using the amplitudes and phases of 32 harmonic constituents (Table 2.1). All except one were obtained for the global tide model FES2012, which provides amplitudes and phases of 32 constituents on a 1/16° grid. Of these only MKS2 is not used, since inclusion in the boundary forcing resulted in a deterioration of results. N4 was initially not recognised by D-HYDRO since it did not have a corresponding constituent with the same name or a similar enough angular frequency. This has since been added.

In addition to the above, the solar annual constituent Sa has also been added based on what was used in DCSMv6 (see Figure 2.19). Even though in the ocean Sa is much less gravitational than meteorological and baroclinic in nature, in the absence of baroclinic forcing it is required to reproduce the observed residual annual cycle, i.e. the signal not captured by annual mean sea-level pressure and wind variations and notably the seasonal temperature cycle. While this is negligible on the shelf, this is less so in the deep ocean.
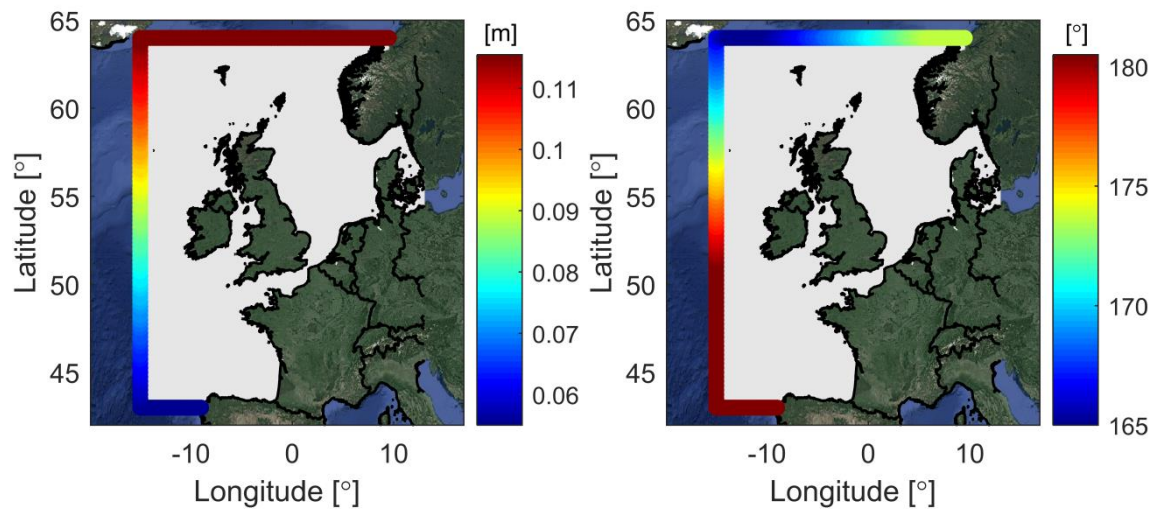
Figure 2.19 Amplitude (left panel) and phase (right panel) of the Sa-component along the open boundaries of the model domain

Table 2.1 Overview of the tidal components prescribed at the open boundaries of DCSM-FM, including their angular frequency (°/h).

Component name	Angular frequency (°/h)	Component name	Angular frequency (°/h)
SA	0.0410686	M2	28.9841042
SSA	0.0821373	LABDA2	29.4556253
MM	0.5443747	NU2	28.5125831
MF	1.0980331	L2	29.5284789
MSF	1.0158958	T2	29.9589333
MFM	1.6424078	S2	30.0000000
Q1	13.3986609	R2	30.0410667
O1	13.9430356	K2	30.0821373
P1	14.9589314	M3	43.4761563
S1	15.0000000	M4	57.9682084
K1	15.0410686	MN4	57.4238337
J1	15.5854433	MS4	58.9841042
MNS2	27.4238337	S4	60.0000000
2N2	27.8953548	M6	86.9523126
MU2	27.9682084	M8	115.9364168
N2	28.4397295		

In the D-HYDRO software the specified amplitudes and phases are converted into timeseries covering the required period by means of harmonic prediction. Implicitly it is assumed that the nodal cycle at the location of the open boundaries can be obtained from the equilibrium tide. The validity of this assumption is corroborated by Zijl (2016b).

Surge

While wind setup at the open boundary can arguably be neglected because of the deep water locally (except near the shoreline), the (non-tidal) effect of local pressure will be significant. The impact of this is approximated by adding an Inverse Barometer Correction (IBC) to the tidal water levels prescribed at the open boundaries. This correction is a function of the time- and space-varying local air pressure.

One can also consider nesting in a model with a larger domain, e.g. a global model. This would also account for the differences due to the mean pressure over the global ocean, which is now assumed to be constant, but in reality varies with the weather.

2.7 Meteorological forcing

For meteorological surface forcing of the model the KNMI provided time- and space-varying wind speed (at 10 m height) and air pressure (at MSL) from the Numerical Weather Prediction (NWP) high-resolution limited area model (HiRLAM; version 7.2). This meteorological model has a spatial resolution of approximately 11 km by 11 km, and a temporal output interval of 1 hour. The wind stress at the surface, associated with the air-sea momentum flux, depends on the square of the local U10 wind speed and the wind drag coefficient, which is a measure of the surface roughness.

To translate wind speed to surface stresses, the local wind speed dependent wind drag coefficient is calculated using the Charnock formulation (Charnock, 1955). The empirically derived dimensionless Charnock coefficient has been set to a constant value of 0.025, which corresponds to the value used in the HiRLAM meteorological model. The resulting Wind drag coefficients are shown in Figure 2.20 as a function of the 10 m wind speed.
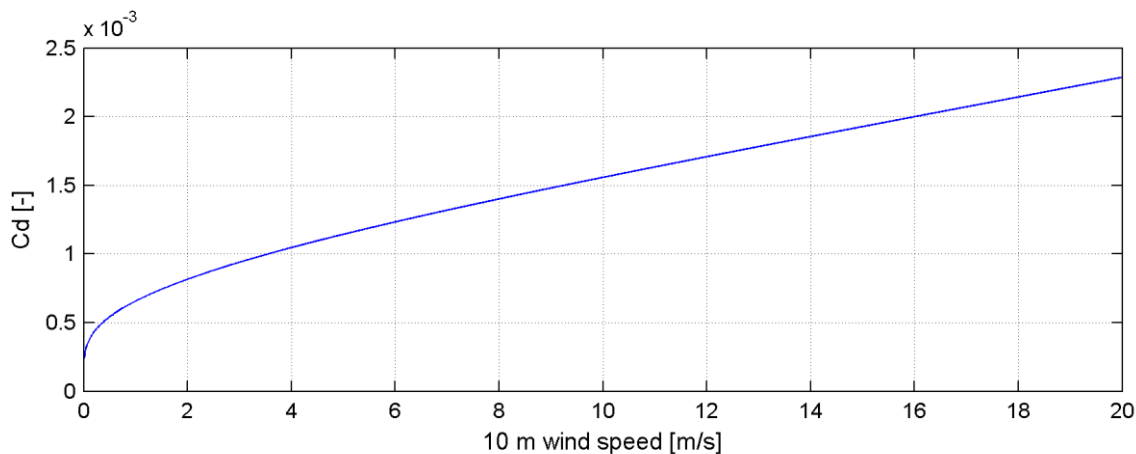
Figure 2.20   Wind drag coefficient (Cd) as a function of the 10 m wind speed, using a Charnock relation with a Charnock parameter of 0.025.

While the calibration and validation as presented in the present report have been performed with Hirlam v7.2 meteorological forcing, the model can be forced with different meteorological model output. The forcing parameters have then to be adjusted accordingly. For example, in the operational ECMWF meteorological model (IFS), the Charnock coefficient is dependent on wind waves (as forecasted with the ECWMF WAM model) and consequently time and space dependent. This implies that when using ECMWF IFS forcing, the Charnock coefficient also has to be prescribed in a time-and space dependent manner.

Relative wind effect

In most wind drag formulations the flow velocity is not taken into account in determining the wind shear stress (i.e., the water is assumed to be stagnant). Even though the assumption of a stagnant water surface is common because it makes computing stresses easier, from a physical perspective the use of relative wind speed makes more sense since all physical laws deal with relative changes. In case the flow of water is in opposite direction to the wind speed, this would contribute to higher wind stresses (and vice-versa). The impact of the water velocity

on the wind stress at the surface, and consequently also on computed water levels, is indicated with the name 'Relative Wind Effect' (RWE).

In general, including RWE leads to a meaningful improvement in (skew) surge quality during calm conditions (see Appendix C). Apparently, RWE adds an effect that cannot fully be incorporated by adjusting the bottom roughness instead. Even though inclusion comes at a cost of an increased systematic underestimation during the two most extreme skew surge events of 1-3 cm, it was decided to include RWE in the final DCSM-FM model schematization. Note that when the wind stress is prescribed directly, this requires switching of the RWE, which would have an adverse effect on the quality of both the surge and tide representation.

2.8 Numerical settings

2.8.1 Theta0
The implicitness of the numerical time integration is specified with the parameter *Teta0*, with *Teta0=1* being fully implicit and *Teta0=0* fully explicit. In accordance with Spruyt et al. (2017) the value of *Teta0* is set to 0.55.

2.8.2 Time step
D-Flow FM automatically limits the time step to prevent numerical instabilities. Since the computation of the advective term is done explicitly in D-Flow FM, the time step limitation is related to the Courant criterion. In accordance with Spruyt et al. (2017) the maximum Courant number is set to 0.7. The maximum computational time step has been set to 2 minutes (120 s).

2.9 Miscellaneous

2.9.1 Tidal potential
The tidal potential representing the direct body force of the gravitational attraction of the moon and sun on the mass of water has been switched on. It is estimated that the effect of these Tide Generating Forces (TGF) has an amplitude in the order of 10 cm throughout the model domain. Components of the tide with a Doodson number from 55.565 to 375.575 have been included.

2.9.2 Horizontal viscosity
The horizontal viscosity is computed with the Smagorinsky sub-grid model, with the coefficient set to 0.20. The use of a Smagorinsky model implies that the viscosity varies in time and space and is dependent on the local cell size. With the exception of a two nodes wide strip along the open boundaries a background value of 0.1 m^2/s is specified. Along the open boundaries a background value of 2000 m^2/s has been used (see Appendix D).

In (Zijl, Irazoqui and Groenenboom 2016) it is concluded that the computed water levels in the North Sea are hardly affected by the use of the Smagorinsky sub-grid model. It is therefore expected that the sensitivity of the water level for the Smagorinsky coefficient is negligible. The impact on currents or the salinity distribution can be larger. The latter is not taken into account in the present model setup.

2.9.3 Movable barriers
There are a number of movable barriers in the model area, such as the Thames Barrier, the Ems Barrier, the Eastern Scheldt Barrier and the Maeslant Barrier. These barriers protect the hinterland from flooding by closing in case of high water is forecasted. The only barrier currently implemented in the model is the Eastern Scheldt Barrier (see Figure 2.21). The other barriers

either have a negligible effect on water levels in the Netherlands (Thames Barrier) of do not have the area upstream of the barrier sufficiently included in this model (Ems Barrier and Maeslant Barrier).

The Eastern Scheldt Barrier consists of 62 separate gates divided over three sections (from north to south: Hammen, Schaar van Roggenplaat and Roompot). These sections are separately schematized in the model. The modelled sill height in each of these three sections is taken to be the average of the sill heights within this section: NAP -6.32 m, NAP -5.75 m and NAP -8.60m. The energy loss coefficients are taken from the sixth generation Oosterschelde model (Tiessen et al., 2019) and have a value of 0.93 and 1.03 for ebb and flood currents, respectively. Furthermore, all gates are assumed to have an infinite height. While in reality this is obviously not the case, this will not affect the calibration and validation, since in these periods flow over the gates has not occurred.

During sensitivity tests the modelled and measured M2 phase and amplitude difference over the Eastern Scheldt barrier was assessed by comparing Roompot Binnen and Roompot Buiten. This has resulted in an increase of the barrier width by 45% compared to the actual width. This was only implemented after making sure, with OpenDA-DUD experiments, that the desired results could not be obtained by adjusting bottom friction. Furthermore, the adjustment of the barrier width could not be avoided by adjusting the energy loss coefficients. Presumably, the need for adjusting the width is related to the coarseness of the model schematization in this area.

The schematization of the three sections of the Eastern Scheldt Barrier on the model grid, are shown in green in Figure 2.21. In this figure, the red lines show the computational network, the red crosses illustrate the dry points (permanently inactive cells) and the thin dams are shown in yellow. The cross-sectional area of the barriers follows from a prescribed gate door height and width. These values are listed in Table 2.2. The width of each of the sections is the summed width of the individual gates in each section.

Table 2.2   Gate door height, width and sill height of the three sections of the Eastern Scheldt Barrier

Section	Gate door height [m]	Width [m]	Sill height [m MSL]
Schaar	11.06	916.40	-5.75
Hammen	11.63	859.13	-6.32
Roompot	13.91	1775.53	-8.60

The effect of the structures on the cross-sectional area at each of the structures is controlled by a timeseries of the gate lower edge level of the three sections (data provided by Rijkswaterstaat). These timeseries are corrected for the presence of a horizontal concrete beam at 1.0m (Roompot en Schaar) and 0.8m (Hammen) above NAP. As the water level at this location sometimes exceeds this vertical level, the flow is partially blocked near the surface. During a closure, see Figure 2.22, the gate lower edge level is almost lowered to the sill height. The timeseries of the gate lower edge level are averaged over the individual gates in each section. The data is corrected for leakage of the hydraulic structure and therefore the gate lower edge level remains above the sill height.
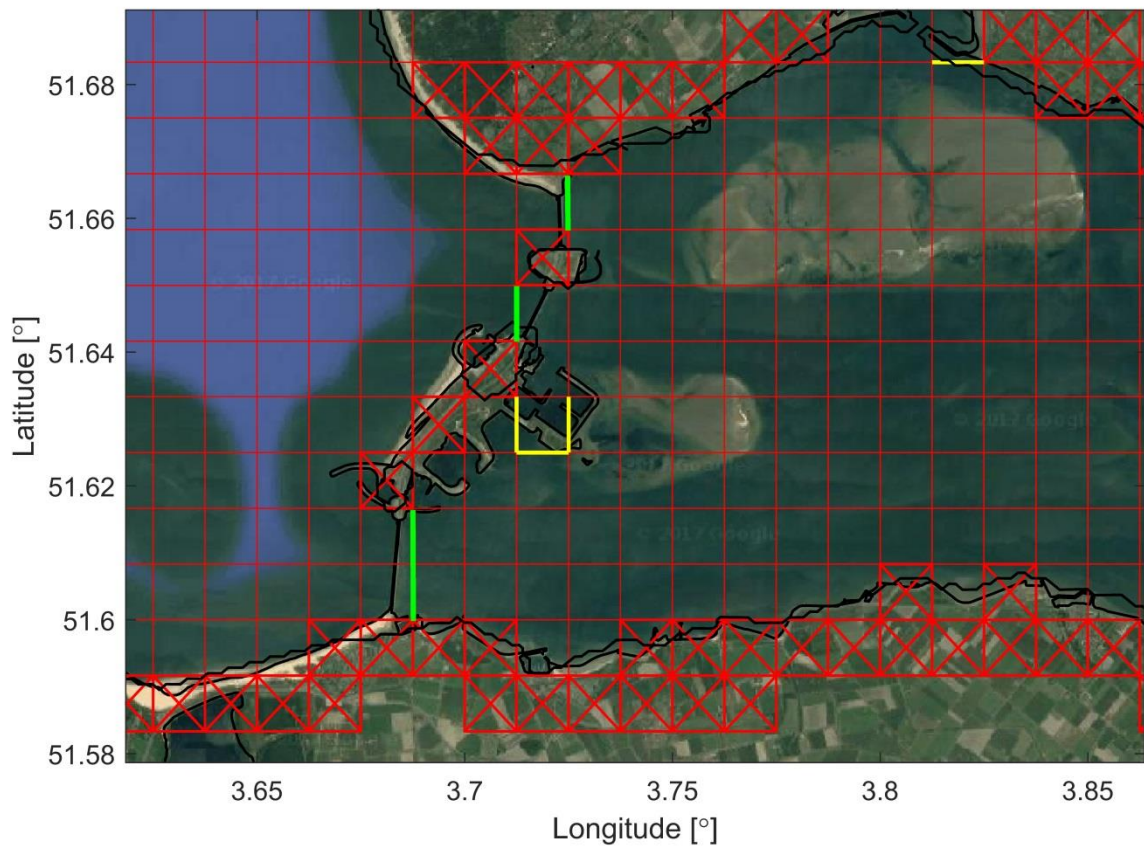
Figure 2.21 Implementation of the Eastern Scheldt Barrier in DCSM-FM (red lines: computational network; red crosses: dry points; yellow lines: thin dams; green lines: movable barriers).
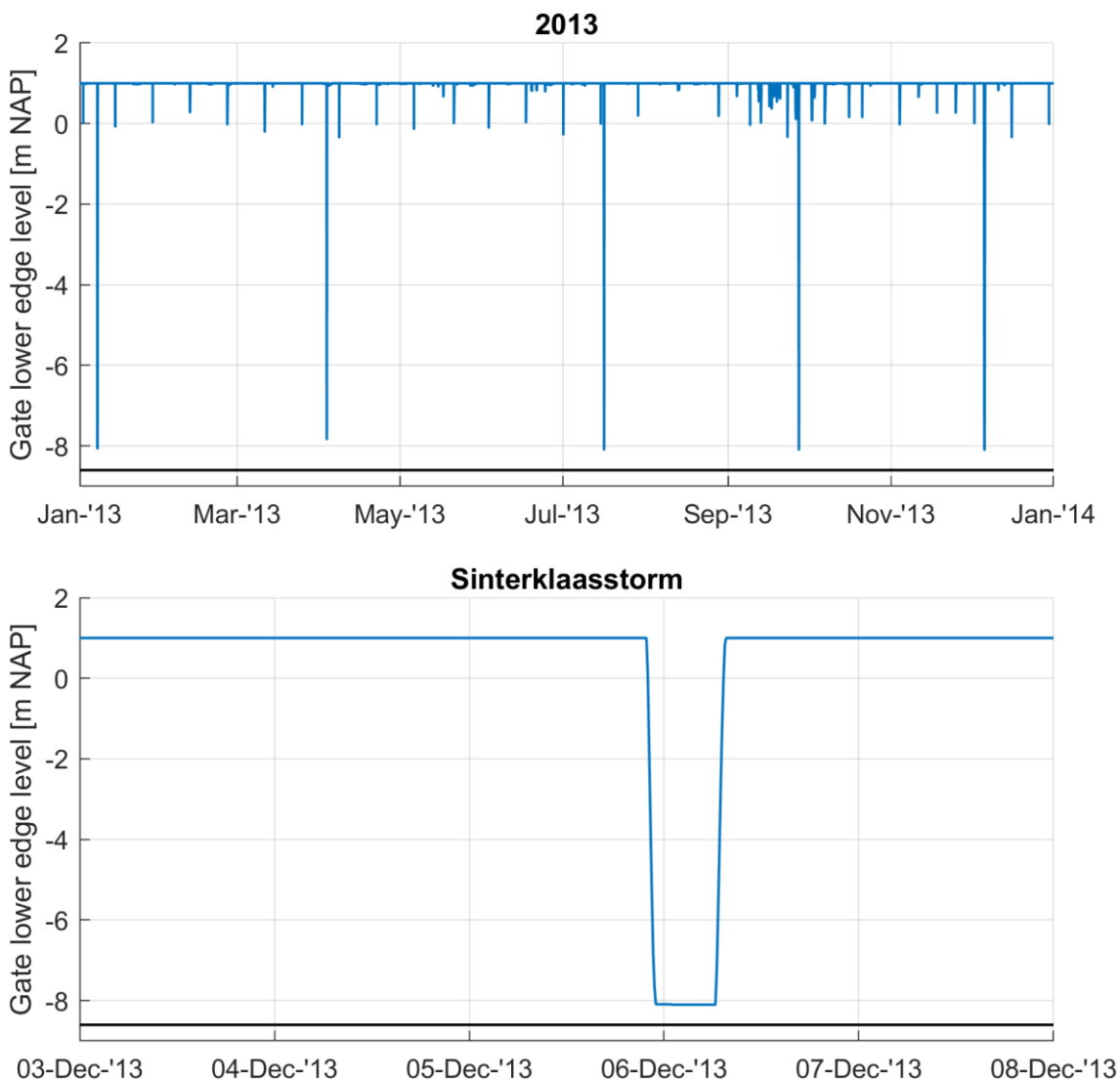
Figure 2.22 Timeseries of the gate lower edge level (in m NAP) of the Eastern Scheldt Barrier section Roompot for year 2013 (top panel) and during the so-called Sinterklaasstorm (lower panel). The black line indicates the sill height of the structure (-8.6 m NAP)

2.9.4 Initial conditions and spin-up period

As the spin-up period for tidal models of this scale are not prohibitively large (10 days is assumed to be sufficient), a uniform initial water level of zero elevation has been specified for the calibration and validation computations. For the initial velocity, stagnant flow conditions have been prescribed. Operationally, the initial model state will be taken from previous hindcast computations (i.e., a so-called warm state).

2.9.5 Time zone

The time zone of DCSM-FM is GMT+0 hr. This means that the phases of the harmonic boundary conditions and the tidal potential are prescribed relative to GMT+0 hr. As a result, the model output is in the same time zone. This time zone is the same as in the previous generation DCSMv6 and DCSMv6-ZUNOv4 models.

2.9.6 Observation points

Since the North Sea is one of the most intensively monitored seas in the world, water level observations are readily available. An overview of the more than 100 tide gauge stations available for calibration and validation are presented in Figure 2.23 (for the entire domain) and Figure 2.24 (Dutch and Belgian stations).

If locations are just outside the model grid, they are manually placed in the closest cell with sufficient depth. One exception is tide gauge location Delfzijl, which is moved to the opening of the harbour breakwater further upstream in the Ems Estuary.
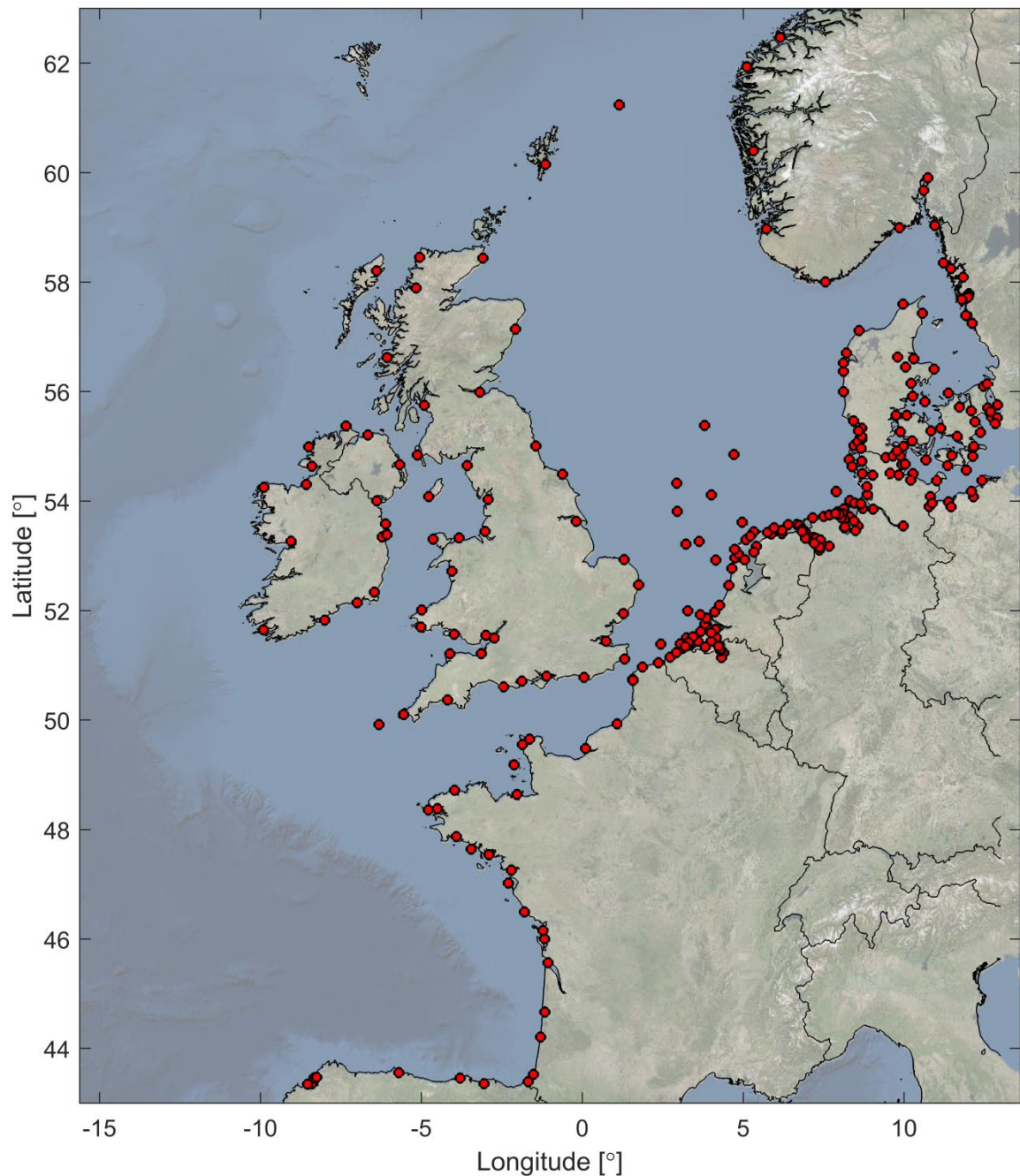
Figure 2.23 Overview of the tide gauge locations used for the model calibration (for Dutch and Belgian locations see Figure 2.24).
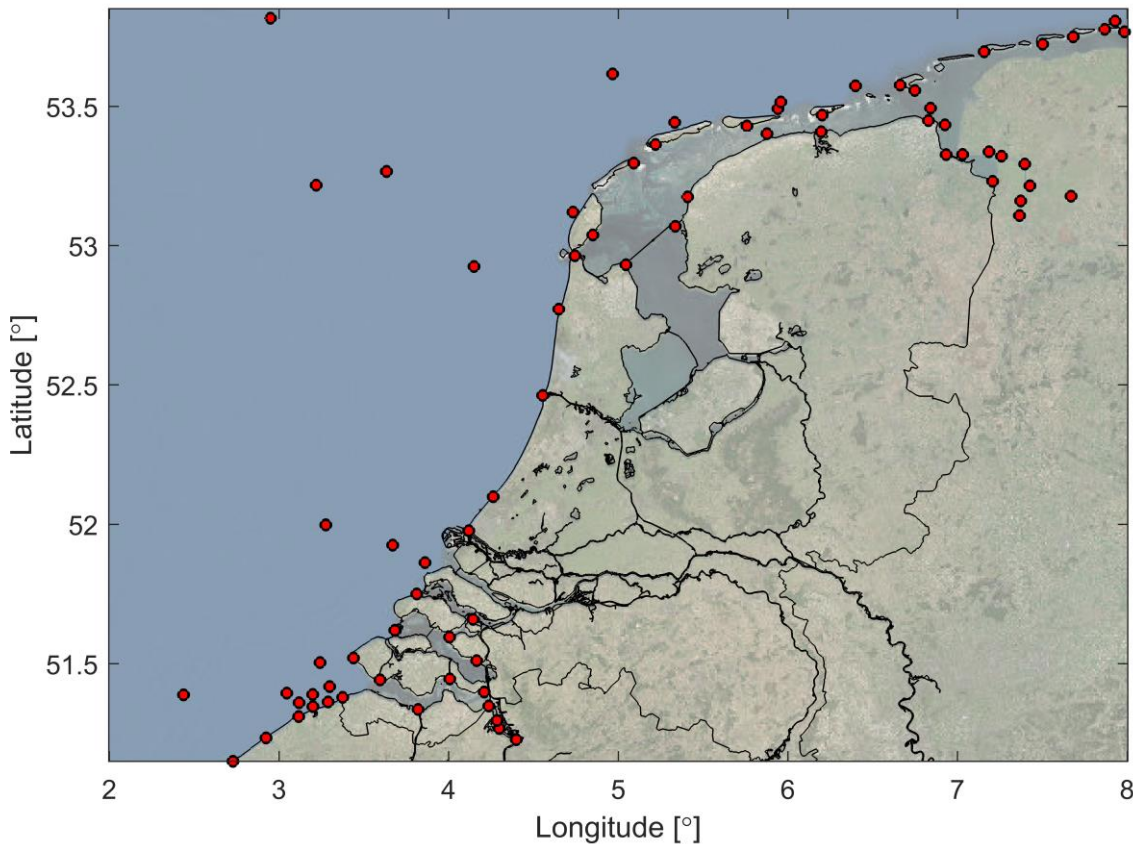
Figure 2.24 Overview of the Dutch and Belgian tide gauge locations used for the model calibration.

2.9.7 Breaking of internal waves

The generation of internal waves on the slope towards the continental shelf precipitates barotropic energy dissipation. Even though the 2D barotropic DCSM-FM model cannot explicitly model internal waves, the energy dissipation this causes can be taken into account through a parametrization that is dependent on the local bathymetry gradient, the local flow velocity perpendicular to the continental slope and the local depth-averaged Brunt–Väisälä frequency. The latter quantity is computed as a pre-processing step on the basis of 3D monthly-averaged temperature and salinity fields.

In Appendix B the impact of taking energy dissipation at the shelf edge into account is quantified. Considering the general improvement in surge quality in both the uncalibrated and calibrated model, it was decided to include the parametrization of energy dissipation by generation of internal waves into the final DCSM-FM model schematization.

2.9.8 Software version

DCSM-FM has been developed as an application of the D-Flow Flexible Mesh module (D-Flow FM) module of the D-HYDRO Suite. With this module is suitable for one-, two-, and three-dimensional hydrodynamic modelling of free surface flows on unstructured grids. Various versions of D-Flow FM have been used during the development of DCSM-FM. For the final validation presented in this report, use has been made of D-Flow FM version 1.2.54.64101 (Jun 12, 2019).

2.9.9 Computational time
In Table 2.3 the computational time of DCSM-FM is presented together with the (average) time step and cell size and the number of network nodes. This is done for a number of configurations of the model (including a 3D version and a test version with a maximum resolution of 1nm), with all computations performed on Deltares' h6 cluster using 5 nodes with 4 cores each.

During the development of DCSM-FM network the minimum size of the network nodes was an important decision since this has a substantial impact on the resulting computations time through the average time step and the number of cells. These results show that halving the minimum cell size more than doubles the computational time. Nonetheless, because of the beneficial impact on the quality of water levels in shallow areas such as the Wadden Sea this is considered acceptable. Even though DCSM-FM (with a minimum cell size of 0.5 nm) has smaller grid cells in the relevant areas, it is still 15% faster than DCSMv6 (1.36 min/day vs. 1.6 min/day).

It can also be observed that the preliminary calibration has increased the average time step and decreased the computational time. This is presumably caused by the higher roughness in the Pentland Firth (i.e., between the north of Scotland and the Orkney Islands), where the remaining restricting cells were located in the uncalibrated model (cf. Figure 2.3).

Three-dimensional configurations
Since DCSM-FM should also be a sound basis for the subsequent development of a 3D baroclinic transport model of the North Sea, the computational time is also assessed using 20 equidistant sigma-layers (Table 2.4)

In 3D barotropic mode (i.e., without temperature and salinity) the model is ~7 times slower than the 2D configuration. Additionally, adding salinity and temperature as state parameters makes it 10 times slower than the 2D model. This amounts to 3.4 days per simulated year, which is considered acceptable.

One computational core
An important criterion for DCSM-FM is that it should be fast enough to produce probability forecasts with a 2 – 10 day lead-time within roughly 2 hours. These forecasts will be based on meteorology of the ECMWF Ensemble Prediction System (EPS) and consist of one control run and 50 perturbed members. It is considered most efficient to run as many of these 51 runs at the same time in sequential mode (i.e., on one computational core), instead of consecutively in parallel. Therefore, the computational time on one core is also determined (Table 2.5). These results show a computational time of 10.9 min/day, which means that running 10 days is possible in 109 minutes, less than the maximum of 120 minutes. Note however, that these results are hardware-dependent and that running multiple computations on one node (on one core each) could increase the required computational time.

Table 2.3 Overview of grid cell size, number of net nodes, maximum and average numerical time step and computational time for various 2D models. The computations were performed on Deltares' h6 cluster using 5 nodes with 4 cores each.

Model	cell size (nm)	# nodes	Maximum time step (s)	Average time step (s)	Comp. time (min/day)	Comp. time (hr/year)
Fifth generation						
DCSMv6	1 nm	859,217	120	120.0	1.6	10.0
DCSMv6-ZUNOv4	4nm – 0.15nm	1,119,106	60	60.0	6.5	40.2
Before calibration						
DCSM-FM (1nm)	4nm-1nm	373,522	200	198.8	0.60	3.7
DCSM-FM (0.5 nm)	4nm-0.5nm	629,187	120	113.8	1.41	8.6
After prel. calibration						
DCSM-FM (1nm)	4nm-1nm	373,522	200	199.8	0.58	3.6
DCSM-FM (0.5 nm)	4nm-0.5nm	629,187	120	118.7	1.36	8.3

Table 2.4 Overview of grid cell size, number of net nodes, maximum and average numerical time step and computational time for various three-dimensional configurations of the model, all using 20 equidistant sigma-layers. The computations were performed on Deltares' h6 cluster using 5 nodes with 4 cores each.

Model	cell size (nm)	# nodes	Maximum time step (s)	Average time step (s)	Comp. time (min/day)	Comp. time (hr/year)
3D (excl S and T)						
3D DCSM-FM (0.5nm)	4nm-0.5nm	629,187	120	114.1	9.4	57
3D (incl S and T)						
3D DCSM-FM (1nm)	4nm-1nm	373,522	200	198.7	4.9	30
3D DCSM-FM (0.5nm)	4nm-0.5nm	629,187	120	113.4	13.5	82

Table 2.5 Overview of grid cell size, number of net nodes, maximum and average numerical time step and computational time for various models. The computations were performed on Deltares' h6 cluster using 1 core.

Model	cell size (nm)	# nodes	Maximum time step (s)	Average time step (s)	Comp. time (min/day)	Comp. time (hr/year)
Fifth generation						
DCSMv6	1 nm	859,217	120	120.0	16	97
Before calibration						
DCSM-FM (1nm)	4nm-1nm	373,522	200	198.9	3.9	24
DCSM-FM (0.5 nm)	4nm-0.5nm	629,187	120	114.0	11.2	68
After prel. calibration						
DCSM-FM (0.5 nm)	4nm-0.5nm	629,187	120	118.7	10.9	66

3 Water level data

3.1 Collection of water level data

Compared to the dataset available for the calibration and validation of the fifth generation models of the North Sea, availability of time series of water level from tide gauges in the model domain has increased significantly. This extended dataset can be used to further improve the model as it will be used in the calibration procedure and for the validation of the model. Various data sources have been used; national organisations of several countries were contacted and water level data from European data networks has been retrieved. Water level data is obtained from the following sources:

- Rijkswaterstaat (RWS) - Waterbase, The Netherlands;
- Meetnet Vlaamse Banken (VB), Belgium;
- Flanders Hydraulics Research (WL-B), Belgium;
- British Oceanographic Data Centre (BODC), Great Britain;
- Bundesanstalt für Gewässerkunde (BAFG), Germany;
- Copernicus Marine Environment Monitoring Service (CMEMS);
- European Marine Observation and Data Network (EMODnet).

The result was a collection of a few hundred raw data files.

3.2 Quality assurance

3.2.1 Selection of the data

The available data was processed, and a first selection of monitoring stations was made based on their location (inside or outside model domain). As data for some stations is available in multiple data sets, priority is given to the data from the national organisations. For the other countries, data from CMEMS and EMODnet is used. As data for some locations is available in both the CMEMS and EMODnet data sets, the data has been checked carefully, merged and where overlaps exist the time series with the highest temporal interval is used.

3.2.2 Removing erroneous data from dataset

Depending on the source of the data, some erroneous data was already removed from the dataset before it was distributed. However, a manual check of all the water level time series was needed as it turned out that erroneous data was still present in all dataset. In general, more erroneous data was found in the CMEMS and EMODnet dataset compared to the data provided by national organisations.

A MATLAB-routine was developed to quickly assess the quality of the provided water level data. All available data for all monitoring stations in the period 2013 – 2017 were manually checked. A visual inspection was performed on plotted time series of the water level (in red in Figure 3.3; each plot has a length of 12 days). To ease the detection of outliers, the modelled (black) and difference between measured and modelled water levels (blue) are plotted as a reference. In addition, a tidal analysis of both the modelled and observed water levels is performed and the surge (total water level minus tidal signal) is plotted in the lower panel of the figure. Again, both the observed (red), modelled (black) and difference (blue) time series of the surge are shown. By using an interactive interface, the user is able to select data and mark times and corresponding water levels as erroneous. These points in the dataset can then be used as a mask (i.e. set to NaN). When using the water level data, for e.g. calibration or validation, the raw data is first read after which the mask is read in and the erroneous data are

removed. This approach of masking the erroneous data is chosen to keep track of applied masked times without changing the original dataset.

Several types of erroneous data were found, and a few examples are listed below.

3.2.2.1 Change in reference level
It was found that the reference level of measurements from several offshore stations was abruptly changed after a certain period (see e.g. Figure 3.3). As these jumps would make these data unsuitable for calibration of validation, short periods where the reference level clearly deviates are masked. In Figure 3.4 the masked values are shown in green, these data will be disregarded during data-model comparisons.

In the Dutch offshore tide gauge stations A12, D15 and J6 some jumps in reference level still remain. This means that these data can only be used when periods without the occurrence of a jump are considered.

3.2.2.2 Constant water level
Figure 3.5 depicts another common error in the water level data. At 9 May 2019, the observed water level at station North Cormorant retains the same value for about an hour. These kinds of errors are sometimes hardly visible in the total water level (top panel). Therefore, the surge (lower panel) is also used during the inspection as erroneous data points (especially outliers) can more easily be detected and marked as data points that should be masked (see Figure 3.6).

3.2.2.3 Phase shift
Some of the monitoring stations contain data that was subjected to a phase shift for a short period. In Figure 3.7 an example of such a phase shift at monitoring location North Cormorant (NORTHCMRT) is shown. The phase shift (which is probably introduced during processing of the data/adjusting the time zone as the shift is usually one hour) in the observed (red) and modelled (black) is not striking since the predicted water level could also be lagging behind (phase error). However, from the lower plot, which illustrates the residual/surge signal (water level minus tides), it is clear that in the period of 11 Sep 2013 to 21 Sep 2013 the provided water level data does not match with the tidal signal that is derived from the tidal analysis. Therefore, the water level data in this period is masked (indicated with green in Figure 3.8).

Note that a tidal signal in the lower plot can also be caused by the absence of harmonic constituents in the harmonic analysis or by non-linear interaction between the tides and surge. A sinusoidal-shaped wave does therefore not always indicate erroneous water level data.

3.2.2.4 Sudden (negative) peak in water level
In Figure 3.9 a sudden negative peak in the observed water level at station Huibertgat is presented. These kinds of sudden peaks are considered to be erroneous because an increase and subsequent decrease in water level in the order of decimetres is not expected to occur within the time interval of 1-10 minutes. Similar to the 'constant water level'-issue, this type of erroneous data is usually more clearly visible in the lower panel that depicts the surge (Figure 3.10). Particularly, when the sudden change occurs when MSL is passed the lower plot is very useful.

In case of doubt, data was not masked (conservative approach). The rare meteo-tsunami of 29 May 2017 caused a rapid increase of water levels along the (southern part of the) Dutch coast. These kinds of phenomena are not correctly modelled and thus during this event, the observed

water levels at e.g. monitoring location Roompot Buiten deviate from the model prediction and were therefore quite noticeable in the Quality-check program. These values have not been masked.

An additional quality check of the data was performed by analysing scatter plots of the measured and preliminarily computed water levels. The left panel of Figure 3.1 shows an example of the scatter plot of the measured (horizontal) and modelled (vertical) water level at station Calais before (left) and after (right) the erroneous data is masked. The circle-shaped pattern in the left panel corresponds to a phase shift during a short period. The highest observed values (>6m) are the result of invalid measured values (constant water level). Furthermore, the scatters that deviate a lot from the line y=x (modelled=observed) can be seen as outliers. By checking the corresponding moments in time in the quality-check program, a lot of these erroneous data points have been masked.
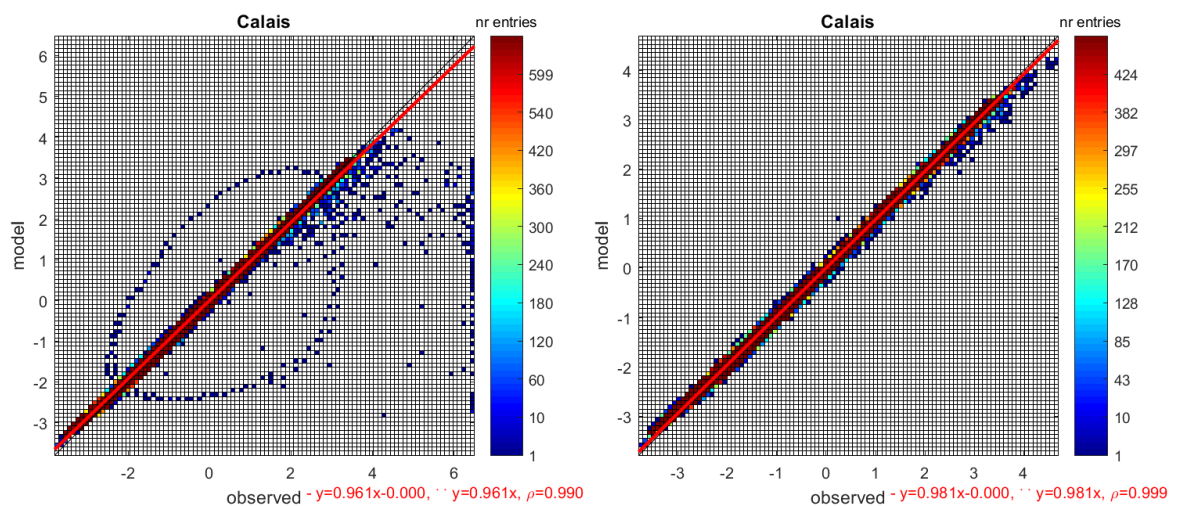
Figure 3.1   Scatter plots of the measured (horizontal) and modelled (vertical) water level at station Calais before (left) and after (right) the erroneous data is masked.

3.2.2.5   *Phase error Dutch offshore platforms (AWGPFM, K14PFM, L9PFM)*
In the comparison of the observed and modelled water level data, it was found that the representation of the water levels at the location of three offshore platforms (AWGPFM, K14PFM and L9PFM) was noticeably different compared to surrounding offshore monitoring stations. The error is caused by the tidal component of the water level signal, the quality of the surge component is comparable to those of the adjacent observation locations (cf. Figure 3.2). As the quality with which tides are reproduced in the Dutch offshore waters is quite uniform, the observation data at these three offshore platforms appears to contain some error. A tidal analysis showed that the difference between the measured and modelled tides are mainly caused by a phase error. This indicates that the timing of the measurement data might be (slightly) off. The water level data of these three Dutch offshore platforms are therefore not considered in the model calibration/validation.
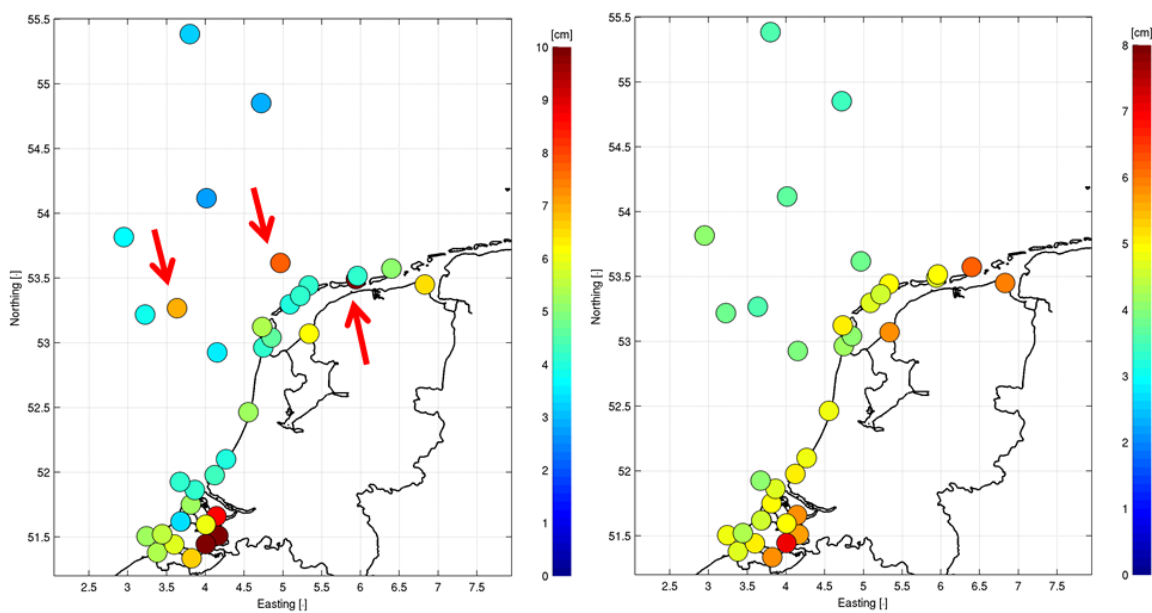
Figure 3.2   Quality of the tide (left) and surge (right) representation of a preliminary version of DCSM-FM. The red arrows indicate the three tide gauge stations which exhibit a phase error.
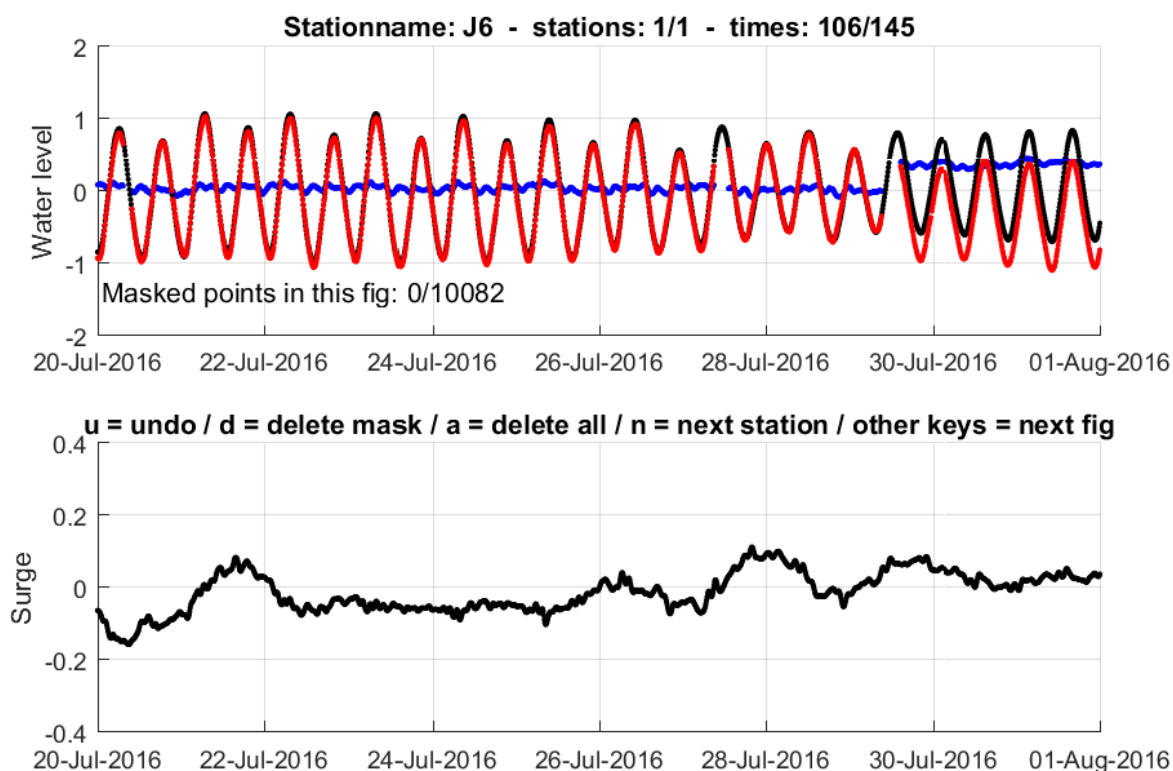
Figure 3.3   Change of vertical reference level at station J6
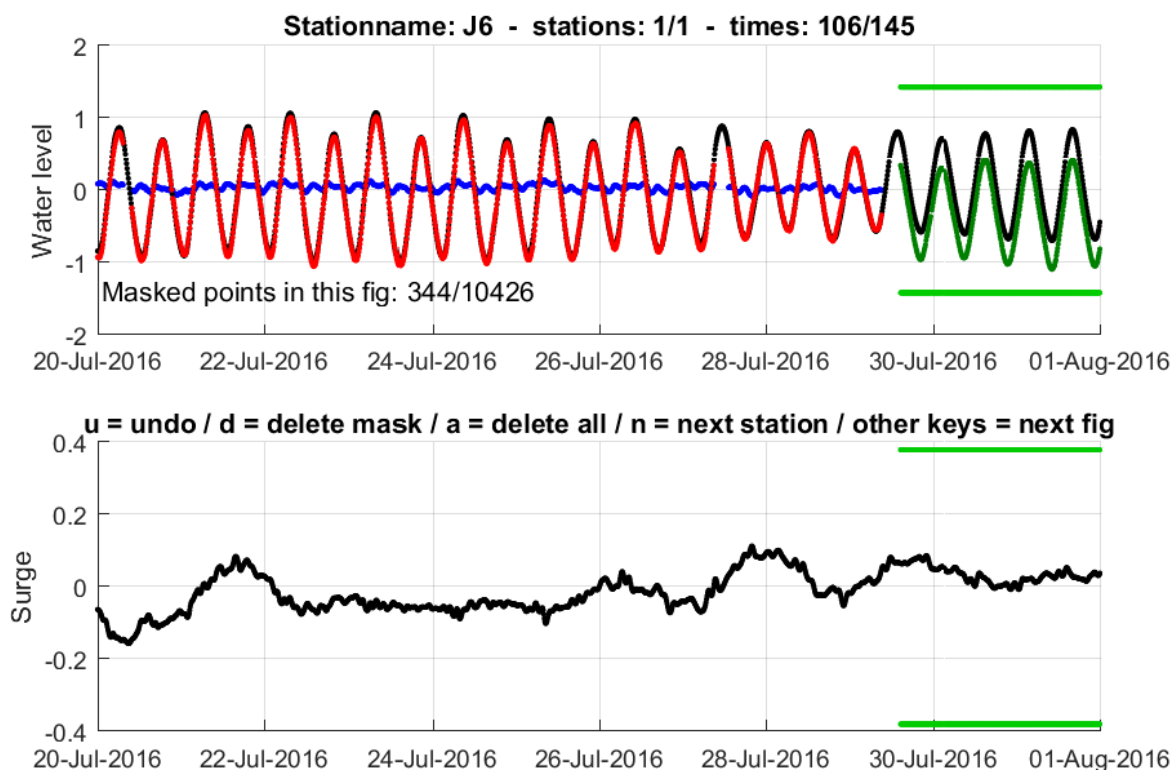
Figure 3.4   Change of vertical reference level at station J6 – Green indicates the masked data
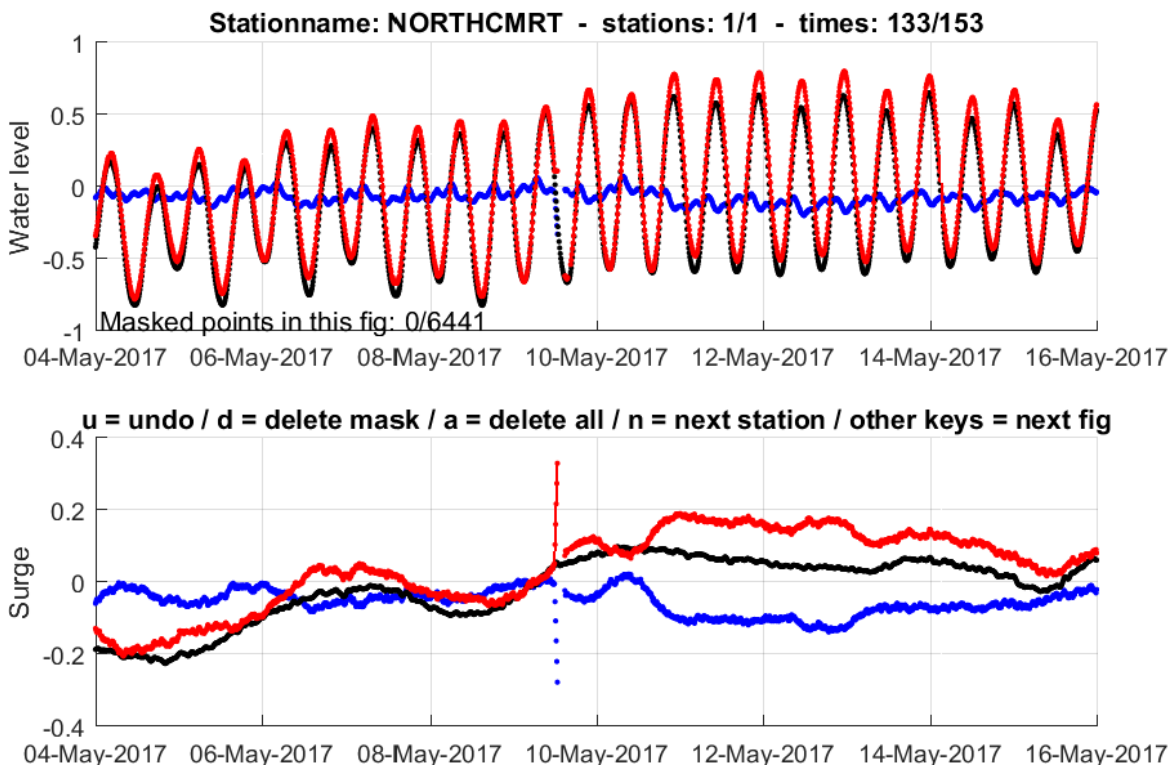
Figure 3.5   Horizontal water level at station NORTHCMRT
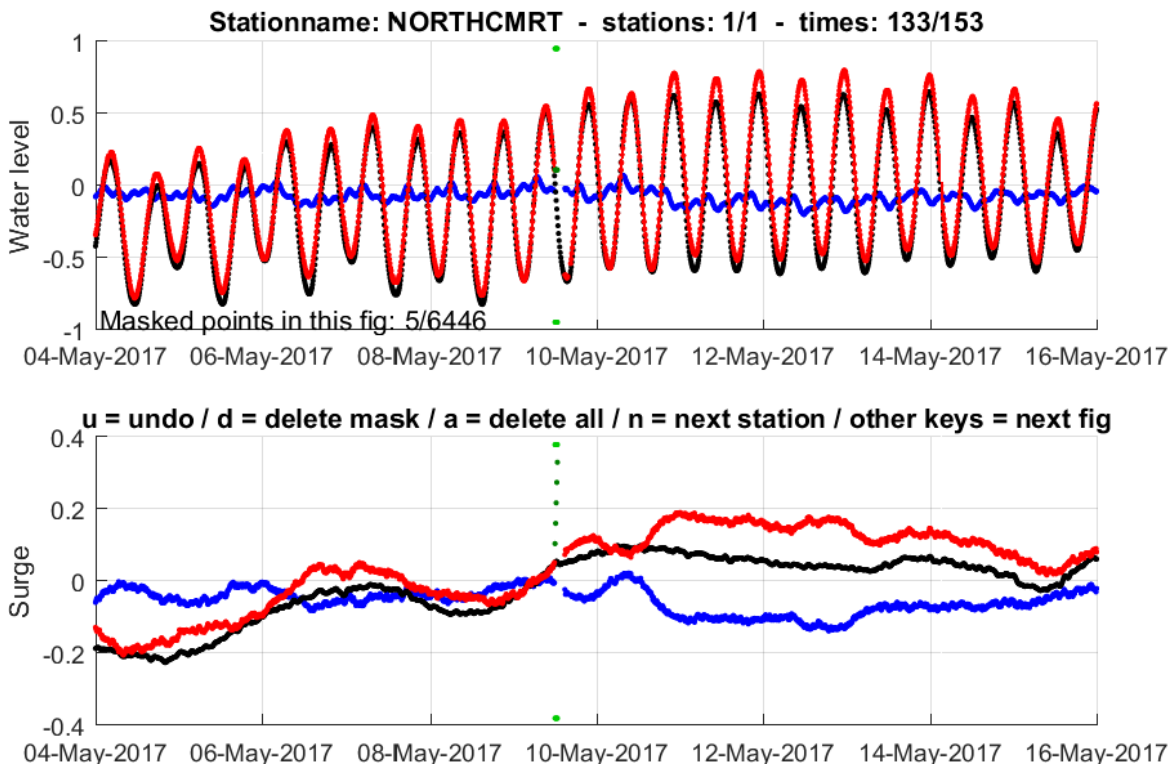
Figure 3.6   Horizontal water level at station NORTHCMRT – Green indicates the masked data
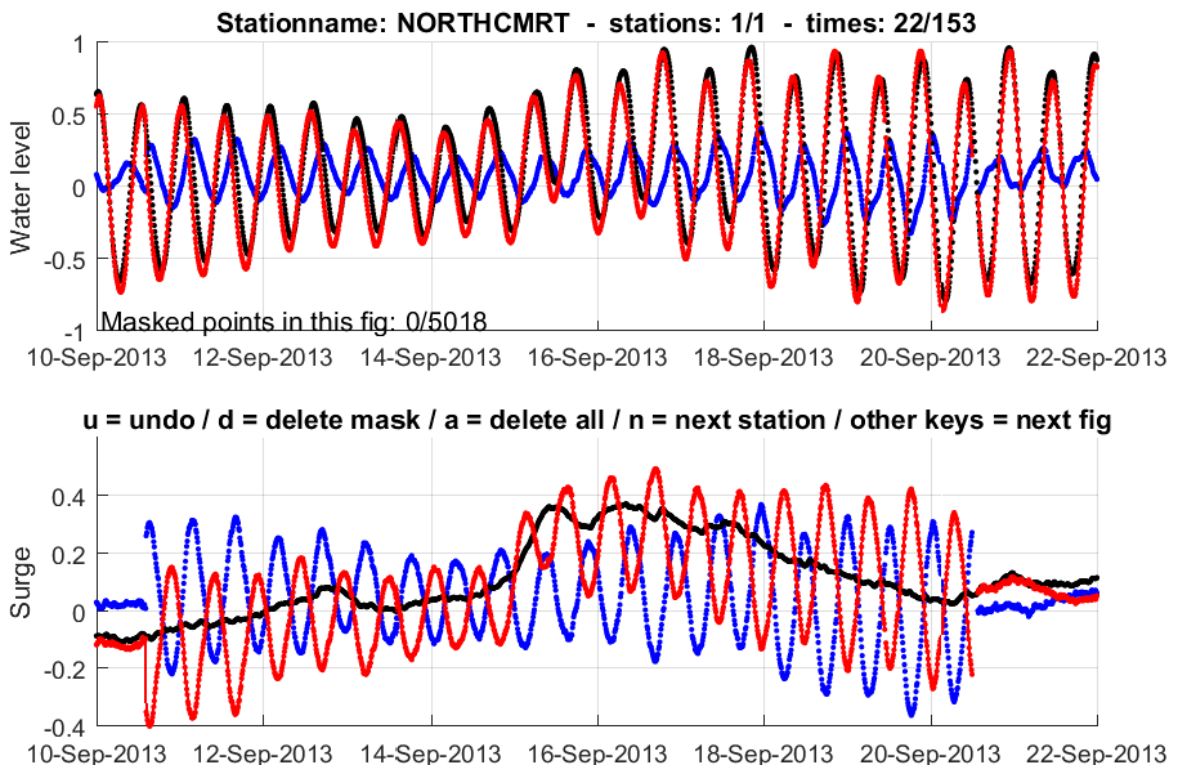
Figure 3.7   Horizontal water level at station NORTHCMRT
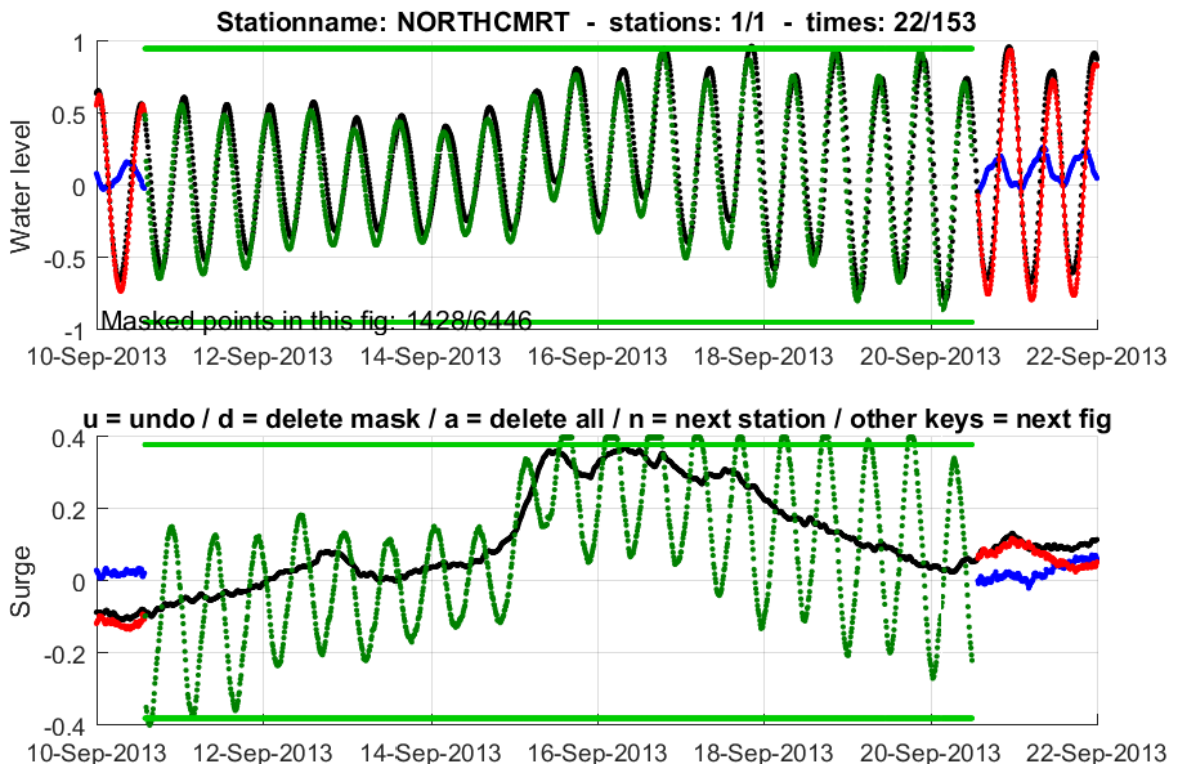
Figure 3.8   Horizontal water level at station NORTHCMRT – Green indicates the masked data
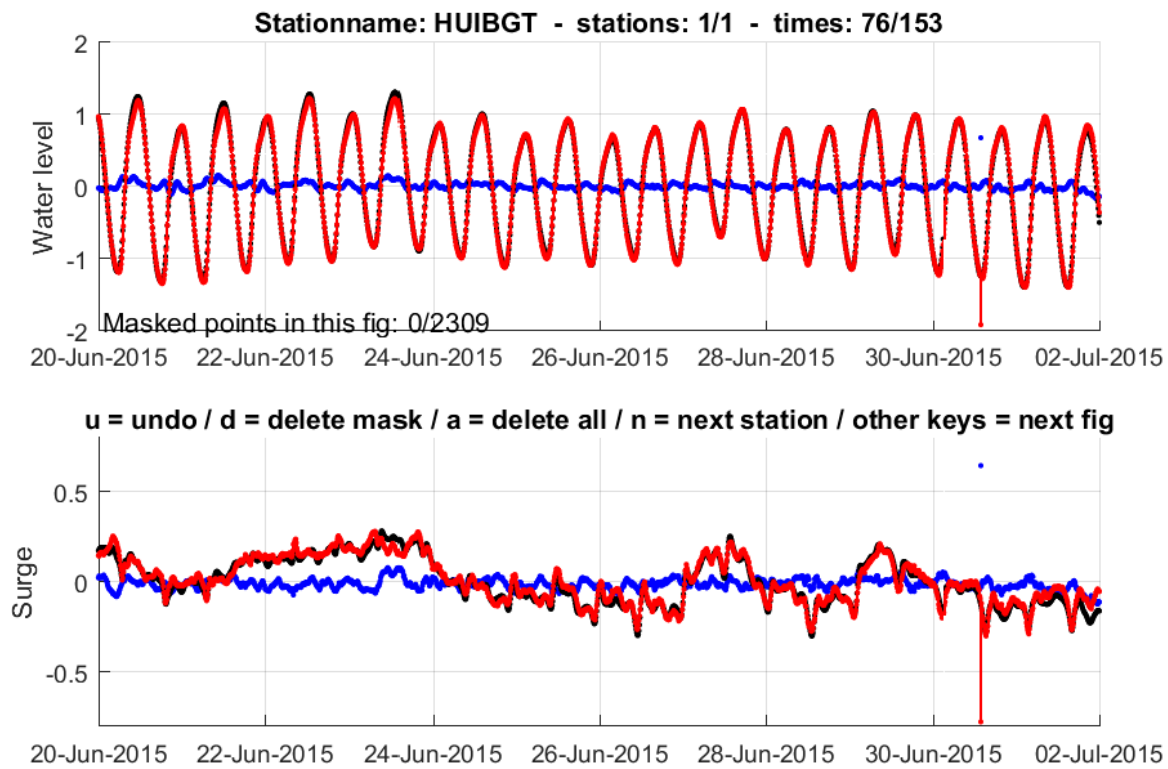
Figure 3.9   Sudden (negative) water level peak at station HUIBGT
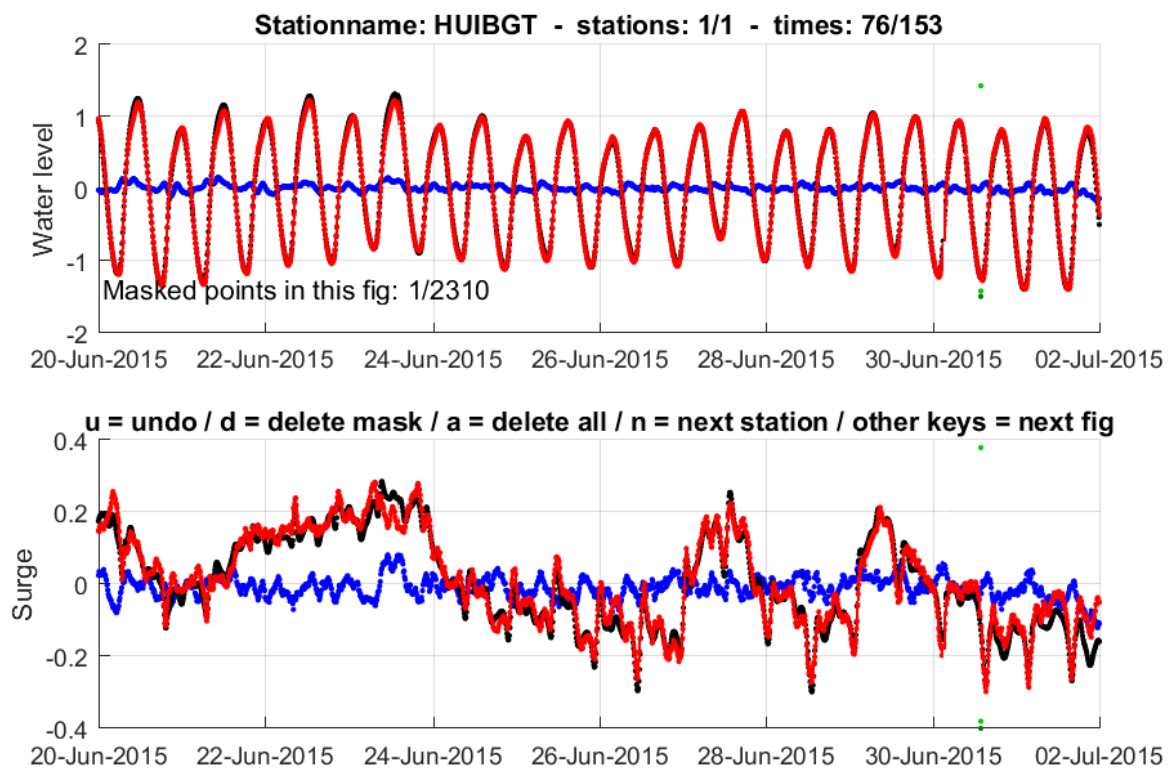
Figure 3.10 Sudden (negative) water level peak at station HUIBGT– Green indicates the masked data

3.3 Tide gauge locations used for the model calibration and validation
After collecting, selecting, merging and quality checking of the water level data, the resulting dataset consists of water level data from 205 tide gauge locations. In these stations water level data is available in the validation period 2013-2017. Furthermore, the model resolution is sufficient to at least reasonably represent these water levels after calibration.

3.3.1 Geographical locations of observation stations
An overview of the 205 tide gauge locations considered for the model calibration and validation is depicted in Figure 3.11. Figure 3.12 shows the observation locations along the Dutch and German Wadden Sea, Skagerrak and Kattegat in more detail. A more detailed overview of the monitoring stations used near the Netherlands can be found in Figure 3.13.
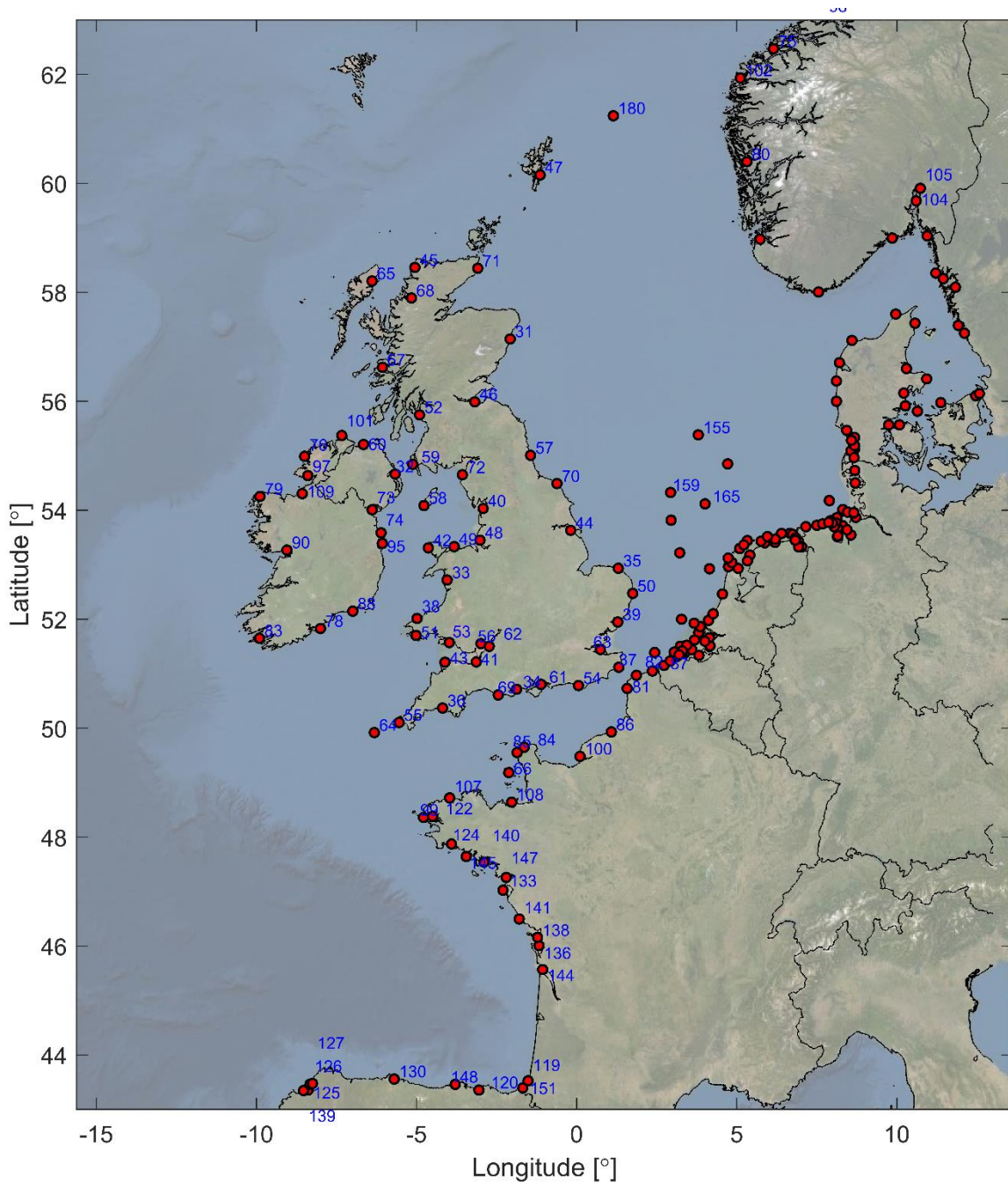
Figure 3.11 Overview of the 205 tide gauge locations used for the model calibration and validation (for the station numbers that are not shown in this figure, see Figure 3.13 and Figure 3.12)

Deltares

Figure 3.12 Overview of the tide gauge locations used for the model calibration and validation
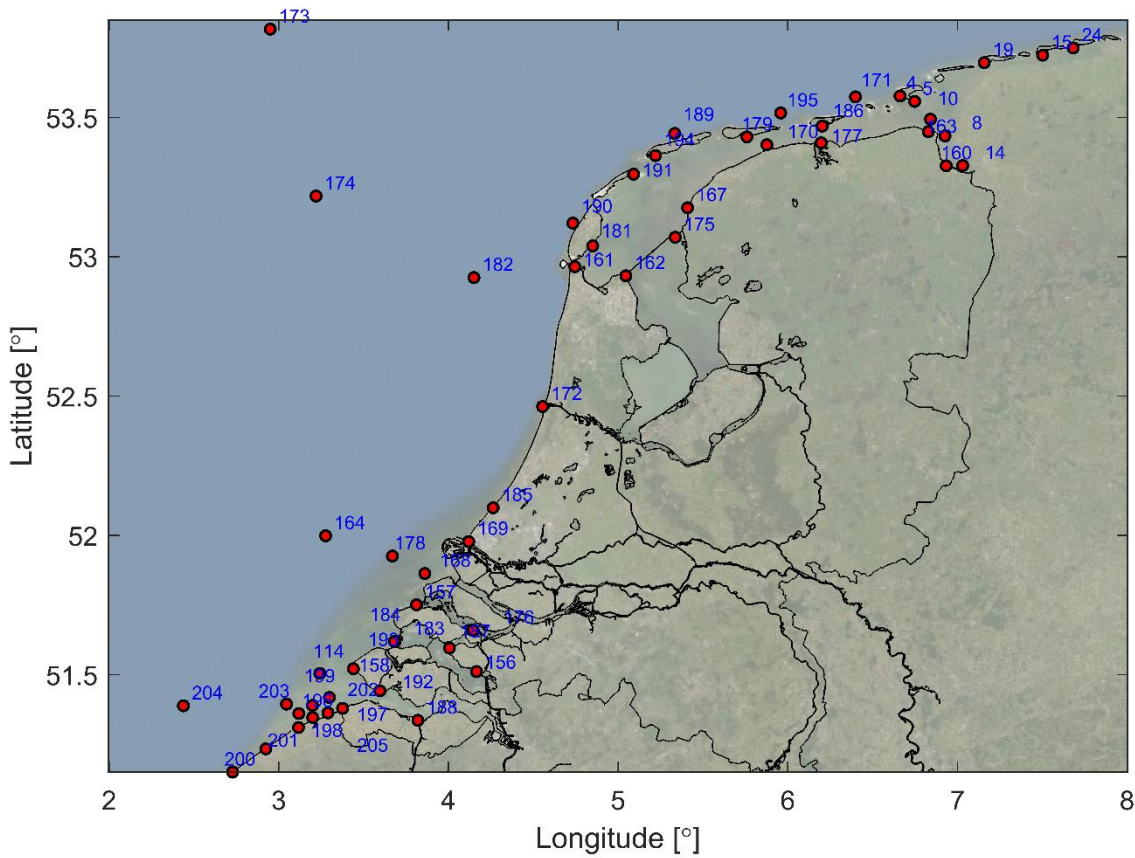
Figure 3.13 Overview of the tide gauge locations used for the model calibration and validation

3.3.2 Temporal availability

The red line in the following figures (Figure 3.14, Figure 3.15, Figure 3.16 and Figure 3.17) shows the temporal availability of data for all tide gauge locations. Each line consists of the station name, data source, station number and availability in the period 2013 – 2018.
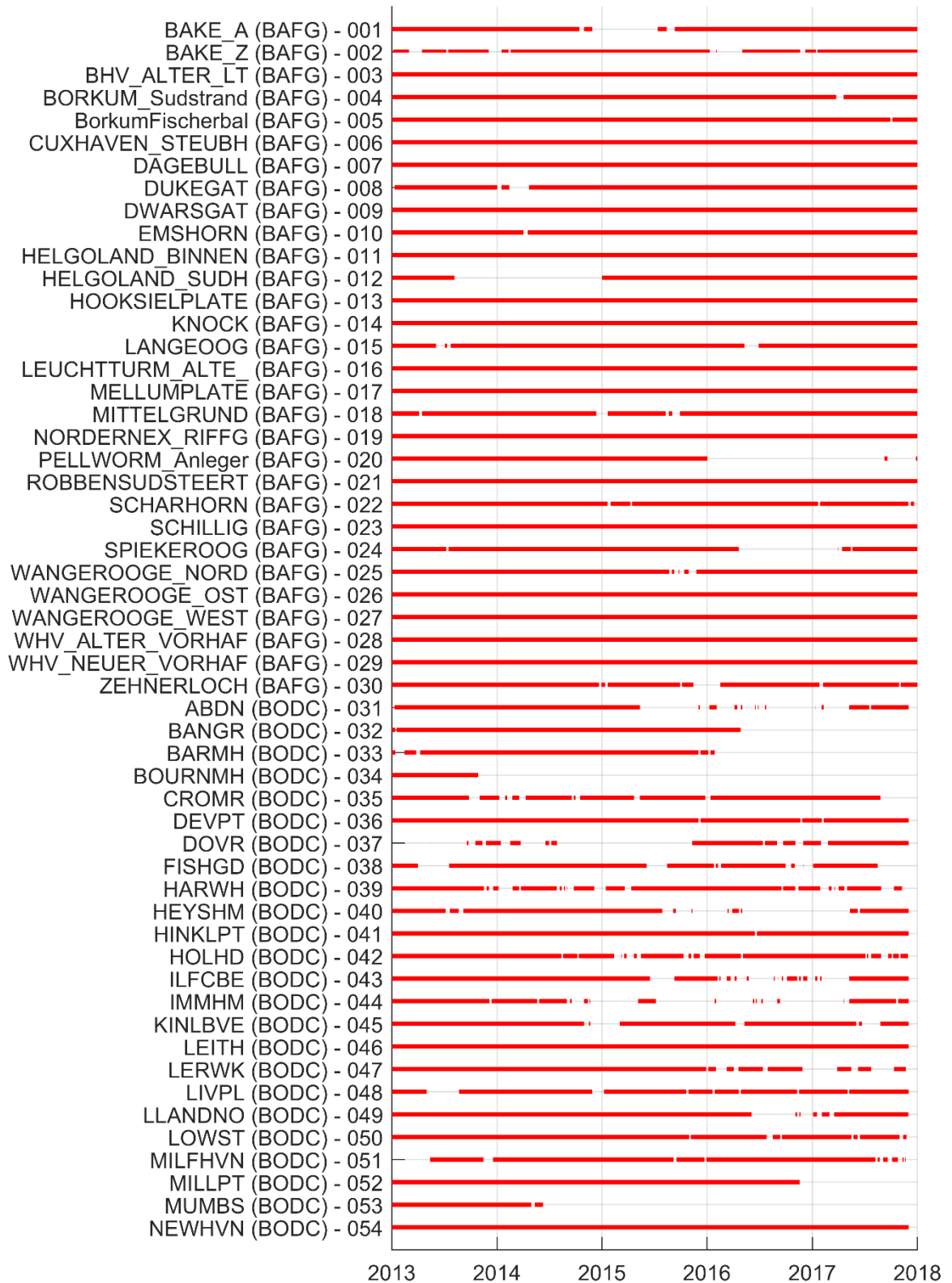
Figure 3.14 Overview of temporal availability of water level data in the period 2013 – 2018 for station numbers 001 – 054
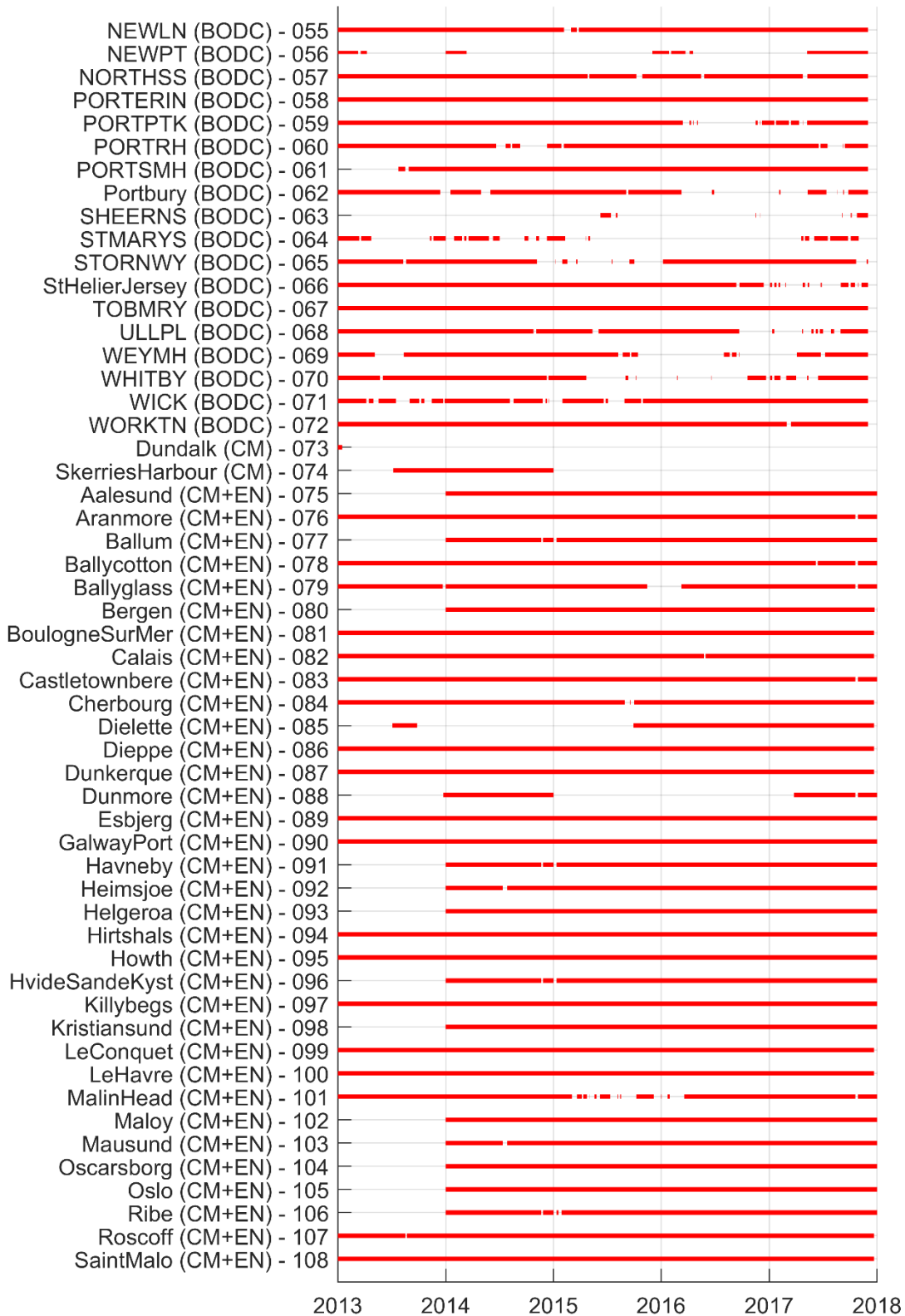
Figure 3.15 Overview of temporal availability of water level data in the period 2013 – 2018 for station numbers 055 – 108 (CM=CMEMS, EN=EMODnet)

Figure 3.16 Overview of temporal availability of water level data in the period 2013 – 2018 for station numbers 109 – 162 (CM=CMEMS, EN=EMODnet, RWS=Rijkswaterstaat)
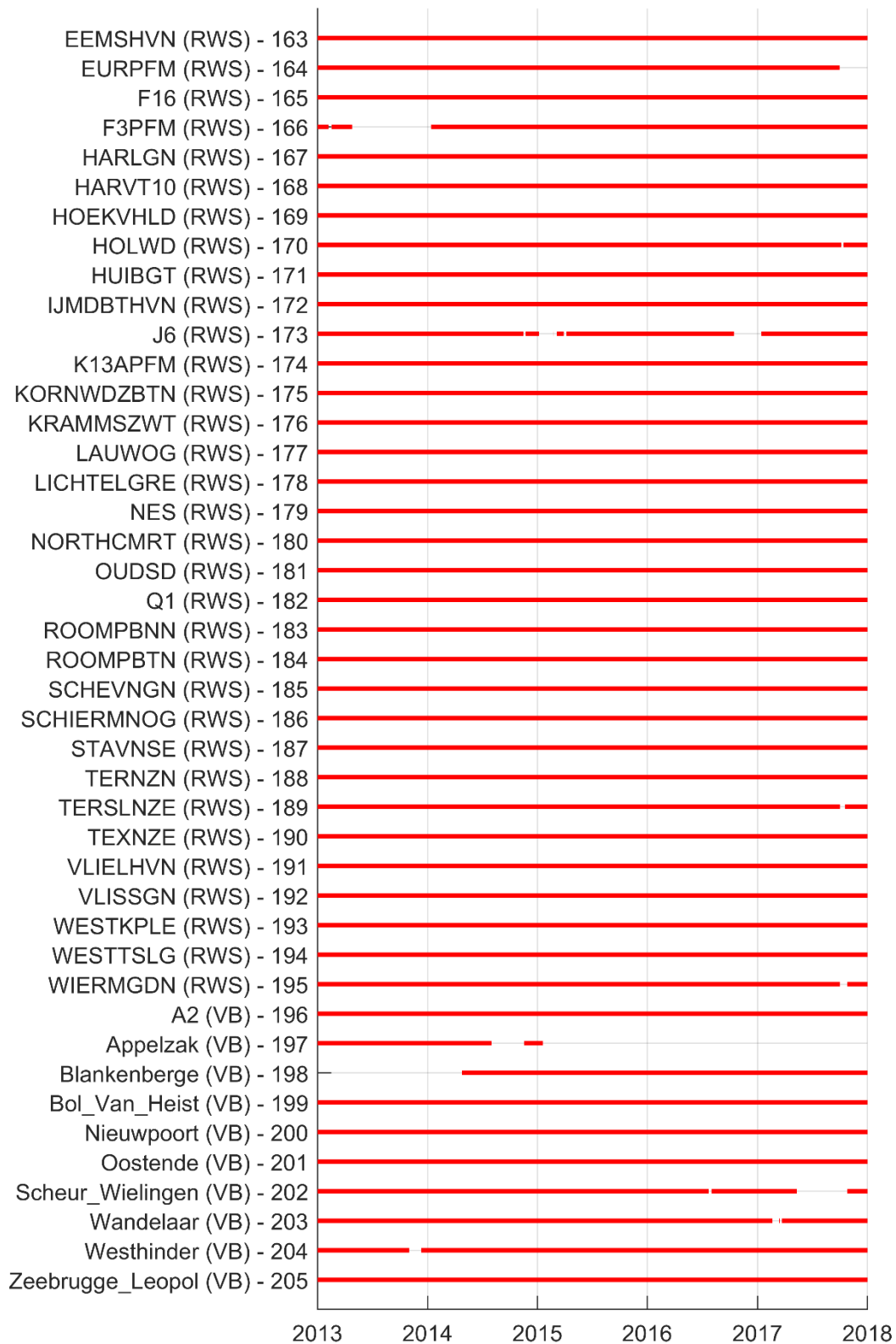
Figure 3.17 Overview of temporal availability of water level data in the period 2013 – 2018 for station numbers 163 – 207 (RWS=Rijkswaterstaat,VB=Vlaamse Banken)

4 Calibration

4.1 Approach

4.1.1 Introduction
Generally, a first simulation with an initial model definition will not lead to an optimal representation of the required parameter (in this case water levels), such as known from measurements. Models contain errors that are generated mainly by errors in the forcing terms (e.g. boundary conditions and meteorological forcing terms), uncertainty in the bathymetry, the model parameters (e.g. bottom friction) and the poorly described or neglected physical processes in the system equations as well as mathematical approximations (e.g. unresolved sub-grid scale motions and exchange of momentum with the atmosphere). In order to reduce the uncertainty of the model parameters and parameterisations used, an automated calibration using the DUD (Doesn't Use Derivative) algorithm (Ralston and Jennrich, 1978) available in the open source data assimilation toolbox OpenDA (version 2.3.1.834) has been performed. This derivative-free algorithm for non-linear least squares transforms a non-linear least square problem onto a well-known least square problem. DUD evaluates and optimizes uncertain model parameters by minimizing a cost function. The parameter values corresponding to the minimum value of the cost function are considered as the optimal parameter values for the given problem. The general methodology followed is similar to the one used for the calibration of the previous generation models DCSMv6 and DCSMv6-ZUNOv4 (Zijl et al., 2013).

4.1.2 Period
It is important to assess model results against sufficiently long measurement series which include all relevant physical processes: e.g. spring and neap tide, various (seasonal) wind patterns, etc. Computing longer periods prevents optimization for specific, unrepresentative events, which would lead to a deterioration of the predictive value of the model.

For the final calibration the entire year of 2017 is therefore used, preceded by a 10-day spin-up period. The use of an entire year is required since the annual modulation of the M2 tide cannot be properly represented in a 2D barotropic model. Optimization for a shorter period would result in an over- or underestimation of dissipation through bottom friction.

4.1.3 Observation data used
The measurement stations described in Chapter 3, with data in the calibration period, have been used for calibration. Accounting for stations without measurements data in the calibration period, a total of 195 stations were eventually used.
The measurements (and model output) were provided with a 60-minute interval because of computer memory restrictions.

Removal of data (thresholds)
In some tide gauge stations, the representation of especially the low waters is negatively affected by the poor resolution of the model in some areas. If these measurements are included in the calibration, this would negatively influence the results. An option could be to exclude these stations altogether from the calibration. While this is done for some stations, for others where the higher water levels are well represented in the model, it was decided to just remove the water level measurements below a certain threshold. This threshold is determined by

making scatter plots of the modelled and measured total water levels, and visually determining from which level the model accuracy is sufficiently accurate. An example for station Nes is presented in Figure 4.1.
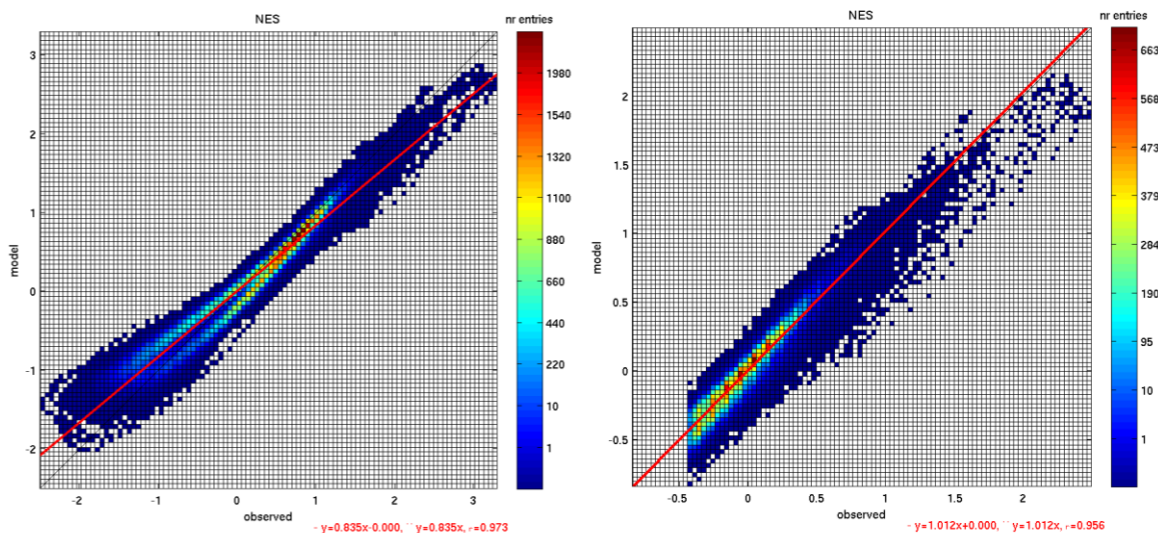
Figure 4.1 Scatter plots of the measured (horizontal) and modelled (vertical) water level at station Nes before (left) and after (right) water levels below the provided threshold are removed.

The resulting thresholds, which will be taken into account in both the calibration and validation, are presented in Table 4.1 and visually shown in Figure 4.2. Note that the thresholds are prescribed relative to MSL, which is determined before the removal of the water levels below the threshold. This causes an apparent mismatch between the threshold in Table 4.1 (Nes: 0.5 m +MSL) and the lowest observed water level in the Figure 4.1 (right; around -0.4 m +MSL);

Table 4.1 Threshold values relative to MSL below which water level measurements are not taken into account during calibration or validation.

Station name	Threshold (m +MSL)	Station name	Threshold (m +MSL)
Ballum	0.5	KNOCK	0.0
BayonneBoucau	-1.0	KORNWDZBTN	-1.0
BHV_ALTER_LT	1.0	LAUWOG	0.5
Brons	0.5	Mando	0.0
Dagebull	-0.5	Nes	0.5
DELFZL	0.0	NEWPT	-1.0
DENOVBTN	0.0	Portbury	1.0
DEVPT	-2.0	PORTSMH	0.0
Dundalk	0.5	ROBBENSUDSTEERT	0.0
Esbjerg	-0.5	SaintNazaire	-2.0
HARLGN	0.5	SCHIERMNOG	0.5
Havneby	0.5	Vidaa	0.0
HOLWD	1.0		
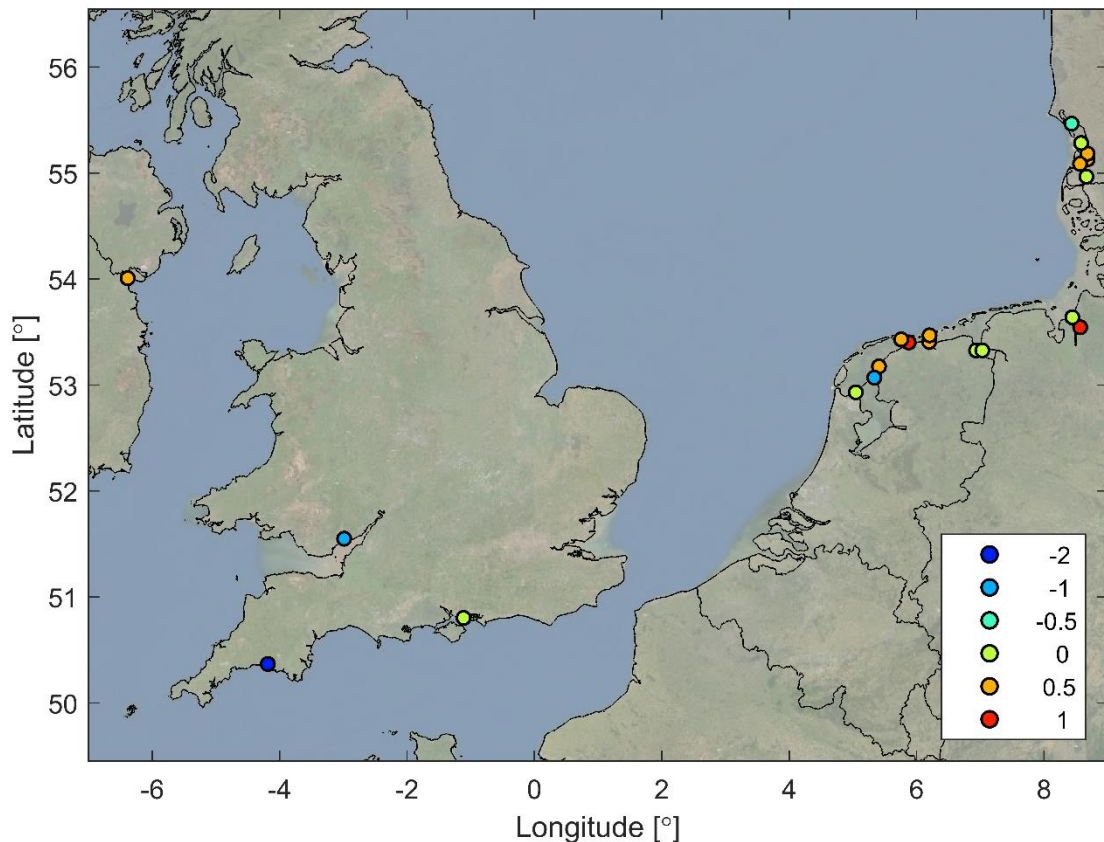
Figure 4.2   Threshold values relative to MSL below which water level measurements are not taken into account during calibration or validation (thresholds for station Bayonne Boucau and Saint Nazaire are not shown).

4.1.4   Cost function and weights

DUD is a derivative-free algorithm for nonlinear least squares that minimises a quadratic cost function by adjusting model parameters. DUD should be initialised with one unperturbed run and n sensitivity run, where n is the number of control parameters.

For the present calibration we have used a quadratic cost function over the complete total water level time series. It is essentially the total sum of squares, made dimensionless with the measurement uncertainty.

In the quadratic cost function minimised during the experiments, the bias between computed and measured water levels is ignored, since this bias is hardly related to the uncertainty in the control parameters, but mostly caused by physical (e.g. baroclinic) processes not considered in this model.

Since the primary focus of this model is the accurate representation of water levels in Dutch waters, additional weight in the cost function has been given to Dutch coastal stations (by a factor 16). This is done by decreasing the uncertainty of the measurements that is specified for each station in the OpenDA-DUD input files. In addition; the WMCN-kust main locations have their weight increased by a factor 4. Stations along the North Sea coast of the UK have their weight increased by a factor 2. This is because of the importance of this region for the correct propagation of the tide towards the Dutch coast. Station in the Skagerrak and Kattegat on the

other hand have been given a reduced weight (by a factor 0.5). In addition, stations which are poorly represented in the model compared to neighbouring stations (but nonetheless retained in the calibration) have also been given a reduced weight. This holds for example for the Dutch Wadden Sea and estuarine stations, as well as stations like Sheerness, where the generation of the complex higher harmonics is hampered by a poor representation of the relatively variable bathymetry. The resulting weights are visually presented in Figure 4.3 for the entire model area, and in Figure 4.4 focussing on Dutch waters.
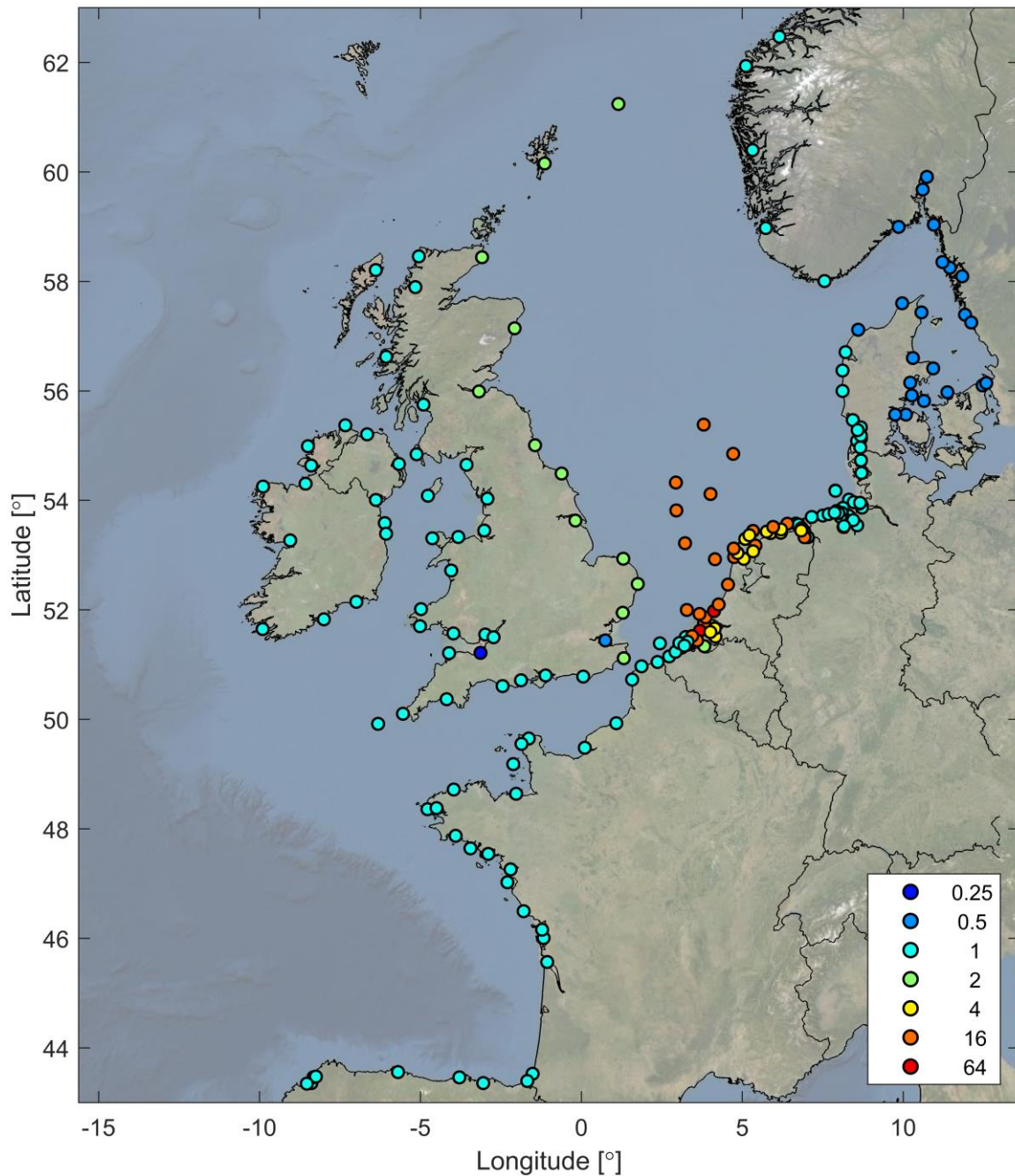
Figure 4.3   Relative weight given to a station in the OpenDA-DUD cost function
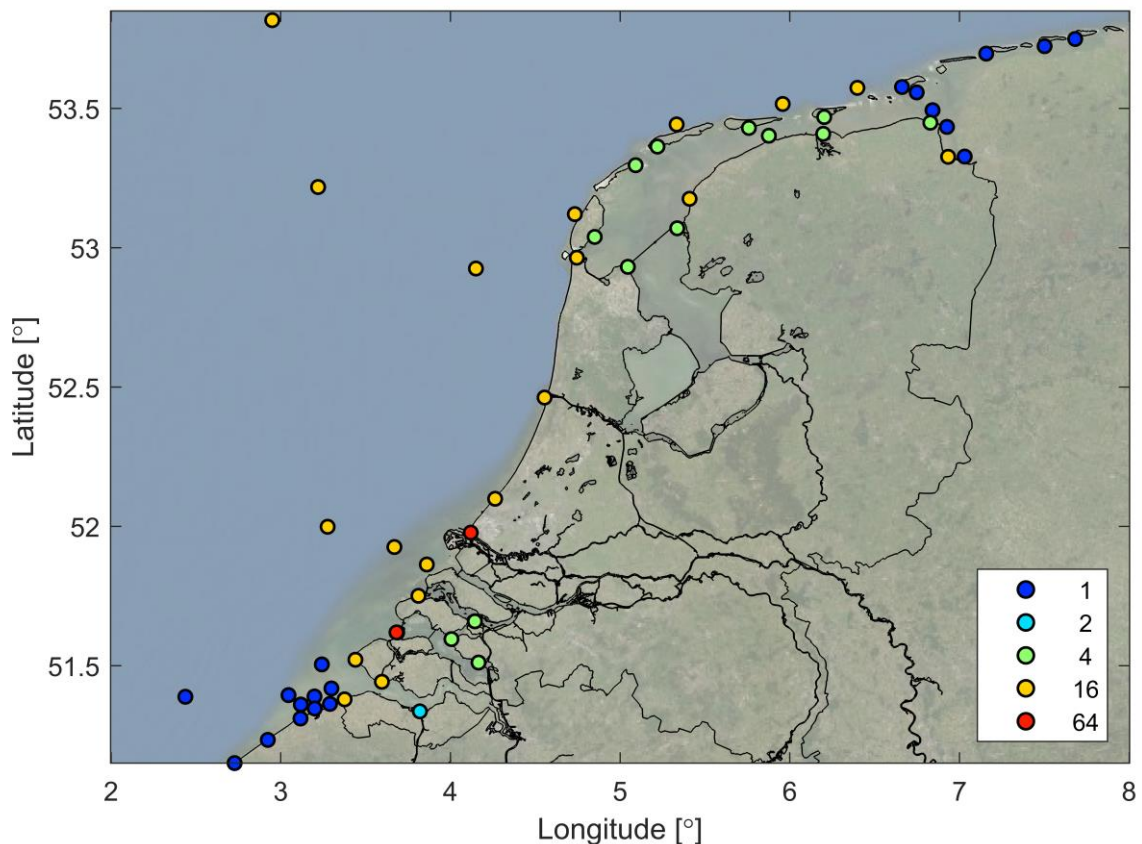
Figure 4.4   Relative weight given to a station in the OpenDA-DUD cost function

4.1.5   Calibration parameters

During the development of the previous generation models for the North Sea uncertainty in both bathymetry and bed roughness coefficients has been reduced during calibration to achieve optimal model representation of water levels (Zijl et al., 2013). At the time, the adjustment of bathymetry was necessary because an M2 phase lag of 15-20° occurred in the uncalibrated model. This phase lag could not be reduced sufficiently by adjusting the bottom roughness.

The use of an improved bathymetry, to a large extent derived from EMODnet (section 2.4), might remove the need to adjust bathymetry during the calibration. To test whether this is the case an experiment was performed with a coarsened, uncalibrated version of DCSM-FM. The coarsening to a minimum grid size of ~1nm was done since the NOOS bathymetry (as used for the previous generation model DCSMv6) has a resolution of ~1 nm x 1 nm. The uniform roughness prescribed in the experiment is 0.028 s/m$^{1/3}$. The results in Figure 4.5 show that the average phase lag along the Dutch coast of 19° with the NOOS bathymetry reduces to 0° with the EMODnet bathymetry. The M2 amplitude also improves, but further improvement is possible with adjustment of the bottom roughness.

These results are used as a justification for excluding the bathymetry and retaining bottom roughness as a calibration parameter in the present model development. Note however that significant bathymetry errors are known to remain in the EMODnet bathymetry dataset (October 2016 version).
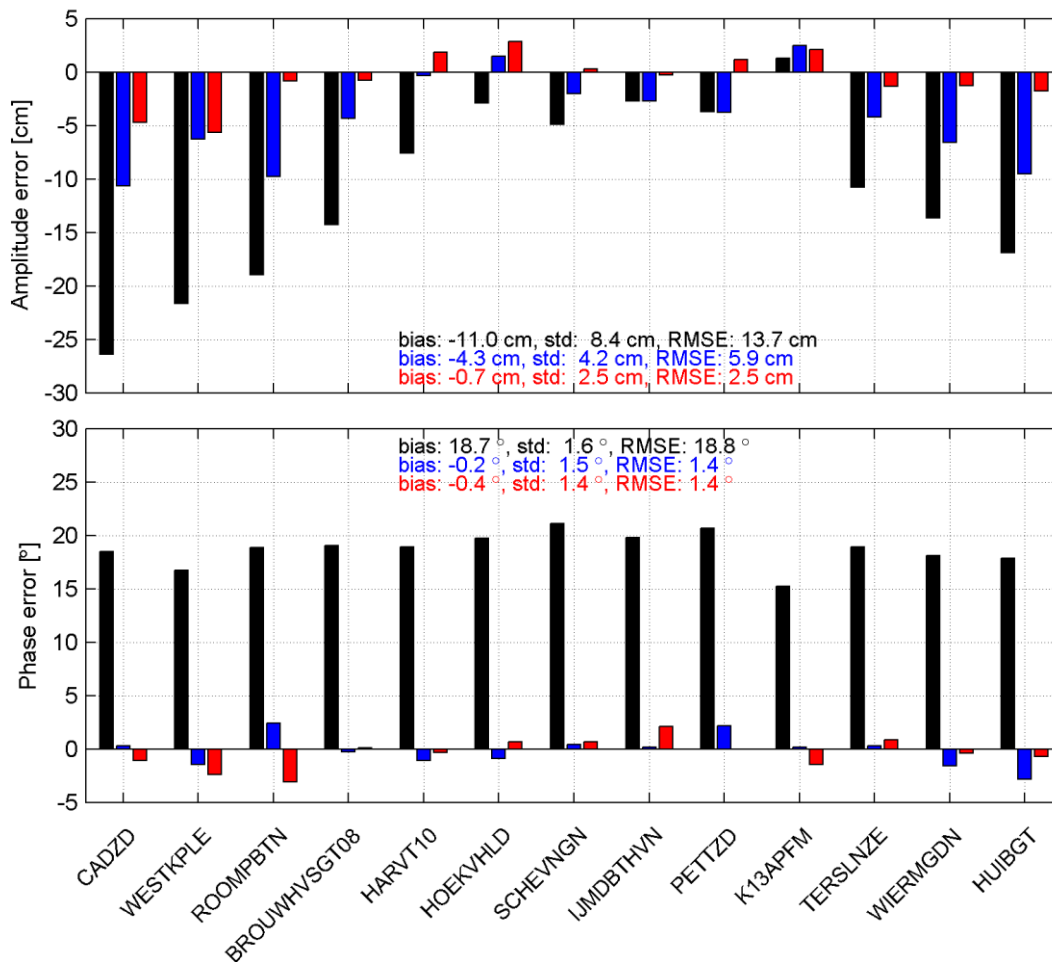
Figure 4.5 M2 amplitude error (upper plot) and phase error (lower plot) using NOOS bathymetry and uniform roughness (black), EMODnet bathymetry and uniform roughness (blue) and EMODnet bathymetry with limited spatially varying roughness calibration (red). The model used is a coarsened version of DCSM-FM with a minimum grid size of ~1nm.

4.1.6 Roughness area distribution

Practically it is not possible to adjust the bottom roughness in each network node since far too many parameters would then have to be estimated in proportion to the available amount of measurement data, which would lead to the problem of identifiability. Therefore, our approach is to specify larger sections as adaptation parameters. These sections are defined as samples with a section number. During the calibration OpenDA-DUD prescribes a uniform adjustment factor to each section, after which these values are interpolated on the network using triangular interpolation. By leaving a distance between the prescribed samples a smooth transition in the resulting bottom roughness is ensured.

After many experiments with various measurement stations, thresholds and number and location of roughness sections, a final set of 60 roughness sections has been chosen. Within these sections an initial bottom roughness of 0.028 $s/m^{1/3}$ is prescribed and deviations between 0.012 $s/m^{1/3}$ and 0.050 $s/m^{1/3}$ are allowed during calibration. On overview of the final roughness sections (samples) is presented in Figure 4.6. In Figure 4.7 and Figure 4.8 the sections in the German Bight and Dutch waters are shown in more detail.

Figure 4.6   Overview of samples used to define roughness adjustments. Each color represents a different calibration area.
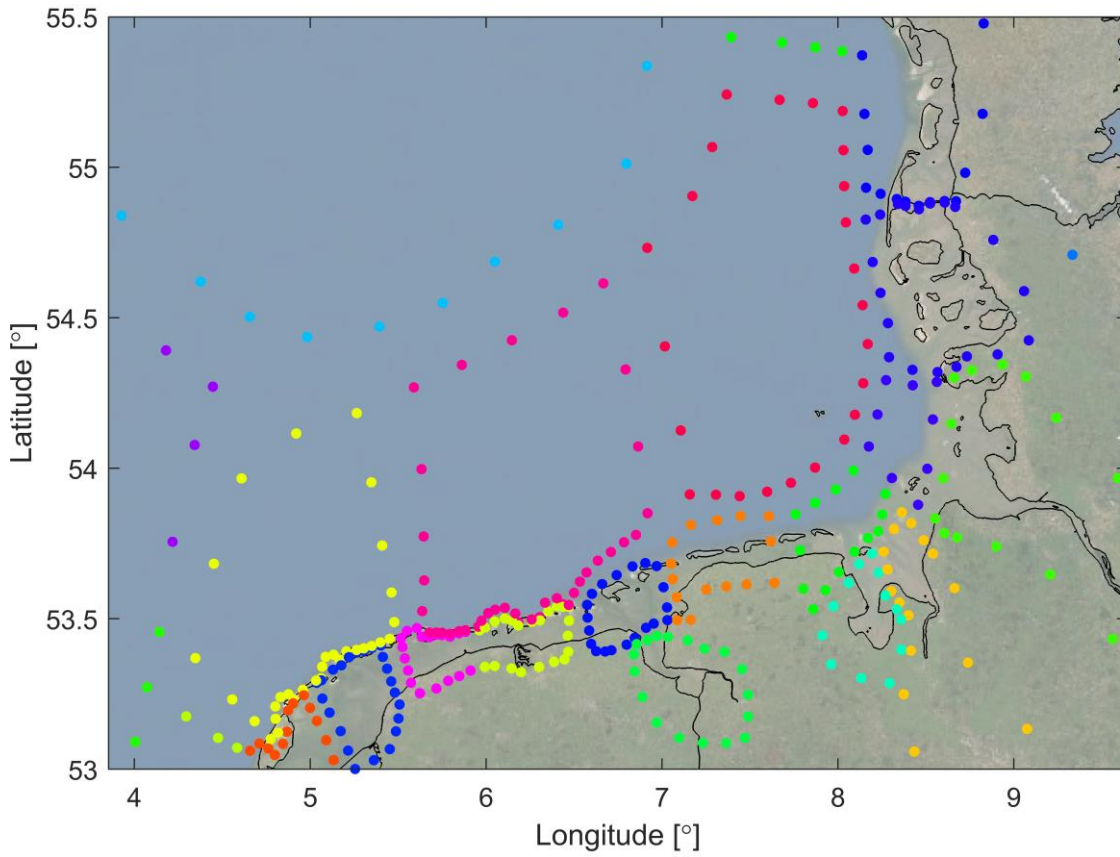
Figure 4.7   Samples used to define roughness adjustments in the German Bight. Each color represents a different calibration area.
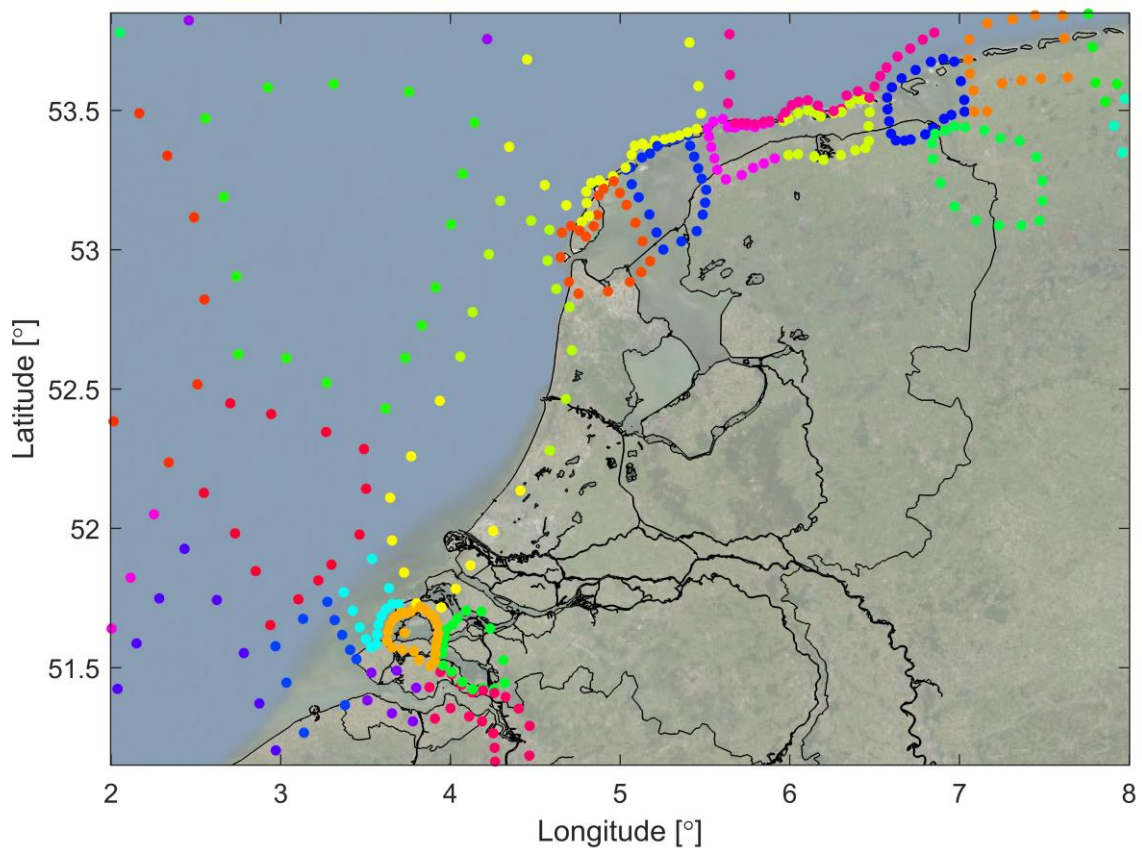
Figure 4.8   Samples used to define roughness adjustments in Dutch waters. Each color represents a different calibration area.

4.2   Calibration results

Various calibration experiments have been performed, with increasing computation length and varying number and shape of the roughness areas. The final calibration experiment, using 60 roughness areas and covering the entire year 2017 is described in this section. For this experiment the initial roughness perturbation for all roughness areas was set to 5% of the initial roughness. With a uniform initial roughness of 0.028 s/m$^{1/3}$ this translates to a perturbation of 0.0014 s/m$^{1/3}$. The calibrated roughness values were constrained between 0.012 s/m$^{1/3}$ and 0.050 s/m$^{1/3}$.

In Figure 4.9, the calibration process and improvement in cost function is visualised. The uncalibrated (unperturbed) run with an initial, uniform roughness value of 0.028 s/m$^{1/3}$, yields a cost function of 17059 (indicated by the yellow dot). The first point on the green line (indicated by the green dot) represents the first guess of the OpenDA-DUD experiment. This already represents an improvement compared to the uncalibrated model (yellow dot) because of earlier experiments. The other small dots on the green line represent the cost function for single perturbations of each roughness area. Once this is known for all roughness areas, the problem is linearized and combinations of adjusted roughness fields are assessed in the optimization (indicated by the blue line) to minimize the cost function.
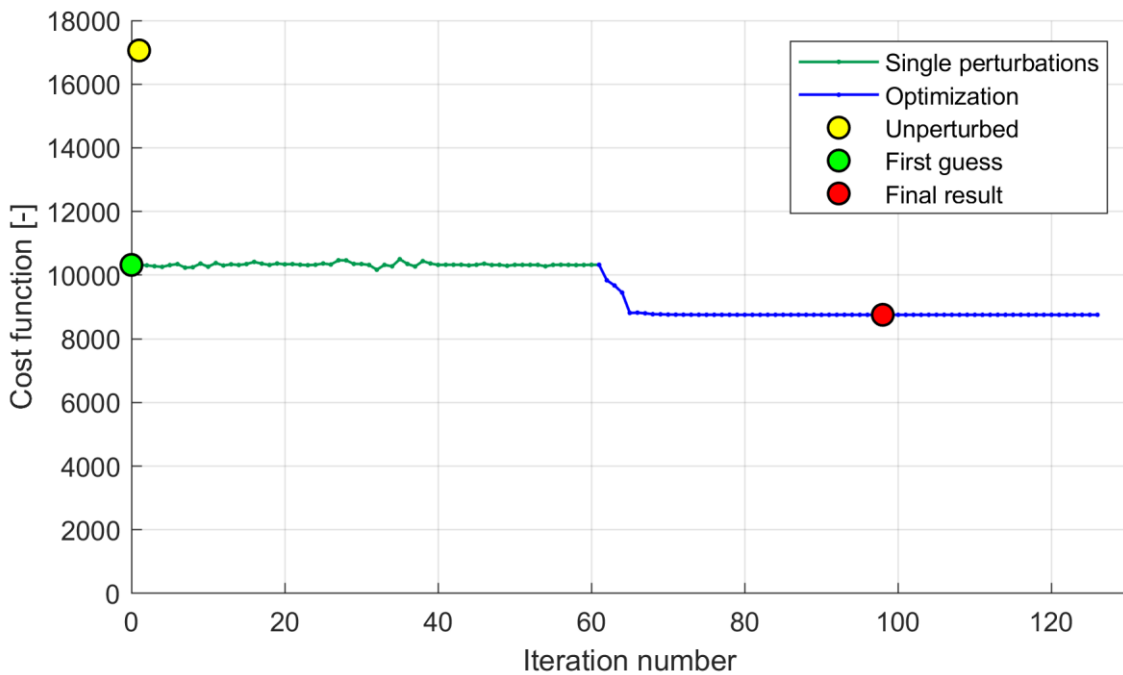
Figure 4.9   Cost function of the OpenDA-dud calibration
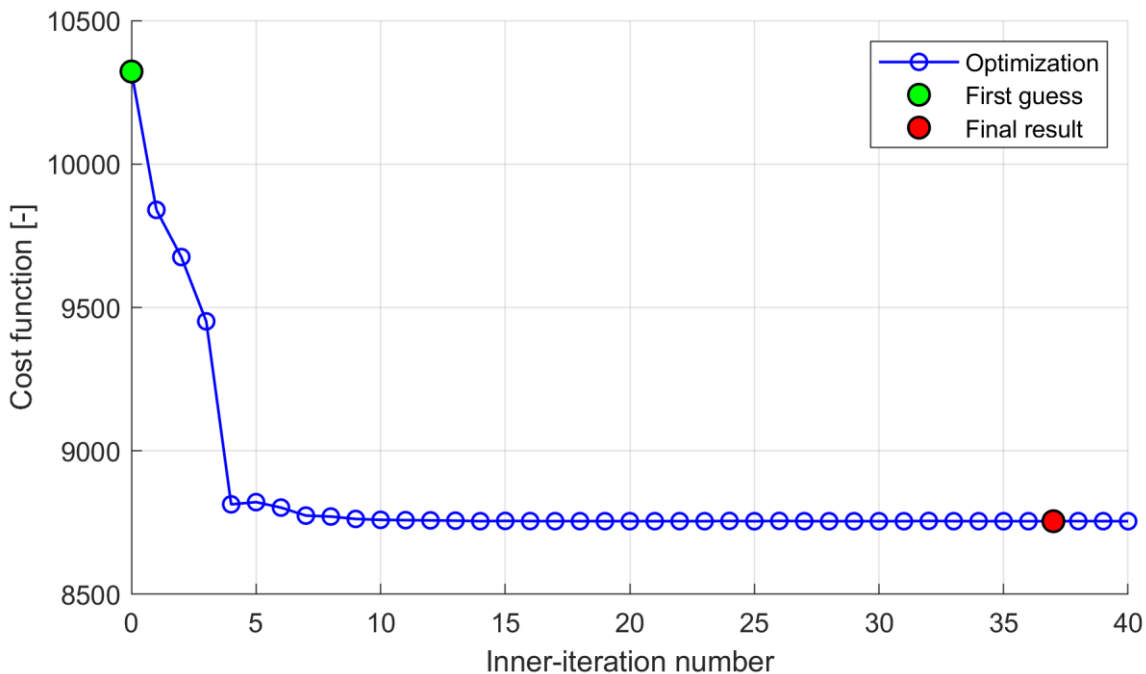
Figure 4.10 Cost function of the OpenDA-dud calibration for the optimization

In Figure 4.10 the iteration part of the optimization is shown in more detail, by leaving out the single perturbations. The green dot represents the first guess of the OpenDA-DUD experiment. This figure illustrates how the cost function reduces substantially during the first four iterations. The iteration with the minimum cost function is picked as the final roughness field, indicated here with a red dot.

During the calibration, the cost function starts at 10322 and reduces to 8755, which is a percentage decrease of about 15%. However, note that this final calibration starts with a roughness field that followed from earlier calibration experiments. The uncalibrated run with an initial, uniform roughness value of 0.028 s/m$^{1/3}$, yields a cost function is 17059. This implies that due to calibration for the bottom roughness a final improvement of 49% is achieved.

The resulting roughness field can be found in section 2.5.

5 Validation

5.1 Introduction

After reducing uncertainty in the bottom roughness by means of an OpenDA-DUD optimization for the year 2017 (Chapter 4), the model is validated against shelf-wide measurements for the five-year period 2013-2017. This period includes the significant 5-6 December 2013 storm Xaver (the so-called 'Sinterklaasstorm' in Dutch). For meteorological forcing Hirlam7.2 has been used (cf. section 2.7). The validation results are presented in this chapter.

5.1.1 Quantitative evaluation measures (Goodness-of-Fit parameters)

Time series: total water level, tide and surge

To assess the quality of the computed water levels, the root-mean-square error (RMSE) is computed based on measured and computed total water levels for the entire 2013-2017 validation period. In addition, as it provides further insight in the origins of remaining errors, the tide and surge component are separated from the total water level (see section 5.1.2) and the quality of both tide and surge is assessed separately.

High waters

The validation results will also be assessed on the capacity to accurately hindcast peaks in water level, including the most extreme high waters in the validation period. Minor differences in timing between computed and measured high waters are less critical than a correct representation of the peak water level. Therefore, the vertical difference between each computed and measured high water (approximately twice a day) is computed and based on this, the error statistics can be determined. Measured and modelled high waters are matched if the difference in timing is less than 4 hrs.

The same can be done for the tidal signal derived from measured and modelled water levels, which yields the quality of the tidal high waters. What remains after subtracting these tidal high waters from the total high waters is called the skew surge, i.e. the difference between the peak water level and the astronomical peak. Note that the skew surge is generally lower than the highest 'normal' surge in the hours surrounding the high water peak.

In addition, a subdivision is made between three categories of high water events, based on the height of the measured skew surge:

- events with the 99% lowest skew surge heights,
- events with skew surge heights between 99.0% and 99.8%
- the highest 0.2% skew surges

The latter category represents storm conditions yielding the most extreme skew surge conditions observed in the years 2013-2017. If measurements are complete, this category consists of 8 values, while the first two categories then contain 3492 and 28 values, respectively.

For the total high waters, tidal high waters and skew surge, the bias, standard deviation (std) and RMSE is determined for each of these categories.

Low waters

Since there is also an interest in the accuracy with which low waters are represented (e.g. relevant for water authorities draining into the sea by gravity flow), especially during storm

surges, the error statistics for low waters are also computed. This is done in a similar manner as for the high waters. This also holds for the subdivision in categories. Note that the skew surge on which the event classification is based is then determined for the low waters.

Mean water level

The water levels computed with DCSM-FM (or any other hydrodynamic model) refer to an equipotential surface of the Earth's gravity field. Gradients in baroclinic pressure (i.e. due to density differences) affect the movement of water and can, consequently, affect the long-term mean water level (or Mean Dynamic Topography). However, the density in the model is assumed to be constant and uniform. Furthermore, while tide and surge caused by variations in atmospheric pressure are accounted for at the open boundaries, steric effects (i.e., changes in sea level due to thermal expansion and salinity variations) are not. This affects the representation of the mean water level. Therefore, the bias between measured and computed water levels in each station, determined over the entire five-year validation period, will be disregarded in all Goodness-of-Fit criteria used here. This is achieved by correcting the measurements for this bias before these criteria are determined. Consequently, when considering the entire period, the Root-Mean-Square (RMS) of the error signal is equal to the standard deviation thereof. Another advantage of this approach is that it removes the need to convert all measurements to a uniform vertical reference plane that is valid for the entire model domain.

5.1.2 Harmonic analysis

The separation of the tide and surge contribution to the total water level is done by means of harmonic analysis using the MATLAB package t_tide (Pawlowicz et al. 2002). After obtaining the tide through harmonic analysis and prediction, the surge (or 'non-tidal residual') is obtained by subtracting the predicted tide from the total water level signal.

Since the 18.6-year nodal cycle is assumed to be constant in the harmonic analysis, we restricted the analysis period to one year. This implies that for each year in the 5-year validation period, the harmonic analysis is performed.

Harmonic analysis is only performed when the completeness index of the measurements is larger than 80% and the length of the available measurements within the analysis period is larger than 300 days.

Based on the possibility to separate constituents using a time series of one year, 118 constituents have been selected to be used in the harmonic analysis. Note that the number of constituents used here is much larger than the number of constituents prescribed on the open boundaries of the model (cf. Table 2.1). This is because many more shallow water constituents, such as compound tides and overtides, are generated inside the model domain, especially in shallow areas where non-linear processes become important. At the location of the open boundaries the amplitudes of these additional constituents are generally assumed to be negligible.

Table 5.1   List of harmonic constituents used for harmonic analysis

Component name	Angular frequency (°/h)	Component name	Angular frequency (°/h)
SA	0.0410667	3MS4	56.9523127
SSA	0.0821373	MN4	57.4238338
MSM	0.4715211	ST9	57.5059711
MM	0.5443746	ST40	57.8860712
MSF	1.0158958	M4	57.9682085

MF	1.0980330	ST10	58.0503457
ALP1	12.3827652	SN4	58.4397296
2Q1	12.8542863	KN4	58.5218669
SIG1	12.9271398	MS4	58.9841042
Q1	13.3986609	MK4	59.0662415
RHO1	13.4715145	SL4	59.5284789
O1	13.9430356	S4	60.0000000
TAU1	14.0251729	SK4	60.0821373
BET1	14.4145567	MNO5	71.3668694
NO1	14.4966940	2MO5	71.9112441
CHI1	14.5695475	MNK5	72.4649025
PI1	14.9178647	2MP5	72.9271398
P1	14.9589314	2MK5	73.0092771
S1	15.0000020	MSK5	74.0251729
K1	15.0410686	2SK5	75.0410686
PSI1	15.0821353	ST11	85.4013260
PHI1	15.1232059	2NM6	85.8635634
THE1	15.5125897	ST12	85.9457007
J1	15.5854433	2MN6	86.4079380
SO1	16.0569644	ST13	86.4900753
OO1	16.1391017	ST41	86.8701754
UPS1	16.6834763	M6	86.9523127
2NS2	26.8794591	MSN6	87.4238338
ST37	26.9523127	MKN6	87.5059711
OQ2	27.3509802	2MS6	87.9682085
EPS2	27.4238338	2MK6	88.0503458
ST2	27.5059711	NSK6	88.5218669
2N2	27.8953549	2SM6	88.9841042
MU2	27.9682085	MSK6	89.0662415
N2	28.4397296	ST16	101.9112441
NU2	28.5125831	3MK7	101.9933814
OP2	28.9019670	ST18	114.8476676
H1	28.9430376	3MN8	115.3920423
M2	28.9841043	ST19	115.4741796
H2	29.0251709	M8	115.9364170
MKS2	29.0662415	ST20	116.4079381
LDA2	29.4556253	ST21	116.4900753
L2	29.5284789	3MS8	116.9523127
T2	29.9589333	3MK8	117.0344500
S2	30.0000000	ST22	117.5059711
R2	30.0410667	ST23	117.9682085
K2	30.0821373	ST24	118.0503458
MSN2	30.5443747	ST26	130.4331109
ETA2	30.6265119	4MK9	130.9774856
2SM2	31.0158958	ST27	131.9933813
SKM2	31.0980330	ST28	144.3761465
NO3	42.3827652	M10	144.9205212

MO3	42.9271398	ST29	145.3920423
M3	43.4761564	ST30	145.9364170
SO3	43.9430356	ST31	146.4900753
MK3	44.0251729	ST32	146.9523127
SK3	45.0410687	M12	173.9046254
ST8	56.4079380	ST34	174.9205212
N4	56.8794591	ST35	175.4741796

5.2 Shelf-wide results

A spatial overview of the RMSE-values of the total water level, tide and surge of all shelf-wide tide gauge stations is given in Figure 5.1 and Figure 5.2 (left- and right-hand side panel), respectively.
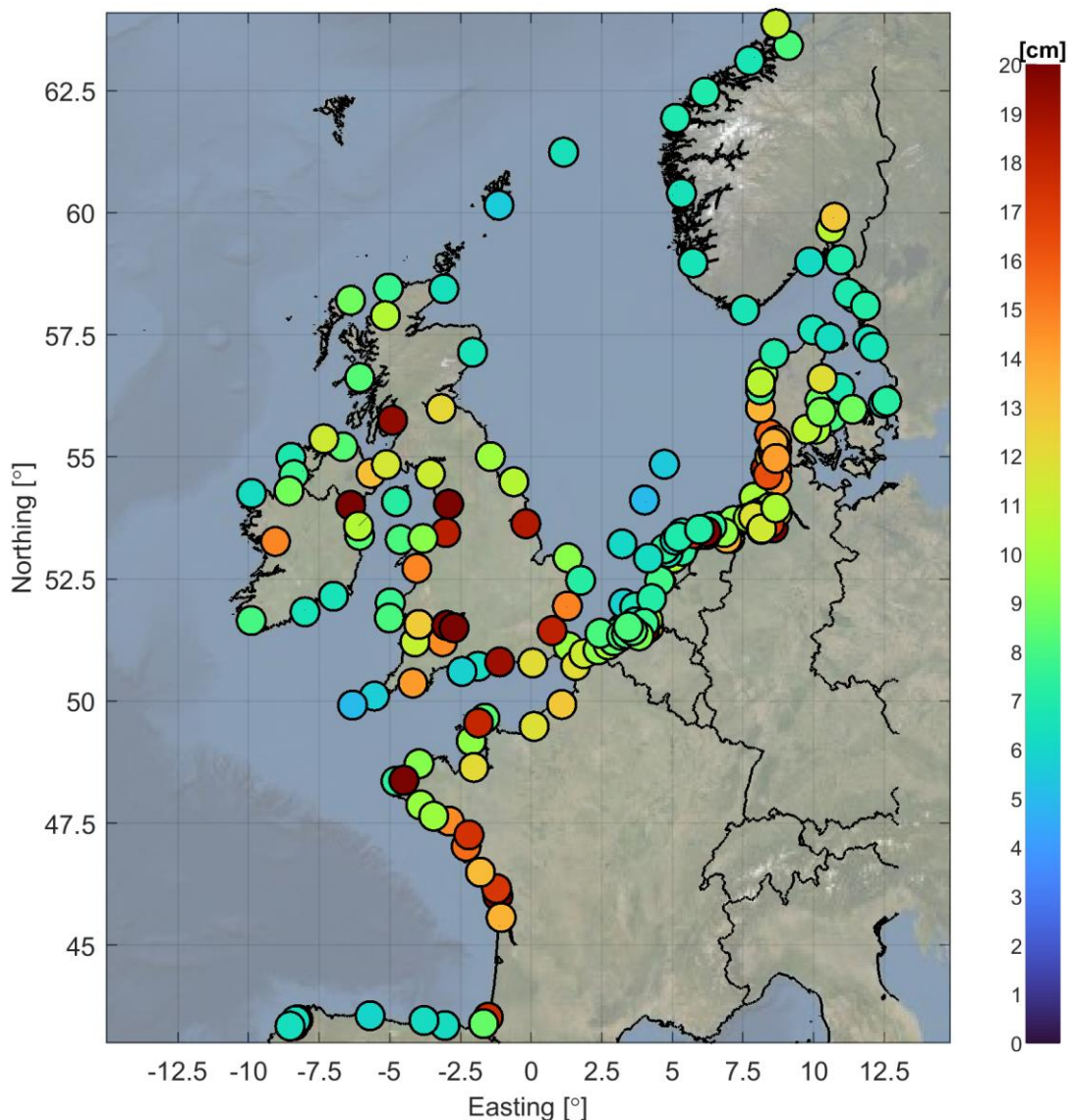
Figure 5.1 Spatial overview of the RMSE-values (cm) of the total water level for the period 2013-2017 of all shelf-wide tide gauge stations
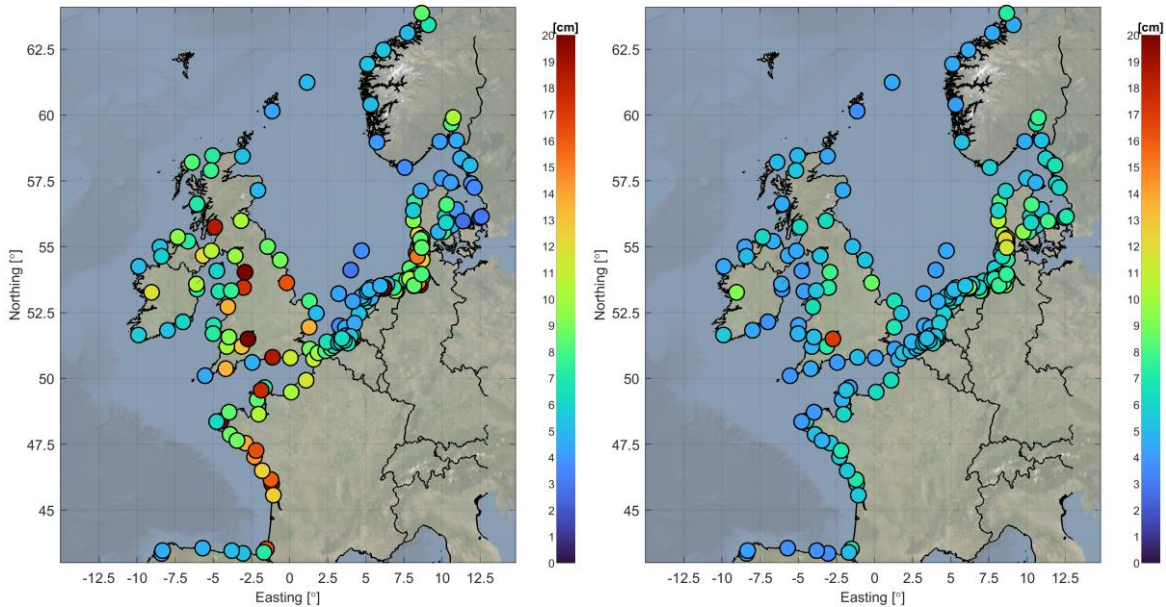
Figure 5.2   Spatial overview of the RMSE-values (cm) of the tide (left panel) and surge (right panel) for the period 2013-2017 of all shelf-wide tide gauge stations

The mean model skill in terms of RMSE for the tide, surge and total water level for all shelf-wide tide gauge stations is summarized in Table 5.2.

Table 5.2   Mean statistics (RMSE in cm) of the tide, surge and total water level for the period 2013-2017 of all shelf-wide tide gauge stations

Stations	RMSE tide (cm)	RMSE surge (cm)	RMSE water level (cm)
Shelf-wide	8.9	6.2	11.1

5.3   Dutch coastal waters

5.3.1   Observation stations

For further analysis of the results, the emphasis will be on a set of 37 Dutch coastal stations with four nearby Belgian and four German stations added. A list of these 45 stations is presented in Table 5.3, in order of increasing M2 phase lag.

To further aid analysis of the model quality, a sub-division is also made in four different sets of stations: 18 stations along the North Sea coast, 5 offshore stations (more than 10-15 km from coast), 6 stations in the Eastern and Western Scheldt and 16 stations in the Wadden Sea and Ems-Dollard.

Table 5.3Names of the tide gauge stations used for quantitative model evaluation in Dutch coastal waters. Some Belgian and German stations nearby have been added, indicated here with BE and DE, respectively. The stations are further subdivided in four groups: coast, offshore, south-western delta (SWD) and Wadden Sea (incl. Ems-Dollard)

1	Wandelaar (BE)	coast	24	Texel Noordzee	coast
2	Zeebrugge (BE)	coast	25	K13a Platform	offshore
3	Bol van Heist (BE)	coast	26	F16	offshore
4	Scheur Wielingen (BE)	coast	27	Oudeschild	Wadden Sea
5	Cadzand	coast	28	Den Oever Buiten	Wadden Sea
6	Westkapelle	coast	29	Terschelling Noordzee	coast
7	Europlatform	offshore	30	Vlieland Haven	Wadden Sea
8	Vlissingen	SWD	31	West-Terschelling	Wadden Sea
9	Roompot Buiten	coast	32	Kornwerderzand Buiten	Wadden Sea
10	Lichteiland Goeree	offshore	33	Wierumergronden	coast
11	Brouwershavense Gat 08	coast	34	Huibertgat	coast
12	Terneuzen	SWD	35	Harlingen	Wadden Sea
13	Haringvliet 10	coast	36	Nes	Wadden Sea
14	Hansweert	coast	37	Lauwersoog	Wadden Sea
15	Roompot Binnen	SWD	38	Schiermonnikoog	Wadden Sea
16	Hoek van Holland	coast	39	Borkum Sudstrand (DE)	Wadden Sea
17	Stavenisse	SWD	40	Borkum Fischerbalje (DE)	Wadden Sea
18	Berge Diepsluis West	SWD	41	Emshorn (DE)	Wadden Sea
19	Krammerssluizen West	SWD	42	Eemshaven	Wadden Sea
20	Scheveningen	coast	43	Dukegat	Wadden Sea
21	IJmuiden Buitenhaven	coast	44	Delfzijl	Wadden Sea
22	Platform Q1	offshore	45	Knock (DE)	Wadden Sea
23	Den Helder	coast			

5.3.2 Total water levels, tide and surge

5.3.2.1 *DCSM-FM 0.5nm*

A spatial overview of the RMSE-values of the total water level, tide and surge of the Dutch coastal stations is presented in Figure 5.3 and Figure 5.4 (left- and right-hand side panel), respectively. Generally, the total water level RMSE is 6-8 cm in North Sea waters. In these stations, the tide and surge RMSE is generally 4-6 cm. The quality deteriorates inside the Dutch estuaries and Wadden Sea, where the model resolution is low compared to the variability in geometry and bathymetry. This is especially noticeable in the eastern Wadden Sea (including the Ems-Dollard estuary) and the eastern part of the Eastern Scheldt where tidal channels are too narrow to properly represent on the model network. The result is a poor representation of the tide, while some impact is also noticeable in the surge quality, presumably due to a poor representation of the non-linear tide-surge interaction.
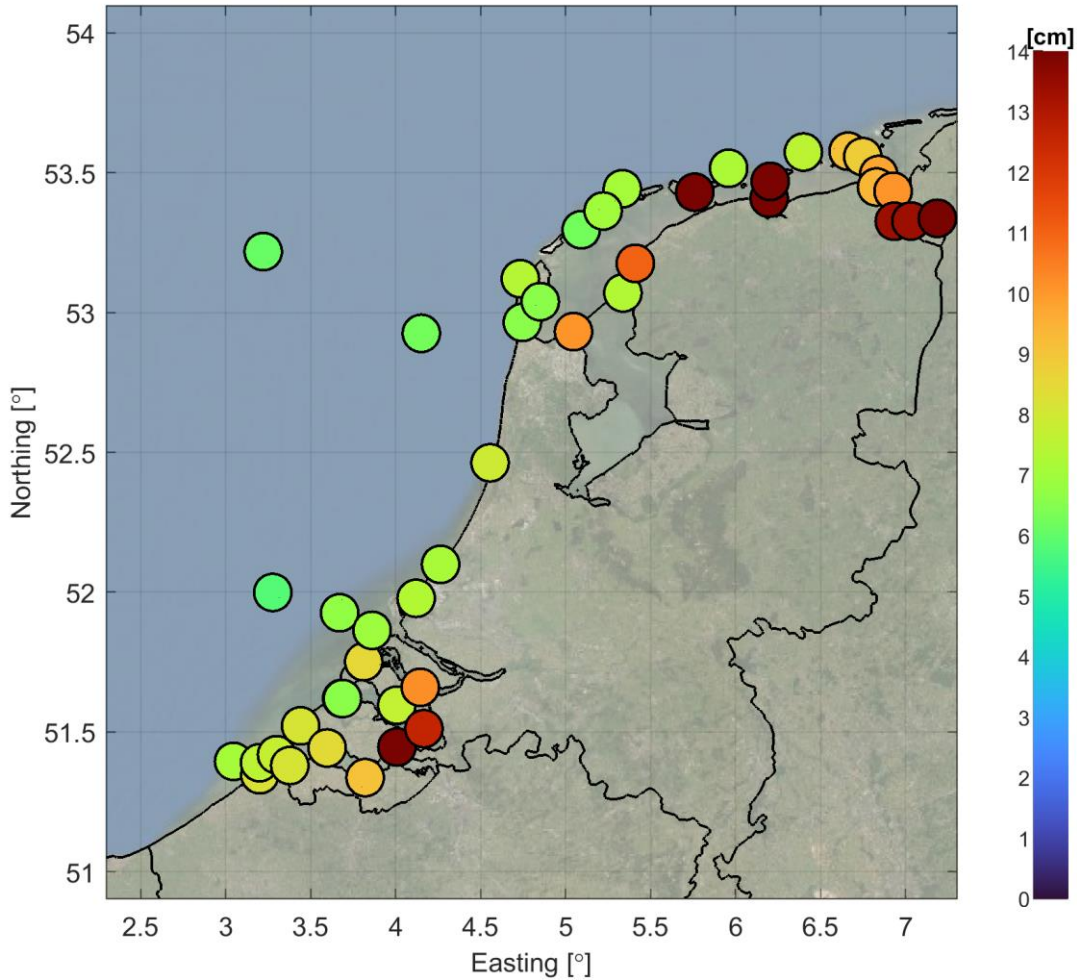
Figure 5.3   Spatial overview of the RMSE-values (cm) of the total water level for the period 2013-2017 of the Dutch coastal stations
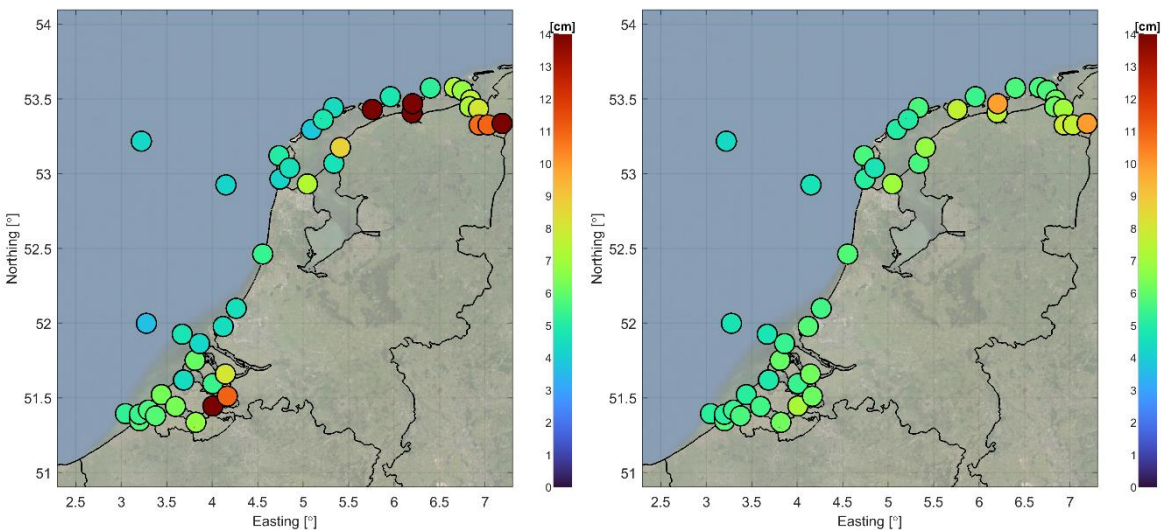
Figure 5.4   Spatial overview of the RMSE-values (cm) of the tide (left panel) and surge (right panel) for the period 2013-2017 of the Dutch coastal stations

5.3.2.2 *Comparison against DCSMv6 and DCSMv6-ZUNOv4 (fifth generation models)*

Table 5.4 shows the RMSE of tide, surge and total water level in Dutch coastal stations, for the sixth generation model DCSM-FM 0.5 nm, in comparison to the fifth generation models DCSMv6 and DCSMv6-ZUNOv4. A spatial overview of the absolute and percentage difference in RMSE (DCSMv6 minus DCSM-FM 0.5nm), for both total water level, tide and surge, is illustrated in Figure 5.5 to Figure 5.7.

These results show that on average the tide representation is slightly worse than both fifth generation models. This is probably because of the exclusion of bathymetry as a calibration parameter in the development of DCSM-FM. Especially in coarsely represented areas, adjustments in bathymetry helped overcome the poor resolution and improve the tide representation locally. Note that in 4 of the 6 main locations (Dutch: 'hoofdlocaties'), Roompot Buiten, Hoek van Holland, Den Helder and Delfzijl, the tide representation of DCMS-FM is better than DCSMv6.

The quality of the surge (RMSE 5.8 cm) is in between the quality of DCSMv6 (RMSE 6.0 cm) and DCSMv6-ZUNOv4 (RMSE 5.7 cm). Compared to DCSMv6, the surge error of DCSM-FM is lower in 32 out of 39 stations, while the surge error is larger in only three stations (Bergse Diepsluis West, Den Oever buiten en Schiermonnikoog). In none of the main locations is the quality worse than DCSMv6. It should however be noted that the quality of the tide representation in DCSMv6 has deteriorated since the year for which it has been calibrated (2007).

Table 5.4 Statistics (RMSE in cm) of tide, surge and total water level of the fifth generation models (DCSMv6 and DCSMv6-ZUNOv4) and the sixth generation model (DCSM-FM 0.5 nm) for the Dutch coastal stations. The main locations (Dutch: 'hoofdlocaties') are shown in bold.

Station	RMSE tide (cm)			RMSE surge (cm)			RMSE water level (cm)		
	DCSMv6	DCSMv6-ZUNOv4	DCSM-FM 0.5nm	DCSMv6	DCSMv6-ZUNOv4	DCSM-FM 0.5nm	DCSMv6	DCSMv6-ZUNOv4	DCSM-FM 0.5nm
Wandelaar	4.9	4.4	5.3	5.4	5.3	5.2	7.0	6.6	7.1
Zeebrugge_Leopoldd.	4.8	4.6	5.8	6.2	6.0	5.8	7.8	7.6	8.2
Bol_Van_Heist	4.3	4.7	5.5	5.5	5.3	5.2	7.0	7.1	7.5
Scheur_Wielingen_Bo.	4.4	5.3	5.7	5.6	5.5	5.4	7.1	7.6	7.7
CADZD	4.3	4.4	5.8	5.9	5.7	5.7	7.3	7.3	8.1
WESTKPLE	3.8	4.4	6.3	5.3	5.2	5.1	6.6	6.8	8.1
EURPFM	4.8	4.0	3.7	4.9	4.7	4.7	6.8	6.1	5.8
VLISSGN	**5.2**	**4.8**	**6.3**	**5.9**	**5.5**	**5.6**	**7.9**	**7.3**	**8.4**
ROOMPBTN	**3.9**	**4.4**	**3.8**	**5.4**	**5.2**	**5.0**	**6.6**	**6.8**	**6.3**
LICHTELGRE	4.1	4.9	4.7	4.9	4.8	4.7	6.4	6.8	6.7
BROUWHVSGT08	4.6	5.0	6.1	6.2	6.1	6.1	7.6	7.8	8.5
TERNZN	7.9	5.6	6.7	6.5	6.0	6.2	10.3	8.2	9.1
HARVT10	4.3	4.4	4.3	5.5	5.4	5.4	7.0	7.0	6.9
HANSWT	14.2	6.1	18.9	7.8	6.2	7.1	16.2	8.6	20.2
ROOMPBNN	7.2	4.3	4.4	5.1	4.9	4.9	8.8	6.4	6.6
HOEKVHLD	**4.8**	**5.0**	**4.4**	**5.8**	**5.3**	**5.8**	**7.5**	**7.3**	**7.3**
STAVNSE	5.8	3.9	5.5	5.5	5.2	5.4	7.9	6.4	7.7
BERGSDSWT	7.1	4.6	11.0	6.0	5.5	6.2	9.2	7.1	12.6
KRAMMSZWT		4.3	8.1		6.4	6.3		7.7	10.2
SCHEVNGN	5.0	5.2	4.5	5.7	5.6	5.6	7.6	7.6	7.1

IJMDBTHVN	5.9	6.3	5.4	6.0	5.9	5.8	8.4	8.7	7.9
Q1	4.7	4.2	4.2	4.6	4.6	4.6	6.6	6.2	6.3
DENHDR	**5.1**	**4.6**	**4.2**	**5.3**	**5.2**	**5.1**	**7.4**	**6.9**	**6.6**
TEXNZE	5.1	4.9	5.0	5.7	5.7	5.6	7.6	7.4	7.4
K13APFM	3.4	3.4	4.3	4.5	4.4	4.4	5.6	5.5	6.1
F16	2.8	2.9	3.0	4.1	4.4	4.1	5.0	5.2	5.0
OUDSD	4.3	4.8	4.6	4.9	4.7	4.7	6.5	6.7	6.6
DENOVBTN	6.0	6.5	7.4	6.8	6.8	6.9	9.1	9.4	10.1
TERSLNZE	4.3	4.1	4.4	5.8	5.8	5.6	7.2	7.0	7.1
VLIELHVN	5.8	4.7	3.8	5.1	5.0	5.0	7.7	6.9	6.3
WESTTSLG	4.5	3.6	4.8	5.5	5.0	5.0	7.1	6.1	7.0
KORNWDZBTN	4.3	3.7	4.6	6.3	5.7	5.7	7.6	6.8	7.3
WIERMGDN	4.8	4.1	4.8	5.7	5.7	5.5	7.4	6.9	7.2
HUIBGT	5.4	4.9	5.2	6.1	6.1	5.7	7.9	7.5	7.5
HARLGN	**8.0**	**4.5**	**8.7**	**7.8**	**5.8**	**6.8**	**11.2**	**7.3**	**11.0**
NES	8.8	5.9	15.4	7.7	6.0	7.6	11.7	8.4	17.2
LAUWOG	9.4	6.5	14.2	7.5	6.8	7.5	12.0	9.4	16.0
SCHIERMNOG	10.3	7.2	24.2	7.9	6.9	9.9	13.0	10.0	26.1
BORKUM_Sudstrand		4.4	7.3		5.8	5.7		7.2	9.2
BorkumFischerbalje		4.7	6.7		5.8	5.7		7.4	8.8
EMSHORN		5.6	7.6		6.2	6.1		8.4	9.7
EEMSHVN	6.3	6.8	7.2	6.8	6.3	6.2	9.3	9.3	9.5
DUKEGAT		8.2	8.0		7.1	7.0		10.5	10.1
DELFZL	**15.4**	**6.8**	**10.8**	**11.1**	**7.5**	**7.9**	**19.0**	**10.1**	**13.4**
KNOCK		7.1	11.0		7.3	7.7		10.2	13.4
Average (total)	5.9	5.0	7.0	6.0	5.7	5.8	8.5	7.6	9.2
Average (offshore)	4.0	3.9	4.0	4.6	4.6	4.5	6.1	6.0	6.0
Average (coast)	5.2	4.8	5.8	5.8	5.6	5.6	7.8	7.4	8.2
Average (SWD)	6.6	4.6	7.0	5.8	5.6	5.7	8.8	7.2	9.1
Average (Wad. S.)	7.6	5.7	9.1	7.0	6.2	6.6	10.4	8.4	11.4
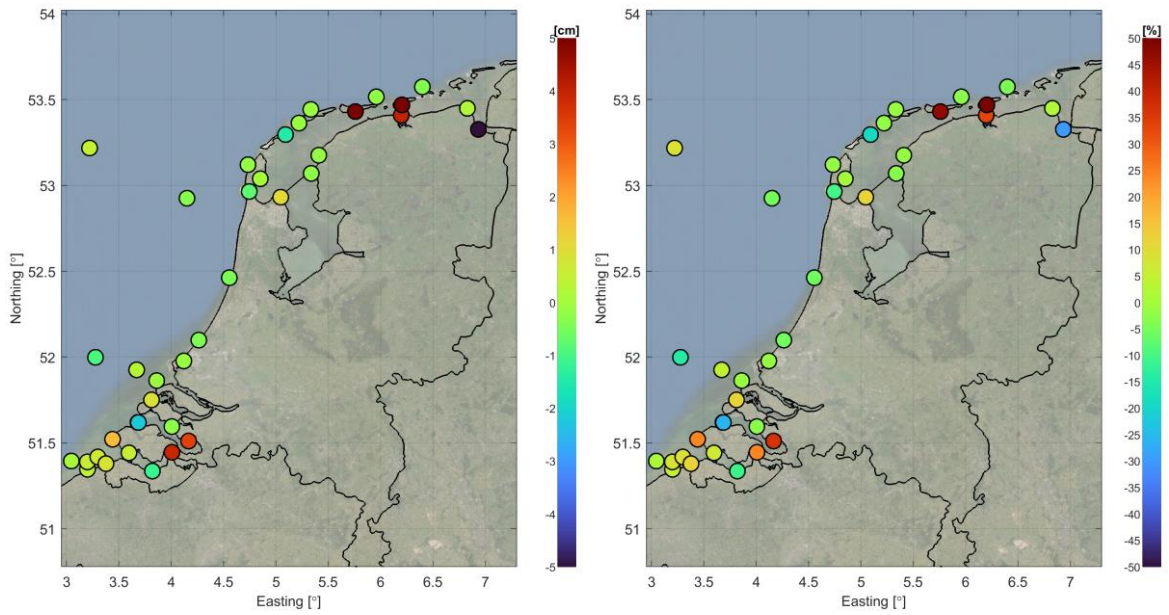
*Figure 5.5   Spatial overview of the difference (DCSM-FM 0.5nm minus DCSMv6) in RMSE of the **total water level** for the period 2013-2017 of the Dutch coastal stations. Left: difference (cm); right: relative difference (%).*
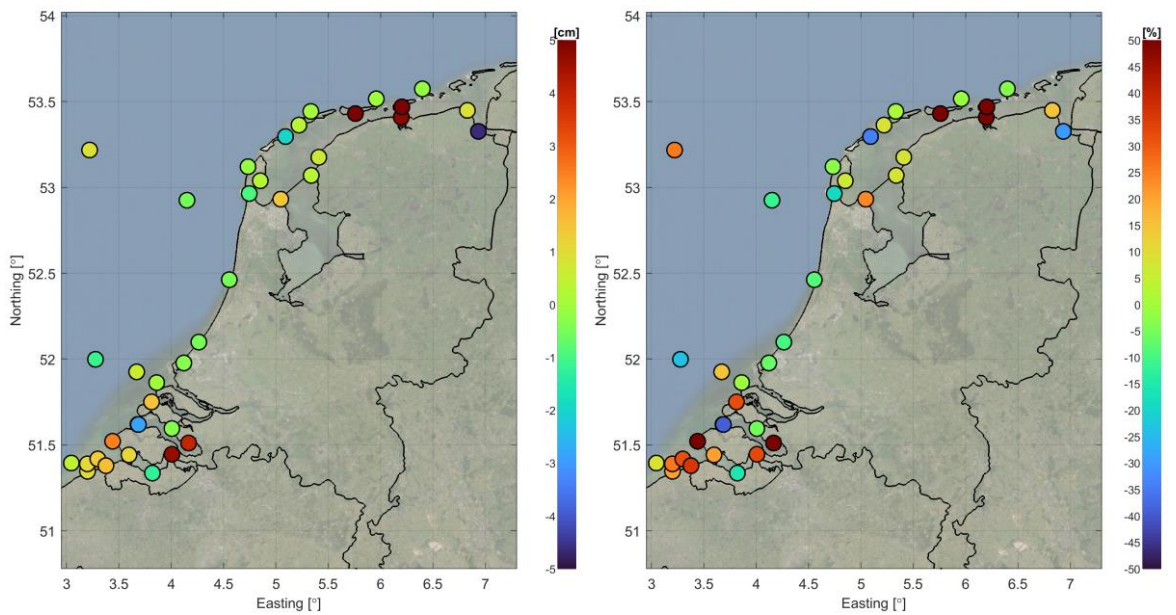
*Figure 5.6   Spatial overview of the difference (DCSM-FM 0.5nm minus DCSMv6) in RMSE of the **tide** for the period 2013-2017 of the Dutch coastal stations. Left: difference (cm); right: relative difference (%).*
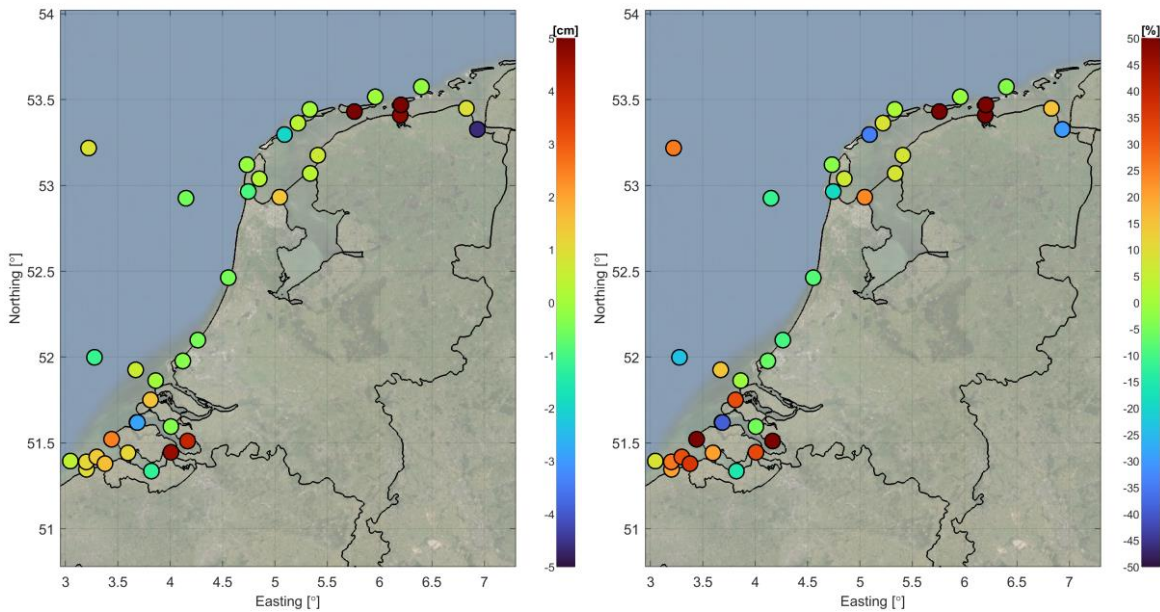
*Figure 5.7   Spatial overview of the difference (DCSM-FM 0.5nm minus DCSMv6) in RMSE of the **surge** for the period 2013-2017 of the Dutch coastal stations. Left: difference (cm); right: relative difference (%).*

5.3.3   Tide (frequency domain)

5.3.3.1   *Amplitude and phase error of the M2-component*

Figure 5.8 illustrates the amplitude and phase error of the M2-component, respectively. These results show that generally, in stations not hampered by a poor model resolution, the amplitude error is less than 4 cm, while the phase error is less than 2°.
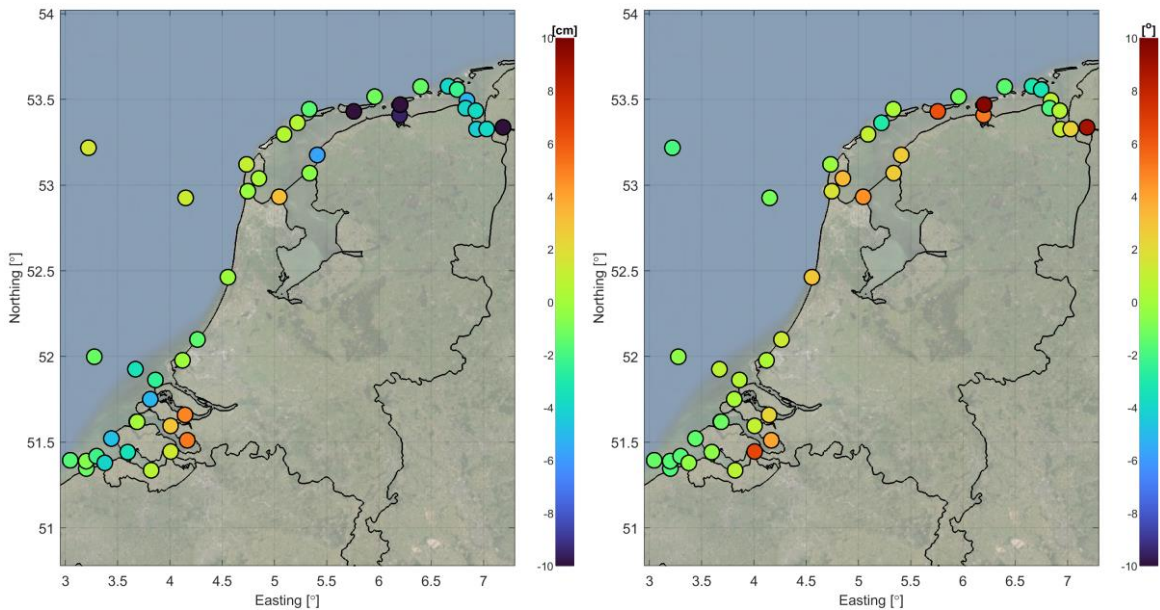
Figure 5.8   Spatial overview of the amplitude error (cm; left) and phase error (º) of the M2-component

5.3.3.2 *Contribution of harmonic components to tidal error*

In Table 5.5 to Table 5.10 an overview is given of the errors in the 10 harmonic constituents with the largest contribution to the tidal error in each of the 6 main locations. These results show that even though M2 is the largest constituent in these stations, it only has the largest contribution to the tidal error in two of the six stations considered here. Remarkably, in Hoek van Holland the M2 tidal error is not among the 10 largest contributions.

In tide gauge stations Roompot buiten and Den Helder, H1 is the harmonic constituent with the largest contribution to the tidal error, while in Hoek van Holland and Delfzijl this constituent has the second largest contribution. H1 (and H2) has an angular frequency that differs one cycle per year from the M2 frequency and represents an annual modulation of the M2 tide. Only a minor part of this modulation is gravitational in nature. While the origin is poorly understood, it is presumably mainly related to the seasonal nature of dissipation due to storms as well as seasonal temperature stratification in the central North Sea. The latter contribution cannot be represented with a 2D barotropic model such as DCSM-FM.

Table 5.5   *Overview of the 10 tidal components that have the largest contribution (in terms of vector difference) to the tidal error for station Vlissingen*

Vlissingen									
Comp.	Obs. ampl. (cm)	Ampl. error (cm)	Phase error (º)	VD (cm)	Comp.	Obs. ampl. (cm)	Ampl. error (cm)	Phase error (º)	VD (cm)
M2	171.6	-3.4	-0.5	3.8	MS4	8.4	-1.6	-1.8	1.6
M4	12.7	-3.0	5.2	3.2	2MS6	8.6	1.2	3.6	1.3
H1	3.6	-2.7	-48.4	3.1	N2	28.3	-1.2	-0.5	1.3
M6	8.6	2.0	0.5	2.0	SSA	2.9	-0.6	22.1	1.2
S2	46.4	-1.8	-0.6	1.9	MU2	12.5	-0.3	4.9	1.1

Table 5.6   *Overview of the 10 tidal components that have the largest contribution (in terms of vector difference) to the tidal error for station Roompot Buiten*

Roompot Buiten									
Comp.	Obs. ampl. (cm)	Ampl. error (cm)	Phase error (º)	VD (cm)	Comp.	Obs. ampl. (cm)	Ampl. error (cm)	Phase error (º)	VD (cm)
H1	2.2	-1.4	-46.9	1.7	NO1	1.1	-0.4	62.2	1.0
M4	12.3	0.6	6.9	1.6	SA	8.3	-1.0	0.8	1.0
M2	133.0	-1.2	-0.4	1.5	M6	6.7	0.4	-7.3	1.0
SSA	3.2	-0.7	23.0	1.3	S1	0.7	0.9	3.9	0.9
K1	7.4	0.2	-7.7	1.0	SIG1	0.3	0.7	-41.8	0.8

Table 5.7   Overview of the 10 tidal components that have the largest contribution (in terms of vector difference) to the tidal error for station Hoek van Holland

Hoek van Holland									
Comp.	Obs. ampl. (cm)	Ampl. error (cm)	Phase error (º)	VD (cm)	Comp.	Obs. ampl. (cm)	Ampl. error (cm)	Phase error (º)	VD (cm)
M4	17.9	1.3	-3.7	1.8	MS4	11.1	0.6	-5.6	1.3
H1	1.6	-0.9	-82.3	1.6	SSA	3.6	-0.7	16.0	1.2
K1	8.0	0.8	-8.8	1.5	H2	0.8	0.0	86.0	1.1
SA	8.6	-0.8	-7.5	1.3	S2	18.1	0.5	2.9	1.1
M6	4.5	-1.2	5.6	1.3	NO1	1.1	-0.4	63.5	1.0

Table 5.8   Overview of the 10 tidal components that have the largest contribution (in terms of vector difference) to the tidal error for station Den Helder

Den Helder									
Comp.	Obs. ampl. (cm)	Ampl. error (cm)	Phase error (º)	VD (cm)	Comp.	Obs. ampl. (cm)	Ampl. error (cm)	Phase error (º)	VD (cm)
H1	2.4	-1.8	-68.2	2.2	H2	0.8	-0.3	150.6	1.2
M2	62.6	-0.3	1.7	1.8	M4	10.3	-0.3	5.8	1.1
SA	10.8	-1.5	-2.0	1.6	M6	5.8	-0.1	-9.7	1.0
SSA	4.7	-0.6	15.8	1.3	NO1	1.0	-0.4	68.4	0.9
2MS6	5.5	0.7	-9.9	1.2	S1	0.9	0.7	29.0	0.9

Table 5.9   Overview of the 10 tidal components that have the largest contribution (in terms of vector difference) to the tidal error for station Harlingen

Harlingen									
Comp.	Obs. ampl. (cm)	Ampl. error (cm)	Phase error (º)	VD (cm)	Comp.	Obs. ampl. (cm)	Ampl. error (cm)	Phase error (º)	VD (cm)
M2	80.8	-5.7	2.6	6.7	MN4	3.4	0.1	35.0	2.1
M4	10.7	-0.5	30.5	5.5	2MS6	3.7	-1.9	10.9	2.0
MS4	5.9	0.1	26.6	2.8	MU2	11.0	-1.2	7.8	1.8
H1	2.5	-2.1	81.8	2.4	3MS4	2.9	-0.1	29.9	1.5
M6	4.2	-2.1	18.7	2.3	SSA	5.9	-0.3	12.9	1.3

Table 5.10   Overview of the 10 tidal components that have the largest contribution (in terms of vector difference) to the tidal error for station Delfzijl

Delfzijl									
Comp.	Obs. ampl. (cm)	Ampl. error (cm)	Phase error (º)	VD (cm)	Comp.	Obs. ampl. (cm)	Ampl. error (cm)	Phase error (º)	VD (cm)
M4	18.1	-5.4	22.4	8.0	MN4	5.9	-1.7	26.7	2.9
H1	6.1	-4.8	-35.6	5.1	M6	6.9	-1.5	17.2	2.3
MS4	10.7	-3.4	23.3	4.9	H2	0.8	0.6	-119.9	1.9
M2	131.7	-4.3	1.1	4.9	3MS4	3.9	-1.0	25.6	1.8
2MS6	6.5	-2.5	19.4	3.1	2MN6	3.6	-1.2	23.4	1.7

5.3.4   Skew surge (high waters)

The error statistics for three skew surge categories, at the Dutch coastal stations, can be found in Table 5.11. A spatial overview of the RMSE of the high water skew surge (<99.0%, i.e., calm conditions) in the Dutch coastal stations is presented in Figure 5.9. This shows a skew surge error of around 5-6 cm in North Sea waters. In the eastern Wadden Sea and Dutch estuaries, the error increases to about 7 cm. The high water skew surge is less sensitive to the quality with which the tide is represented (compared to the surge), which yields a more uniform model quality.
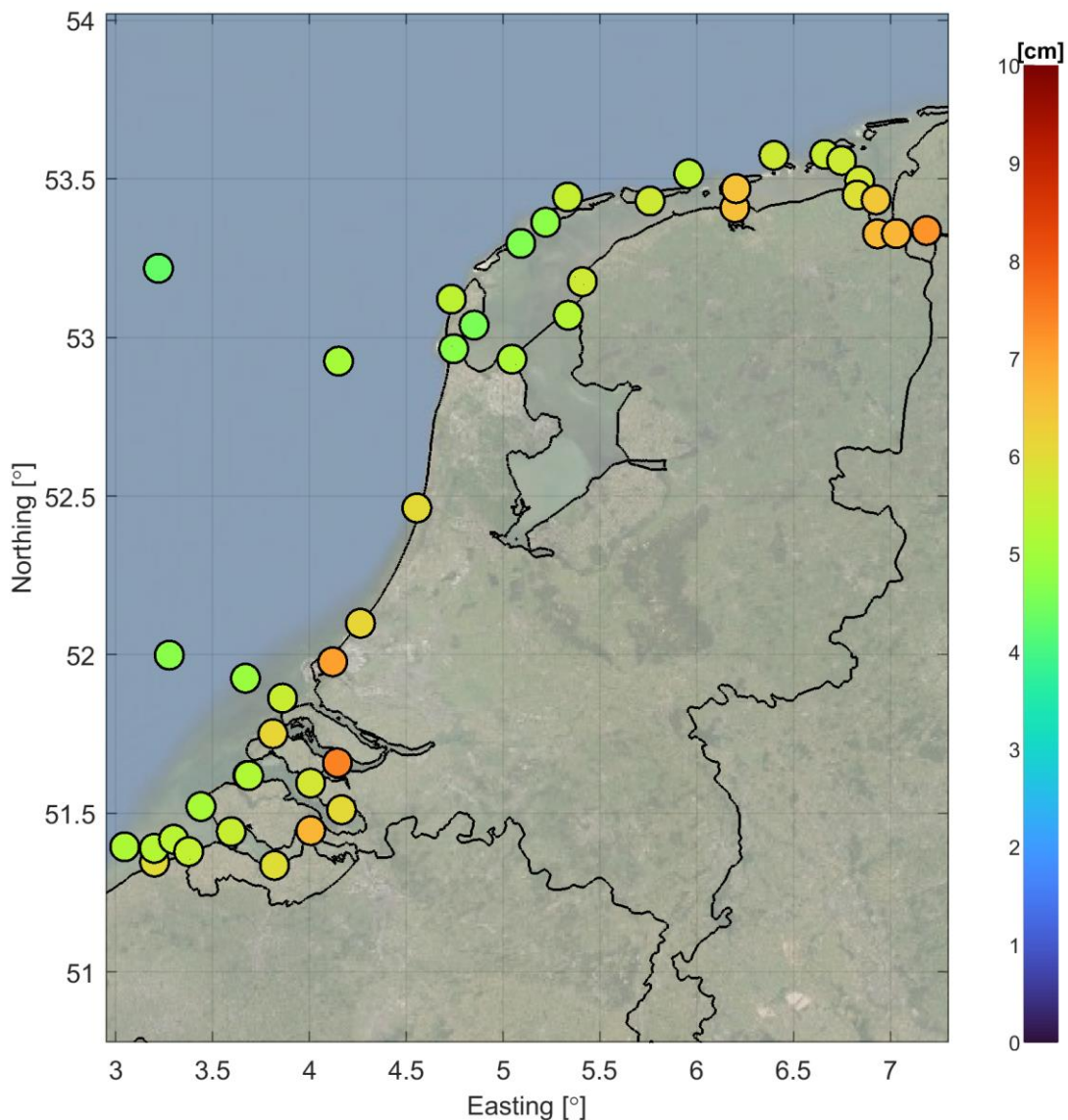
Figure 5.9   Spatial overview of the RMSE (cm) of the skew surge height for high waters (<99.0% skew surges)

In Figure 5.10, the bias and RMSE of the most extreme (>99.8%) skew surge events are presented. This shows an excellent quality in southern waters, with RMSE values less than 10-15 cm. One notable exception in that region is Brouwershavense Gat, which exhibits a bias of -15.4 cm and consequently has an RMSE of 21.2 cm. This is presumably cause by the presence of seiches during storms, which are not represented in the model.

Stations in the north, especially inside the Wadden Sea show larger skew surge errors. This is mostly due to a large systematic underestimation of the skew surge during storms. The bias is generally largest in the eastern part of the Wadden Sea and increases from north to south. In the Ems-Dollard the bias can reach 30-40 cm.
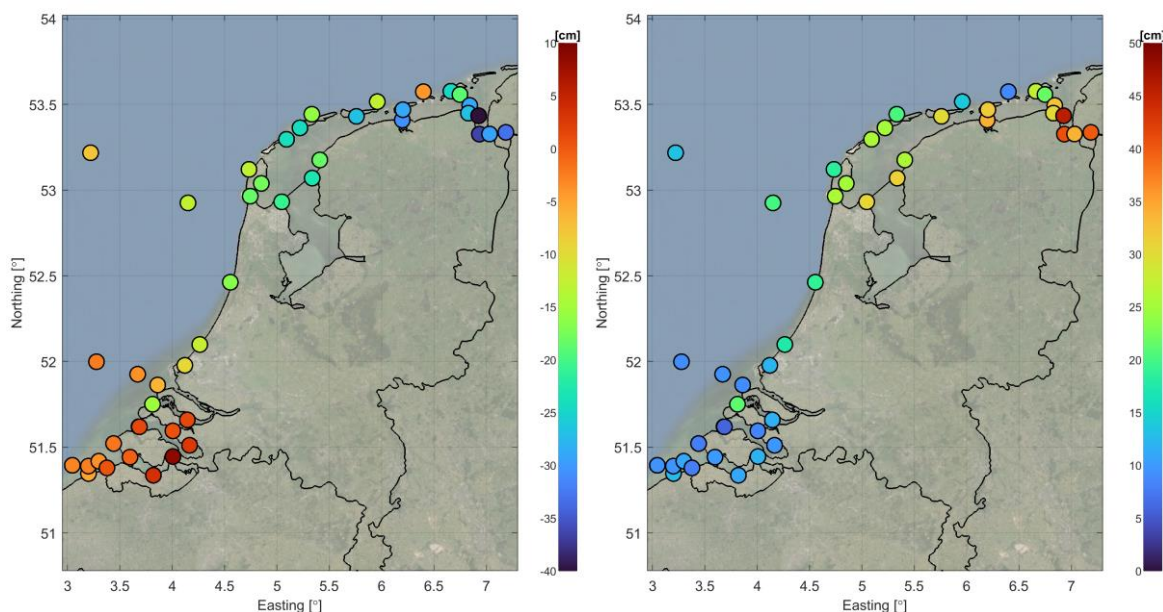
Figure 5.10 Spatial overview of the bias in cm (left panel) and RMSE in cm (right panel) of the skew surge height for high waters (>99.8% skew surges)

Table 5.11 Overview of the model skill to represent skew surge heights (high waters), for three different event classes, in terms of bias (cm) and the RMSE (cm) for Dutch coastal stations

Station	<99.0% skew surges		99.0% - 99.8% skew surges		>99.8% skew surges		
	bias (cm)	RMSE (cm)	bias (cm)	RMSE (cm)	bias (cm)	std (cm)	RMSE (cm)
Wandelaar	-0.2	5.2	0.7	8.1	-2.9	8.9	9.4
Zeebrugge_Leopold.	-1.5	6.0	0.9	10.2	-5.1	11.5	12.6
Bol_Van_Heist	-1.0	5.3	0.3	7.5	-2.6	9.2	9.6
Scheur_Wielingen_.	-0.2	5.3	0.1	9.3	-3.7	10.4	11.1
CADZD	0.0	5.5	1.5	8.2	0.4	7.9	7.9
WESTKPLE	0.5	5.1	3.0	7.2	-2.0	7.7	8.0
EURPFM	0.1	4.7	0.4	7.1	-2.4	8.8	9.2
VLISSGN	0.1	5.6	2.7	8.5	-0.4	10.1	10.1
ROOMPBTN	-0.5	5.0	-0.6	9.7	-8.2	8.9	12.1
LICHTELGRE	-0.5	4.9	0.0	7.8	-3.7	8.8	9.6
BROUWHVSGT08	-1.4	6.2	-5.3	13.8	-15.4	14.6	21.2
TERNZN	1.0	6.0	1.9	10.1	3.6	10.4	11.0
HARVT10	-0.9	5.6	-0.7	10.7	-6.3	6.5	9.0
HANSWT	0.0	6.7	9.8	14.4	8.7	8.3	12.1
ROOMPBNN	-0.8	5.2	5.2	10.0	1.2	5.9	6.0
HOEKVHLD	-3.9	7.1	-2.6	13.2	-9.7	7.4	12.2
STAVNSE	0.1	5.8	8.1	12.3	0.6	8.4	8.4
BERGSDSWT	0.9	6.0	12.6	15.6	2.6	9.5	9.9

KRAMMSZWT	-0.9	7.5	2.8	11.8	1.4	11.7	11.8
SCHEVNGN	-1.6	6.2	-3.8	10.5	-12.1	12.8	17.6
IJMDBTHVN	-1.5	6.1	-4.6	12.9	-16.7	8.5	18.8
Q1	-0.6	5.1	-1.8	10.1	-12.7	15.5	20.1
DENHDR	-0.7	4.8	-5.7	9.0	-18.4	17.8	25.6
TEXNZE	-1.2	5.4	-5.9	13.9	-12.7	13.5	18.5
K13APFM	-0.1	4.3	0.3	6.6	-7.9	10.6	13.2
F16	-0.4	4.2	-0.6	5.3	-11.8	5.2	12.9
OUDSD	-0.3	4.5	-2.6	7.2	-17.7	17.7	25.0
DENOVBTN	-0.8	5.2	-5.3	9.6	-20.8	22.5	30.6
TERSLNZE	-1.0	5.5	-5.1	11.9	-15.9	12.5	20.2
VLIELHVN	-0.2	4.6	-3.4	9.0	-24.0	9.0	25.6
WESTTSLG	-0.3	4.7	-2.2	9.0	-24.1	7.6	25.3
KORNWDZBTN	-0.5	5.3	-4.0	10.3	-22.9	21.1	31.2
WIERMGDN	-0.4	5.3	4.2	10.2	-12.7	5.5	13.8
HUIBGT	-0.7	5.7	8.0	11.9	-4.1	7.7	8.7
HARLGN	0.1	5.7	-3.2	11.4	-18.1	18.4	25.8
NES	0.5	5.7	-7.1	13.6	-26.8	13.9	30.2
LAUWOG	0.6	6.5	-5.5	13.0	-30.8	14.8	34.1
SCHIERMNOG	0.8	6.5	-4.5	12.7	-28.8	13.1	31.6
BORKUM_Sudstran.	-0.2	5.6	-0.3	9.5	-24.6	11.7	27.2
BorkumFischerbalje	-0.1	5.6	3.3	9.8	-18.8	11.1	21.8
EMSHORN	0.0	5.7	-3.2	11.7	-29.0	13.8	32.1
EEMSHVN	-0.3	5.9	-3.2	11.7	-27.1	13.1	30.1
DUKEGAT	-0.3	6.4	-2.6	16.4	-42.7	15.8	45.6
DELFZL	-0.6	6.7	0.6	13.5	-36.5	17.5	40.4
KNOCK	0.3	6.7	3.1	13.6	-29.3	17.2	34.0
Average (total)	-0.4	5.6	-0.2	10.8	-13.6	11.9	19.6
Average (offshore)	-0.3	4.6	-0.4	7.4	-7.7	9.8	13.0
Average (coast)	-0.9	5.7	-0.3	10.7	-7.8	10.0	13.8
Average (SWD)	0.1	6.0	5.5	11.4	1.5	9.3	9.5
Average (Wad. S.)	-0.1	5.7	-2.5	11.4	-26.4	14.9	30.7

Comparison against DCSMv6 and DCSMv6-ZUNOv4 (fifth generation models)
The error statistics for the fifth generation models (at the Dutch coastal stations) can be found in the Appendix (DCSMv6: Table E.4; DCSMv6-ZUNOv4: Table E.5). These results are summarised in Table 5.12, where the station-averaged error statistics are compared against those of the fifth generation models. This shows that on average the quality with which the skew surge is represented is similar in all three models.

Table 5.12 Comparison of the station-averaged model skill to represent skew surge heights (high waters), for three different event classes, in terms of bias (cm) and the RMSE (cm) for Dutch coastal stations.

Total	<99.0% skew surges		99.0% - 99.8% skew surges		>99.8% skew surges		
	bias (cm)	RMSE (cm)	bias (cm)	RMSE (cm)	bias (cm)	std (cm)	RMSE (cm)
DCSMv6	-0.3	5.7	1.5	11.4	-10.3	12.2	17.4
DCSMv6-ZUNOv4	-0.3	5.6	-0.3	11.0	-14.4	12.4	19.8
DCSM-FM 0.5nm	-0.4	5.6	-0.2	10.8	-13.6	11.9	19.6
Offshore							
DCSMv6	-0.1	4.7	-0.1	7.3	-9.1	11.6	15.6
DCSMv6-ZUNOv4	-0.2	4.6	0.1	7.5	-9.0	9.4	13.5
DCSM-FM 0.5nm	-0.3	4.6	-0.4	7.4	-7.7	9.8	13.0
Coast							
DCSMv6	-0.6	5.7	1.1	11.1	-7.6	11.2	14.6
DCSMv6-ZUNOv4	-0.6	5.5	-0.9	10.9	-9.8	11.1	15.3
DCSM-FM 0.5nm	-0.9	5.7	-0.3	10.7	-7.8	10.0	13.8
South-western Delta							
DCSMv6	0.0	6.0	5.1	11.9	-0.5	10.1	11.3
DCSMv6-ZUNOv4	0.2	5.8	3.0	10.2	-2.5	9.4	9.9
DCSM-FM 0.5nm	0.1	6.0	5.5	11.4	1.5	9.3	9.5
Wadden Sea							
DCSMv6	0.0	6.1	0.8	13.7	-21.5	15.6	27.0
DCSMv6-ZUNOv4	-0.1	5.8	-0.9	12.4	-25.8	15.7	30.6
DCSM-FM 0.5nm	-0.1	5.7	-2.5	11.4	-26.4	14.9	30.7

5.3.5   Skew surge (low waters)

The error statistics for three low water skew surge categories, at the Dutch coastal stations, can be found in Table 5.13. A spatial overview of the RMSE of the low water skew surge (<99.0%, i.e., calm conditions) in the Dutch coastal stations is presented in Figure 5.11. This shows a skew surge error of around 5-6 cm in North Sea waters. In the eastern Wadden Sea and Dutch estuaries, the error increases to about 7 cm and up to 10 cm in Schiermonnikoog. While the low water skew surge is less sensitive to the quality with which the tide is represented (compared to the surge, and similar to the high water skew surge), it is sensitive to the accuracy with which the bathymetry is represented. Especially in areas where the resolution of the model is coarse relative to the variability in bathymetry, this hampers the quality of the low water skew surge representation.
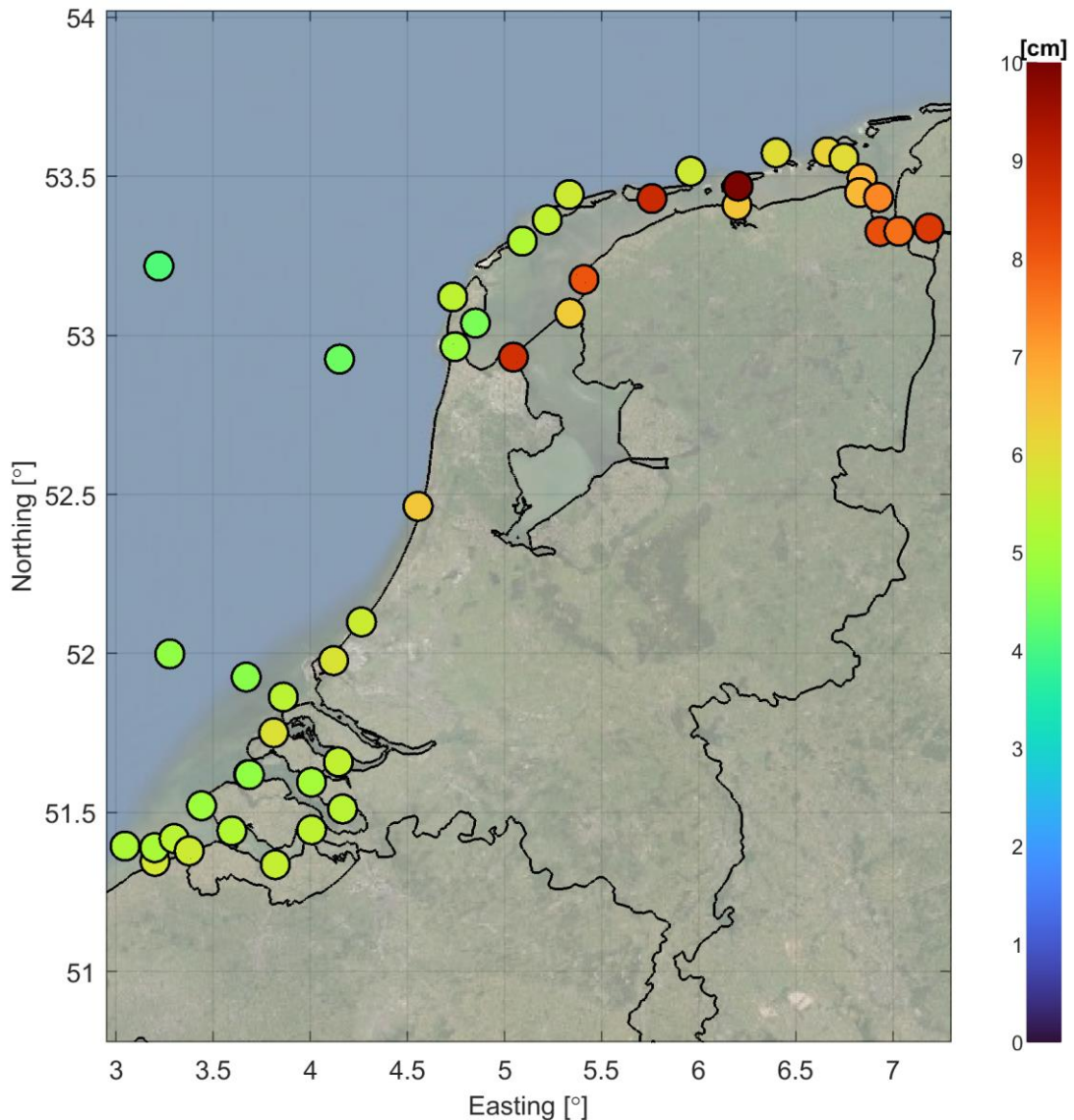
Figure 5.11 Spatial overview of the RMSE (cm) of the skew surge height for low waters (<99.0% skew surges)

In Figure 5.12, the bias and RMSE of the low water skew surge during the most extreme (>99.8%) skew surge events is presented. In southern waters this shows a larger systematic underestimation of low waters, than for high waters during the same category of events. The underestimation increases in upstream direction inside the Eastern and Western Scheldt. On the other hand, in northern waters, the systematic error (bias) is less severe than for the high water skew surge, with a bias of 10-20 cm in the Ems-Dollard (compared to 30-40 cm for the high water skew surge). The most extreme biases are presumably caused by a poor representation of the local bathymetry due to the coarseness of the network.
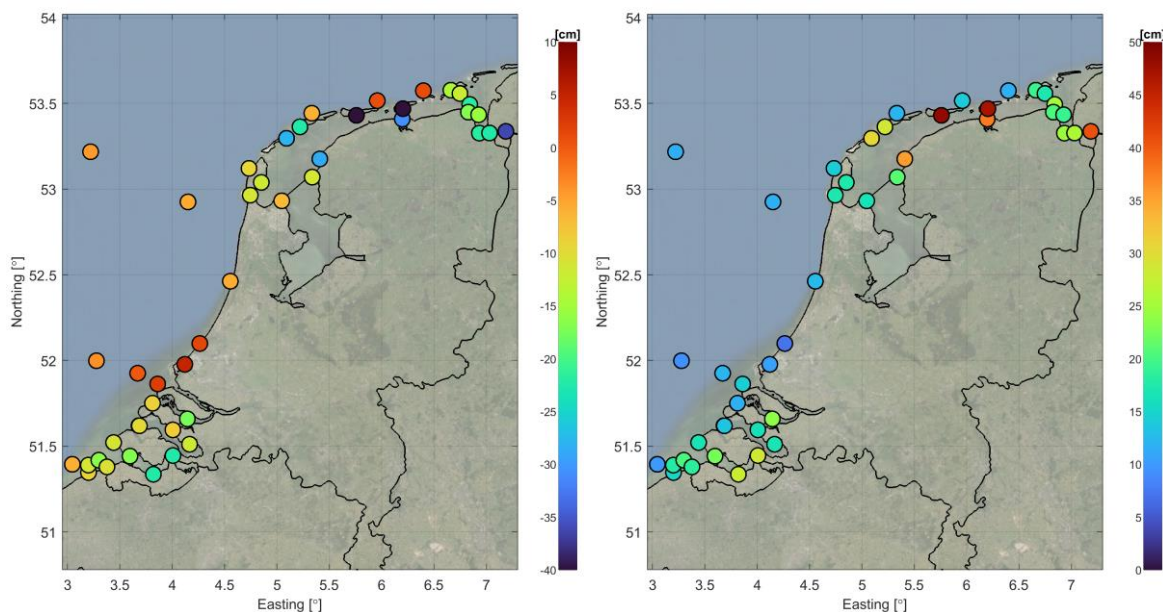
Figure 5.12 Spatial overview of the bias in cm (left panel) and RMSE in cm (right panel) of the skew surge height for low waters (>99.8% skew surges)

Table 5.13 Overview of the model skill to represent skew surge heights (low waters), for three different event classes, in terms of bias (cm) and the RMSE (cm) for Dutch coastal stations

Station	<99.0% skew surges		99.0% - 99.8% skew surges		>99.8% skew surges		
	bias (cm)	RMSE (cm)	bias (cm)	RMSE (cm)	bias (cm)	std (cm)	RMSE (cm)
Wandelaar	0.3	5.2	-2.9	10.9	-6.0	8.2	10.1
Zeebrugge_Leopold.	0.3	5.8	0.1	11.5	-9.1	12.2	15.2
Bol_Van_Heist	0.0	5.1	-1.2	10.1	-11.1	13.9	17.8
Scheur_Wielingen_.	-0.5	5.3	-1.3	10.8	-16.5	11.4	20.1
CADZD	-0.6	5.6	-0.1	9.8	-10.5	15.2	18.4
WESTKPLE	-0.1	4.9	0.6	8.6	-11.1	12.7	16.9
EURPFM	0.6	4.8	3.4	7.9	-3.8	8.4	9.2
VLISSGN	-0.2	5.3	-1.2	8.6	-16.8	15.1	22.6
ROOMPBTN	0.2	4.8	-0.7	10.3	-10.4	12.4	16.1
LICHTELGRE	0.2	4.7	1.0	7.5	0.1	12.2	12.2
BROUWHVSGT08	-0.3	5.9	-2.1	9.9	-8.8	7.7	11.7
TERNZN	0.0	5.5	-2.4	9.7	-22.3	16.9	28.0
HARVT10	0.3	5.4	4.3	9.2	2.2	14.1	14.3
HANSWT	-1.0	5.4	-7.9	15.5	-22.2	18.1	28.7
ROOMPBNN	-0.3	4.8	-2.8	9.7	-9.9	9.3	13.6
HOEKVHLD	0.8	5.8	4.3	9.9	4.8	9.6	10.7
STAVNSE	0.6	5.1	-5.2	10.8	-8.4	14.1	16.4
BERGSDSWT	1.1	5.3	-5.9	14.1	-11.5	12.2	16.8
KRAMMSZWT	0.9	5.4	-3.1	11.0	-17.4	16.0	23.7
SCHEVNGN	1.1	5.6	4.0	9.4	1.5	7.0	7.1
IJMDBTHVN	1.8	6.4	3.3	9.0	-5.6	11.3	12.6
Q1	0.4	4.4	1.6	7.2	-5.6	10.2	11.7

DENHDR	0.6	4.9	-1.5	8.8	-11.1	13.1	17.2
TEXNZE	1.3	5.4	3.9	8.0	-9.7	10.2	14.1
K13APFM	0.4	4.1	-0.4	4.8	-4.3	10.9	11.7
F16	0.3	4.0	0.6	5.8	-3.1	5.3	6.1
OUDSD	0.3	4.5	-3.2	8.6	-11.6	13.0	17.4
DENOVBTN	-0.4	8.7	3.9	11.2	-7.0	15.0	16.6
TERSLNZE	0.7	5.6	5.0	10.7	-6.1	10.7	12.3
VLIELHVN	0.4	5.3	-8.4	13.6	-27.8	12.7	30.6
WESTTSLG	0.4	5.5	-7.7	13.8	-22.3	17.8	28.5
KORNWDZBTN	0.1	6.3	1.4	11.1	-11.3	17.8	21.1
WIERMGDN	0.1	5.7	4.5	10.8	0.7	14.0	14.0
HUIBGT	0.1	5.9	4.1	9.3	0.9	11.7	11.7
HARLGN	-0.1	8.1	-12.0	15.8	-28.6	20.8	35.4
NES	-0.2	8.9	-28.4	30.5	-44.1	20.1	48.4
LAUWOG	-0.1	6.4	-20.7	23.5	-30.7	21.8	37.7
SCHIERMNOG	-1.6	10.0	-34.5	36.9	-41.8	21.3	46.9
BORKUM_Sudstran.	0.4	6.2	-10.7	15.0	-14.3	13.3	19.5
BorkumFischerbalje	0.1	6.0	-7.9	12.9	-12.0	12.4	17.2
EMSHORN	0.6	6.7	-14.2	17.3	-22.0	12.6	25.4
EEMSHVN	1.1	6.7	-10.6	15.2	-16.9	11.4	20.3
DUKEGAT	1.1	7.4	-11.1	15.1	-15.7	11.3	19.3
DELFZL	1.6	8.1	-15.0	19.5	-21.8	11.7	24.7
KNOCK	0.7	7.7	-15.3	19.6	-22.3	13.0	25.8
Average (total)	0.3	5.9	-4.8	12.8	-13.4	13.2	19.9
Average (offshore)	0.4	4.4	1.2	6.7	-3.3	9.4	10.2
Average (coast)	0.3	5.5	0.9	10.1	-7.1	11.9	15.0
Average (SWD)	0.4	5.2	-3.4	10.6	-14.4	14.0	20.2
Average (Wad. S.)	0.3	7.0	-12.1	17.5	-21.9	15.4	27.2

Comparison against DCSMv6 and DCSMv6-ZUNOv4 (fifth generation models)
The error statistics of the fifth generation models (at the Dutch coastal stations) can be found in the Appendix (DCSMv6: Table E.6; DCSMv6-ZUNOv4: Table E.7). These results are summarised in Table 5.14, where the station-averaged error statistics are compared against those of the fifth generation models. This shows that on average the quality with which the lowest two classes of skew surge are represented is slightly better compared to the fifth generation models in three of the four sub-areas. The quality of the highest low water skew surge events is slightly worse than the fifth generation models, mainly due to worse results in the South-western Delta and Wadden Sea. This is presumably due to the exclusion of bathymetry as a calibration parameter in the development of DCSM-FM (as opposed to the fifth generation models, where the bathymetry was adjusted).

Table 5.14 Comparison of the station-averaged model skill to represent skew surge heights (low waters), for three different event classes, in terms of bias (cm) and the RMSE (cm) for Dutch coastal stations.

	<99.0% skew surges		99.0% - 99.8% skew surges		>99.8% skew surges		
Total	bias (cm)	RMSE (cm)	bias (cm)	RMSE (cm)	bias (cm)	std (cm)	RMSE (cm)
DCSMv6	0.2	5.9	-2.1	12.2	-10.1	12.7	17.5
DCSMv6-ZUNOv4	0.3	5.8	-0.2	11.2	-7.6	12.1	15.4
DCSM-FM 0.5nm	0.3	5.9	-4.8	12.8	-13.4	13.2	19.9
Offshore							
DCSMv6	0.5	4.8	0.0	8.0	-6.5	9.4	11.9
DCSMv6-ZUNOv4	0.4	4.5	1.8	7.2	-3.9	8.6	9.5
DCSM-FM 0.5nm	0.4	4.4	1.2	6.7	-3.3	9.4	10.2
Coast							
DCSMv6	0.2	5.7	-0.1	11.0	-9.1	11.9	16.4
DCSMv6-ZUNOv4	0.4	5.6	1.7	11.0	-5.6	11.4	14.5
DCSM-FM 0.5nm	0.3	5.5	0.9	10.1	-7.1	11.9	15.0
South-western Delta							
DCSMv6	0.4	5.4	0.2	10.9	-8.5	11.0	15.4
DCSMv6-ZUNOv4	0.1	5.4	1.1	11.1	-9.0	12.3	16.0
DCSM-FM 0.5nm	0.4	5.2	-3.4	10.6	-14.4	14.0	20.2
Wadden Sea							
DCSMv6	0.1	7.2	-7.9	17.1	-14.8	16.7	23.7
DCSMv6-ZUNOv4	0.2	6.6	-3.4	12.7	-10.5	13.9	18.1
DCSM-FM 0.5nm	0.3	7.0	-12.1	17.5	-21.9	15.4	27.2

6 Conclusions and recommendations

6.1 Conclusions

Upon request of Rijkswaterstaat (RWS) Deltares has developed a sixth-generation hydrodynamic model of the Northwest European Shelf: the Dutch Continental Shelf Model – Flexible Mesh (DCSM-FM). Specifically, this model covers the North Sea and adjacent shallow seas and estuaries in the Netherlands, such as the Wadden Sea, the Ems-Dollard estuary, the Western Scheldt and the Eastern Scheldt.

The development of the present model is part of a more comprehensive project in which sixth-generation models are developed for all waters managed and maintained by RWS. An important difference with the previous fifth generation models is the use of the D-HYDRO Suite, the new software framework for modelling free surface flows, which was first released in 2015 and allows for the use of unstructured grids.

Since the proposed applications on the North Sea pose a wide range and sometimes mutually exclusive demands on a model, two horizontal schematizations were proposed: a relatively coarse two-dimensional model (DCSM-FM 0.5nm; described in the present report) and a relatively fine schematization (DCSM-FM 100m; not described here) with further refinement in most Dutch coastal waters. DCSM-FM 0.5nm is primarily aimed at ensemble forecasting, but also forms a sound basis for a subsequent 3D model development, including temperature and salinity as state parameters.

The bottom roughness in DCSM-FM was calibrated using the open-source data assimilation toolbox OpenDA. This was done against 205 shelf-wide tide-gauge measurements, covering the entire calendar year 2017. Compared to the uncalibrated version of the model, this has led to a 49% reduction in the cost function. Before being used, the measurements were extensively checked on quality.

DCSM-FM was validated against measurements for the period 2013-2017 and compared against the fifth generation models DCSMv6 and DCSMv6-ZUNOv4. An analysis of total water levels as well as the contribution of tide and surge in Dutch waters showed that:

- Generally, the total water level RMSE is 6-8 cm in North Sea waters. In these stations, the tide and surge RMSE is generally 4-6 cm. The quality deteriorates inside the Dutch estuaries and Wadden Sea, where the model resolution is low compared to the variability in geometry and bathymetry.
- These results show that on average the tide representation is slightly worse than both fifth generation models. This is probably because of the exclusion of bathymetry as a calibration parameter in the development of DCSM-FM.
- Compared to DCSMv6, the surge error of DCSM-FM is lower in 32 out of 39 stations, while the surge error is larger in only three stations. In none of the six main locations (Dutch: 'hoofdlocaties') is the quality worse than the fifth generation model DCSMv6.

The model is also assessed with respect of its capacity to represent the high water skew surge, i.e., the difference between a total high water and the associated astronomical high water, ignoring small differences in timing. This is done for three categories of events, subdivided based on the height of the measured skew surge. With respect to the skew surge the following can be concluded:

- The RMSE of the high water skew surge (<99.0%, i.e., calm conditions) in the Dutch coastal stations is around 5-6 cm in North Sea waters and increases to about 7 cm in the eastern Wadden Sea and Dutch estuaries.
- The most extreme (>99.8%) skew surge events shows an excellent quality in southern waters, with RMSE values less than 10-15 cm. Errors are much larger inside the (eastern) Wadden Sea, mostly due to a large systematic underestimation of the skew surge during storms. In the Ems-Dollard the bias can reach 30-40 cm during these events.
- With respect to the high water skew surge, DCSM-FM has on average a similar quality compared the fifth generation models DCSMv6 and DCSMv6-ZUNOv4.

Since there is also an interest in the accuracy with which low waters are represented (e.g. relevant for water authorities draining into the sea by gravity flow), especially during storm surges, the error statistics for low waters are also computed. With respect to the low water skew surge, the following can be concluded:

- In North Sea waters a skew surge RMSE of around 5-6 cm is found. In the eastern Wadden Sea and Dutch estuaries, the error increases to about 7 cm.
- The low water skew surge (and low water representation in general) is sensitive to the accuracy with which the bathymetry is represented. Especially in areas where the resolution of the model is coarse relative to the variability in bathymetry, this hampers the quality of the low water skew surge representation.
- The low water skew surge during the most extreme (>99.8%) skew surge events shows a larger systematic underestimation of low waters, than for high waters during the same category of events. The underestimation increases in upstream direction inside the Eastern and Western Scheldt. On the other hand, in northern Dutch waters, the systematic error (bias) is less severe than for the high water skew surge, with a bias of 10-20 cm in the Ems-Dollard (compared to 30-40 cm for the high water skew surge).
- On average the quality with which the lowest two classes of low water skew surge are represented is slightly better than the fifth generation models in most areas.
- The quality of the highest low water skew surge events is slightly worse than the fifth generation models, mainly due to worse results in the South-western Delta and Wadden Sea.

6.2 Recommendations

6.2.1 Bathymetry

Outside Dutch coastal waters, the model bathymetry is based on the EMODnet October 2016 version. In the meantime, the more recent September 2018 version has become available. Since significant bathymetry errors are known to exist in the October 2016 EMODnet bathymetry dataset, it is recommended to update the model bathymetry with the most recent version.

Furthermore, the quality of the tide representation of DCSM-FM 0.5nm has deteriorated slightly compared to the fifth generation models DCSMv6 and DCSMv6-ZUNOv4. This is based on the validation for the years 2013-2017 and is all the more striking, since the quality of the tide representation in the fifth generation models has deteriorated since the year for which these have been calibrated (2007). A possible reason for the slightly worse tide representation in the sixth generation model is the exclusion of bathymetry as a calibration parameter. It is therefore

recommended to investigate whether adjusting the bathymetry within reasonable bounds would be beneficial to the quality of the tide.

6.2.2 Boundary conditions
The tidal boundary conditions are based on the FES2012 global tide model. It is recommended to upgrade this to the most recent available version FES2014.

6.2.3 Annual M2 modulation
In tide gauge stations Roompot buiten and Den Helder, H1 is the harmonic constituent with the largest contribution to the tidal error, while in Hoek van Holland and Delfzijl this constituent has the second largest contribution. H1 (and H2) has an angular frequency that differs one cycle per year from the M2 frequency and represents an annual modulation of the M2 tide. Only a minor part of this modulation is gravitational in nature. While the origin is poorly understood, it is presumably mainly related to the seasonal nature of dissipation due to storms as well as seasonal temperature stratification in the central North Sea. The latter contribution cannot be represented with a 2D barotropic model such as DCSM-FM. It is therefore recommended to investigate whether a better tide quality can be achieved by using a 3D baroclinic version of DCSM-FM.

6.2.4 Meteorological forcing
The present calibration and validation were performed using Hirlam7.2 meteorological forcing, even though an important application will be the use for probability forecasting using the ECMWF EPS meteorological product. It is therefore recommended to further validate DCSM-FM using ECWMF meteorological forcing. Also, since Hirlam7.2 will be replaced by Harmonie, the validation should also be performed using the latter forcing.

6.2.5 Forecast accuracy
The validation in the present report is based on hindcast computations. Since the model will be used for forecasting applications, it is recommended to also assess the forecast quality as a function of the lead time.

6.2.6 Mean Dynamic Topography
The water levels computed with DCSM-FM (or any other hydrodynamic model) refer to an equipotential surface of the Earth's gravity field. Gradients in baroclinic pressure (i.e. due to density differences) affect the movement of water and can, consequently, affect the long-term mean water level (or Mean Dynamic Topography). Salinity and temperature are not included in DCSM-FM as state parameters, since in a 2D model this would not produce a realistic solution. Consequently, the density is assumed to be constant and uniform. Furthermore, at the open boundaries, steric effects (i.e., changes in sea level due to thermal expansion and salinity variations) are not taken into account. This affects the representation of the Mean Dynamic Topography (MDT). Therefore, the bias between measured and computed water levels in each station, determined over the entire five-year validation period, is disregarded in all Goodness-of-Fit criteria used here.

One approach to properly compute the MDT is to use a 3D model with salinity and temperature as state parameters. While this is feasible and useful for many applications, for some this would result in an unacceptably high computational burden. An alternative approach would then be to

add the depth-averaged horizontal baroclinic pressure gradients obtained from an external solution to the 2D model equations (Slobbe et al., 2013). It is recommended to consider both the first and second solution.

Development of a sixth generation model for the NW European Shelf (DCSM-FM 0.5nm)

Literature

Charnock, H. (1955). *Wind stress on a water surface.* Quarterly Journal of the Royal Meteorological Society, 81(350), 639-640.

EMODnet Bathymetry Consortium (2016). *EMODnet Digital Bathymetry (DTM).* http://doi.org/10.12770/c7b53704-999d-4721-b1a3-04ec60c87238

Pawlowicz, R., Beardsley, B., Lentz, S. (2002). *Classical tidal harmonic analysis including error estimates in MATLAB using T_TIDE.* Computers and Geosciences 28 (2002), 929-937.

Slobbe, D. C., Verlaan, M., Klees, R., & Gerritsen, H. (2013). *Obtaining instantaneous water levels relative to a geoid with a 2D storm surge model.* Continental Shelf Research, 52, 172-189.

Spruyt, A., Minns, A.W., Zijl, F., Genseberger, M., Yossef, M.F.M., van der Kaaij, Th., de Goede, E.D. (2017). *Ontwikkeling zesde-generatie modellen met D-HYDRO - Generieke technische en functionele specificaties.* Deltares, report 11200569-000.

Tiessen, M., Plieger, R., Groenenboom, J., Winter, G., Sumihar, J. (2019). *Modelontwikkeling D-HYDRO Oosterschelde en Veerse Meer – Twee zesde generatie Rijkswaterstaatmodellen.* Deltares report 11202221-008-ZKS-0005.

Zijl, F., Verlaan, M., Gerritsen, H., (2013). *Improved water-level forecasting for the Northwest European Shelf and North Sea through direct modelling of tide, surge and non-linear interaction.* Ocean Dyn. 63 (7).

Zijl, F., Irazoqui Apecechea, M., Groenenboom, J. (2016). *Kustmodellen in D-HYDRO - Pilot-applicatie Noordzee; Advies voor algemeen functioneel ontwerp voor de zesde-generatie modellen van RWS.* Deltares, report 1230071-011-ZWS-0018.

Zijl, F. (2016a). *On the impact of hydrodynamic model resolution on water levels.* Deltares, memo 1220073-003-ZKS-0009.

Zijl, F. (2016b). *Representation of the 18.6-year nodal cycle in DCSMv6.* Deltares, memo 1230072-003-ZKS-0007.

Zijl, F. (2016c). *The impact of relative wind effect on water levels.* Deltares, memo 1230072-003-ZKS-0008.

A Impact of model domain extension

At the open boundaries the surge component of the water level is imposed by means of an Inverse Barometer Correction (IBC). This approximation is based on the local deviation of air pressure compared the mean pressure over the global ocean, while surface stresses are ignored. Even though the contribution of the latter is thought to be limited in deep water (where most of the open boundaries are located), an extension of the model domain might have a beneficial impact on the surge representation inside the model domain. An expansion implies that that a larger part of the surge signal is generated inside the model by means of wind stress and atmospheric pressure gradients, and consequently a smaller part has to enter the domain through the IBC. Due to the possibility to use large grid cells in the grid extension, the impact on computational times is expected to be limited.

The existing fifth generation models DCSMv6 and DCSMv6-ZUNOv4 cover the area from 15° W to 13° E and 43° N to 64° N. This extent is also used in DCSM-FM, alongside a version that is extended in northern and western direction (with 3.5° and 1.5°, respectively). This means that the ('virtual') north-western corner of the network is then located above Iceland (see Figure A.1). As a result of the extension the number of grid cells (in the preliminary test model) increased by 4% from 626,673 to 650,271.

With both models (using preliminary versions of the schematisation and settings) a four-year period from 2013 to 2016 was computed and the resulting model skill to represent skew surge heights was assessed. The results are presented in Table A.1 and show that the impact during calm conditions is negligible. However, during the most extreme conditions, the bias and RMSE improve by 1.5 cm (9%) and 1.0 cm (5%), respectively. This comes at an increase in computational cost of 15%, from 1.35 min/day to 1.55 min/day, even though the average time step remains virtually the same. Because of this increase in computational time, it was decided to retain the original extent of the network.

Note that improvements can be larger during individual storms. Furthermore, the timing and shape of the surge signal is not assessed here, but can also be affected. Also, the increase in computational time of 15% cannot be fully explained by the increase in network cells of 4%. Before making a decision on the boundary locations of the DCSM-FM refined model this should be investigated in more detail.

Table A.1   Comparison of DCSM-FM model skill to represent skew surge heights, for three different event classes, in terms of mean bias and the RMS over the RMSE's at 9 locations along the Dutch coast in the period 2013-2016.

	<99.0% skew surges		99.0% - 99.8% skew surges		>99.8% skew surges	
	bias (cm)	RMSE (cm)	bias (cm)	RMSE (cm)	bias (cm)	RMSE (cm)
Original size	-1.3	6.2	-3.4	11.2	-15.9	21.4
Extended size	-1.3	6.2	-3.1	11.4	-14.4	20.4
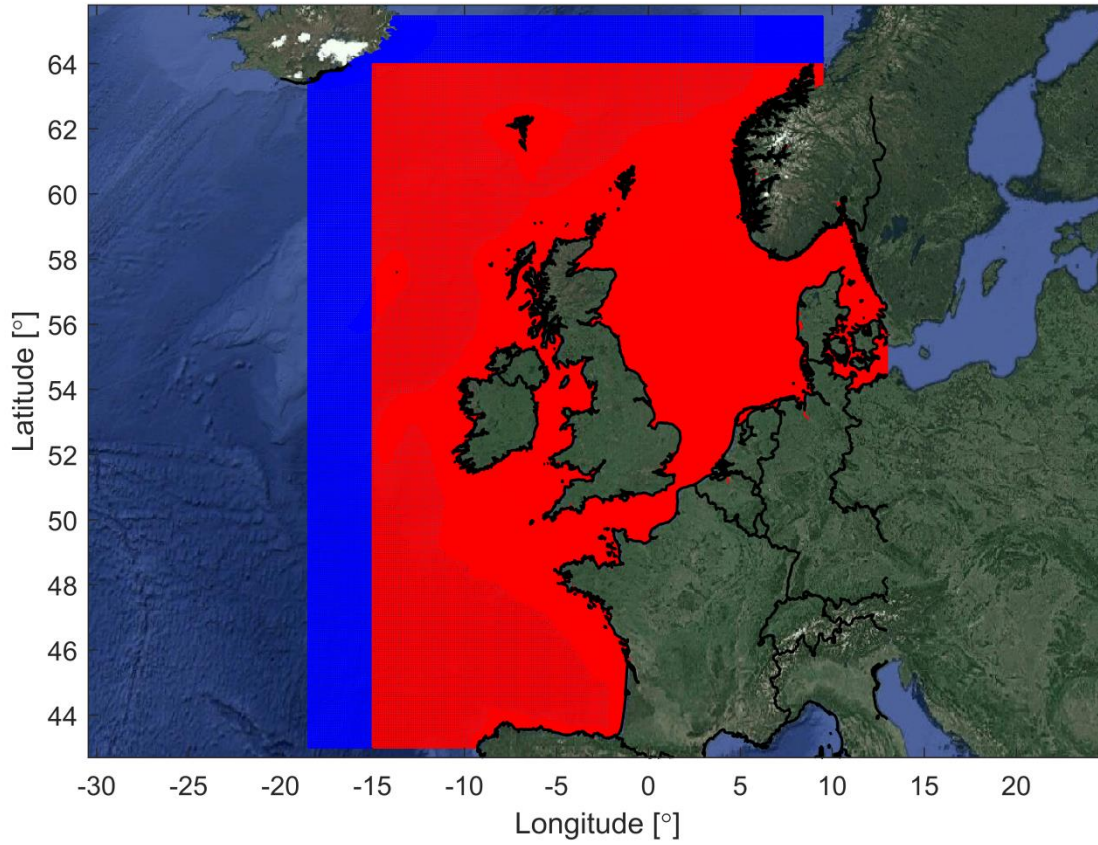
Figure A.1 Computational network of the original and extended version of DCSM-FM.

B Energy dissipation by generation of internal waves

The generation of internal waves on the slope towards the continental shelf precipitates barotropic energy dissipation. Even though the 2D barotropic DCSM-FM model cannot explicitly model internal waves, the energy dissipation this causes can be taken into account through a parametrization that is dependent on the local bathymetry gradient, the local flow velocity perpendicular to the continental slope and the local depth-averaged Brunt–Väisälä frequency (with the bottom values having more weight than the surface values). The latter quantity is computed as a pre-processing step on the basis of 3D monthly-averaged temperature and salinity fields.

In this appendix the impact of taking energy dissipation at the shelf edge into account is quantified. First of all, in Table B.1 the aggregated model skill is presented, based on 13 stations along the Dutch coast and considering the year 2007. This is done for the uncalibrated model, including and excluding the additional dissipation. The results show that the tide representation deteriorates slightly. This is mainly because an already too low mean M2 amplitude and phase decreases even further. These decreases are consistent with increased dissipation. It should however be noted that the uncalibrated model used here uses a somewhat arbitrary, uniform bottom roughness. It is likely that with a lower roughness value the impact of the additional dissipation would actually be beneficial. More importantly, the results in Table B.1 also show an improvement in surge and skew surge representation quality.

When considering the impact at 111 shelf-wide stations, the average surge error in 2007 reduces from 6.3 cm to 6.2 cm. This improvement is relatively evenly spread over the model domain, with only one station deteriorating (by 0.1 cm), 44 stations where the impact is less than 0.1 cm and 66 stations where the improvement is 0.1 cm or larger.

*Table B.1 Model skill **before calibration** (determined over the entire year 2007), including and excluding energy dissipation through generation of internal waves, aggregated from 13 locations along the Dutch coast, for tide, surge, total water level, and skew surge.*

Station	Mean M2 ampl. error (cm)	Mean M2 phase error (°)	RMSE tide (cm)	RMSE surge (cm)	RMSE water level (cm)	RMSE skew surge (cm)
Excluding dissipation	-3.8	-2.5	7.5	6.0	9.6	5.8
Including dissipation	-5.0	-2.2	7.8	5.9	9.8	5.7

After limited calibration
To further corroborate the positive impact of the parameterization of this dissipative mechanism, the above comparison is repeated after a limited calibration of roughness values based on computation with duration of one month and 40 roughness areas. This calibration is done separately for the model including and excluding generation of internal waves. The results are presented in Table B.2 and again show an improvement in surge representation. When considering the impact at 111 shelf-wide stations, the average surge error in 2007 reduces from 6.3 cm to 6.2 cm (which is the same as in the uncalibrated model).

Considering the general improvement in surge quality in both the uncalibrated and calibrated model, it was decided to include the parametrization of energy dissipation by generation of internal waves into the final DCSM-FM model schematization.

*Table B.2   Model skill **after calibration** (determined over the entire year 2007), including and excluding energy dissipation through generation of internal waves, aggregated from 13 locations along the Dutch coast, for tide, surge, total water level, and skew surge.*

Station	Mean M2 ampl. error (cm)	Mean M2 phase error (°)	RMSE tide (cm)	RMSE surge (cm)	RMSE water level (cm)	RMSE skew surge (cm)
Excluding dissipation	2.5	-0.5	5.7	5.9	8.3	5.8
Including dissipation	2.4	-0.5	5.9	5.8	8.3	5.8

C Relative wind effect

In most wind drag formulations, and indeed the wind drag formulation used for the previous generation model DCSMv6 and in WAQUA in general, the flow velocity is not taken into account in determining the wind shear stress (i.e., the water is assumed to be stagnant). Even though the assumption of a stagnant water surface is common because it makes computing stresses easier, from a physical perspective the use of relative wind speed makes more sense since all physical laws deal with relative changes. In case the flow of water is in opposite direction to the wind speed, this would contribute to higher wind stresses (and vice-versa).

The impact of the water velocity on the wind stress at the surface, and consequently also on computed water levels, is indicated with the name 'Relative Wind Effect' (RWE). This was investigated in Zijl (2016c), where it was concluded that the inclusion of RWE resulted in an average improvement in the skew surge representation quality during calm condition of 0-2% along the Dutch coast, 3% in the Dutch estuaries and Wadden Sea and 5-7% in Delfzijl. These results were notable since they also occurred in the period for which the models were calibrated without taking RWE into account. This led to the hypothesis that improvements might be larger if RWE is taken into account during calibration. It was recommended to assess whether further improvements are possible when taking RWE into account during renewed calibration.

In this appendix the impact of taking RWE into account is quantified comparing model results for the year 2007. The model including and excluding RWE were calibrated separately based on computations with a duration of one month (April 2007) and 40 roughness areas.

The quality of the water level representation with and without RWE is assessed on the basis of statistics covering the entire year of 2007. Moreover, a distinction is made between tide and surge. The results for stations along the Dutch coast are presented in Table C.1, while the results for the stations in the Western Scheldt and Wadden Sea are presented in Table C.2. In addition, the results for tide gauge station Delfzijl are given in Table C.3. From these results the following can be concluded the quality of tide, surge and total water levels improves as a result of including RWE. The only exception is the tide along the Dutch coast, which remains unchanged.

Table C.1 Comparison of the tide, surge and total water level accuracy, aggregated from 13 locations along the ***Dutch coast****. The accuracy is given for computations with and without RWE.*

Station	Mean M2 ampl. error (cm)	Mean M2 phase error (°)	RMSE tide (cm)	RMSE surge (cm)	RMSE water level (cm)
Excluding RWE	2.6	-0.6	5.9	6.0	8.4
Including RWE	2.4	-0.5	5.9	5.8	8.3
Difference	-0.2	0.1	0.0	-0.1	-0.1

Table C.2 Comparison of the tide, surge and total water level accuracy, aggregated from 16 locations along the ***Dutch estuaries and Wadden Sea****. The accuracy is given for computations with and without RWE.*

Station	Mean M2 ampl. error (cm)	Mean M2 phase error (°)	RMSE tide (cm)	RMSE surge (cm)	RMSE water level (cm)
Excluding RWE	0.8	1.8	9.9	7.3	12.3
Including RWE	1.5	1.4	9.0	7.1	11.5
Difference	0.7	-0.4	-0.9	-0.2	-0.8

*Table C.3 Comparison of the tide, surge and total water level accuracy at tide gauge location **Delfzijl**. The accuracy is given for computations with and without RWE.*

Station	Mean M2 ampl. error (cm)	Mean M2 phase error (°)	RMSE tide (cm)	RMSE surge (cm)	RMSE water level (cm)
Excluding RWE	-5.1	2.4	11.3	9.3	14.6
Including RWE	-1.5	1.3	9.3	9.0	12.9
Difference	3.6	-1.1	-2.0	-0.3	-1.7

To look at the impact of RWE during storm events, the skew surge error is also assessed, distinguishing between two different categories of skew surge events. A synthesis of results is presented here for a selection of stations along the Dutch coast (Table C.4), in the Dutch estuaries and Wadden Sea (Table C.5) and at tide gauge station Delfzijl (Table C.6). From these results it can be concluded that during calm conditions there is an average improvement in the skew surge quality of 0.2 - 0.4 cm (or 4-5%). However, this comes at a cost of an increased systematic underestimation (bias) during the two most extreme skew surge events of 1 – 3 cm.

*Table C.4 Comparison of model skill to represent skew surge heights, for two different event classes, in terms of mean bias and the RMS over the RMSE's of a selection of 13 stations along the **Dutch coast**. The accuracy is given for computations with and without RWE.*

Station	RMSE <99% (cm)	Bias >99.8% (cm)	RMSE >99.8% (cm)
Excluding RWE	5.7	-15.5	26.4
Including RWE	5.5	-16.5	26.4
Difference	-0.2	-1.0	0.1

*Table C.5 Comparison of the M2 amplitude error, phase error and Vector Difference, averaged over 13 locations along the **Dutch estuaries and Wadden Sea.** The accuracy is given for computations with and without RWE.*

Station	RMSE <99% (cm)	Bias >99.8% (cm)	RMSE >99.8% (cm)
Excluding RWE	6.2	-17.5	23.8
Including RWE	6.0	-20.8	27.0
Difference	-0.3	-3.3	3.1

*Table C.6 Comparison of the M2 amplitude error, phase error and Vector Difference at tide gauge location **Delfzijl.** The accuracy is given for computations with and without RWE.*

Station	RMSE <99% (cm)	Bias >99.8% (cm)	RMSE >99.8% (cm)
Excluding RWE	8.3	-37.4	37.9
Including RWE	7.9	-40.0	40.4
Difference	-0.4	-2.6	2.5

Discussion

Results found are similar to what was reported in Zijl (2016c). In general, there is a meaningful improvement in (skew) surge quality during calm conditions, but at a cost of an increased systematic underestimation (bias) during the two most extreme skew surge events of 1 – 3 cm. The latter is significantly smaller than what was found in Zijl (2016c).

Apparently, RWE adds an effect that cannot fully be incorporated by adjusting the bottom roughness instead. Therefore, it was decided to include RWE in the final DCSM-FM model schematization.

D Viscosity along the open boundaries

At an initial stage of setting-up the model, the refinement of the grid at certain isobaths seemed to substantially improve the modelled surge levels. While a more accurate prediction of the tides was expected (especially in the refined areas), but due to the improved surge even the total RMSE at offshore stations decreased. Considering the Dutch coastal systems, the refinement of the Wadden Sea improved the model water levels at offshore station K13.

The above described effect turned out to be caused by a different mechanism. Due to the refinement of the grid, the flow links became smaller in certain areas and thus the time step was automatically limited based on the Courant criterium. Later, it was found that a subtle numerical instability (that did not affect the automatically chosen time step) occurred at the northern boundary of the model domain. As the refinement of e.g. the Wadden Sea decreased the time step that was used in the computation, the numerical instability did not arise and hence the model results improved.

By manually limiting the maximum time step in the model to 60 instead of 200 seconds, in a test model with a 1nm-grid, the modelled surge levels significantly improved. To supress the numerical instability at the northern boundary without limiting the time step to 60s, several tests were performed with imposing additional viscosity at the northern boundary. Ultimately, additional viscosity (with a value of 2000 m^2/s) is added to the two outer cells of the open boundaries. This suppresses the numerical instability and therewith improves the modelled surge levels.

Deltares

E Model validation

E.1 Shelf-wide results

E.1.1 Tide, surge and total water level

Table E.1   Statistics (RMSE-values in cm) of tide, surge and total water level of the fifth generation models (DCSMv6 and DCSMv6-ZUNOv4) and the sixth generation model (DCSM-FM 0.5 nm) for all shelf-wide tide gauge stations.

Station	RMSE tide (cm)			RMSE surge (cm)			RMSE water level (cm)		
	DCSMv6	DCSMv6-ZUNOv4	DCSM-FM 0.5nm	DCSMv6	DCSMv6-ZUNOv4	DCSM-FM 0.5nm	DCSMv6	DCSMv6-ZUNOv4	DCSM-FM 0.5nm
BAKE_A			9.2			7.9			10.2
BAKE_Z			8.0			7.2			10.5
BHV_ALTER_LT			30.5			9.9			32.0
BORKUM_Sudstrand	4.4		7.3	5.8		5.7		7.2	9.2
BorkumFischerbalje	4.7		6.7	5.8		5.7		7.4	8.8
CUXHAVEN_STEUBH			8.6			7.7			11.5
DAGEBULL			14.6			8.5			16.9
DUKEGAT	8.2		8.0	7.1		7.0		10.5	10.1
DWARSGAT			12.4			7.6			14.5
EMSHORN	5.6		7.6	6.2		6.1		8.4	9.7
HELGOLAND_BINNE.			7.7			5.5			9.4
HELGOLAND_SUDH			8.2			5.8			10.1
HOOKSIELPLATE			7.6			6.9			10.3
HORNUM			16.8			5.6			17.7
KNOCK	7.1		11.0	7.3		7.7		10.2	13.4
LANGEOOG			7.7			7.0			9.6
LEUCHTTURM_ALT.			7.2			6.2			9.5
LIST			11.3			5.9			12.7
MELLUMPLATE			7.4			6.8			10.1
MITTELGRUND			9.8			8.0			11.3
NORDERNEX_RIFFG			7.3			6.0			9.4
PELLWORM_Anleger			12.4			7.4			14.4
ROBBENSUDSTEER.			14.9			8.1			16.9
SCHARHORN			7.3			7.0			9.9
SCHILLIG			6.7			6.5			9.3
SPIEKEROOG			7.4			6.5			9.8
WANGEROOGE_NO.			7.8			6.5			10.4
WANGEROOGE_OST			6.0			6.5			8.7
WANGEROOGE_WE.			9.6			7.0			11.8
WHV_ALTER_VORH.			9.4			7.8			12.2
WHV_NEUER_VORH.			8.5			7.6			11.5
WITTDUN			15.2			6.3			16.3
ZEHNERLOCH			8.1			7.5			10.3

ABDN			4.8			4.6		6.6
BANGR			12.2			4.6		13.1
BARMH			13.5			6.6		14.8
BOURNMH								6.3
CROMR			8.0			6.7		9.4
DEVPT			13.4			4.5		14.2
DOVR			8.9			4.4		9.7
FISHGD			6.8			4.4		7.7
HARWH			13.6			6.9		14.9
HEYSHM			28.7			7.8		29.6
HINKLPT			13.0			7.2		14.7
HOLHD			6.8			4.3		8.1
ILFCBE			10.0			4.9		11.0
IMMHM			16.2			8.7		18.5
KINLBVE			7.3			5.0		7.7
LEITH			10.3			6.4		12.1
LERWK			4.3			3.7		5.6
LIVPL			17.4			7.1		18.3
LLANDNO			7.6			5.5		9.4
LOWST			5.1			5.3		7.2
MILFHVN			7.1			4.9		8.1
MILLPT			18.5			6.2		19.4
MUMBS			9.3			5.2		12.7
NEWHVN			11.2			4.2		12.0
NEWLN			4.4			3.8		5.7
NEWPT								29.0
NORTHSS			8.6			5.0		9.9
PORTERIN			5.9			4.1		7.2
Portbury			59.2			17.0		62.1
PORTPTK			10.6			4.4		11.5
PORTRH			7.2			4.6		8.3
PORTSMH			18.6			5.1		19.1
SHEERNS								18.2
StHelierJersey			8.6			4.8		9.5
STMARYS								5.0
STORNWY			8.3			5.0		8.8
TOBMRY			7.0			4.5		8.3
ULLPL			7.7			5.4		10.4
WEYMH			4.7			4.0		5.8
WHITBY			8.9			5.5		10.6
WICK			5.3			4.5		6.5
WORKTN			9.8			5.4		11.2
Aalesund			5.4			4.5		7.0
Aranmore			5.3			4.4		6.8
Ballum			14.8			14.2		19.8
Ballycotton			5.2			4.4		6.6
Ballyglass			5.0			4.4		6.3

Development of a sixth generation model for the NW European Shelf (DCSM-FM 0.5nm)

Bergen			5.1			4.1		6.5
BoulogneSurMer			11.0			4.9		12.0
Brest			20.4			6.7		21.2
Calais			9.9			5.3		11.2
Castletownbere			5.7			5.7		8.0
Cherbourg			7.2			4.4		8.4
Dielette			17.8			5.3		18.0
Dieppe			11.5			6.3		12.8
Dundalk								36.9
Dunkerque			7.8			5.2		9.4
Dunmore			6.0			3.8		6.6
Esbjerg			12.2			10.1		15.7
GalwayPort			11.6			9.2		14.8
Havneby			23.2			10.2		24.9
Heimsjoe			6.8			4.6		8.2
Helgeroa			4.2			4.6		6.2
Hirtshals			4.2			5.1		6.6
Howth			7.4			4.0		8.4
HvideSandeKyst			9.2			10.4		13.5
Killybegs			5.8			5.1		7.7
Kristiansund			5.0			4.5		6.7
LeConquet			6.2			4.1		7.4
LeHavre			10.1			6.3		11.9
MalinHead			9.5			6.2		11.3
Maloy			5.3			4.4		6.9
Mausund			8.5			7.2		11.1
Oscarsborg			8.2			6.8		10.7
Oslo			10.2			7.7		12.8
Ribe			8.4			11.5		13.7
Roscoff			8.5			4.0		9.4
SaintMalo			10.5			6.0		12.1
SkerriesHarbour			10.3			4.7		10.5
Sligo								9.0
Stavanger			4.0			5.3		6.6
ThyboronKyst			7.6			7.9		9.5
TorsmindeKyst			5.6			6.1		7.8
Tregde			3.5			5.7		6.7
Viker			4.6			5.3		7.0
VLAKTVDRN			5.6			5.9		7.9
Aarhus			6.3			6.2		8.7
Ballen			4.8			5.9		8.0
BayonneBoucau			16.4			6.9		17.7
Bilbao			5.2			3.7		6.3
Bogense			7.6			7.3		10.1
BrestNus30								23.8
Brons			31.1			21.3		37.0
Concarneau			8.6			5.2		9.7

Coruna			4.7			4.1		6.3
Ferring								10.6
Ferrol2								6.8
Ferrol			4.7			4.2		6.3
Fredericia			4.8			9.3		10.7
Frederikshavn			4.2			4.8		6.3
Gijon			4.7			3.7		5.9
Grena			4.0			5.5		6.9
Hanstholm			4.5			5.9		7.1
Herbaudiere			14.4			5.5		15.4
Hornbaek			3.0			5.3		6.3
Hov			6.1			6.1		9.1
Langosteira								6.4
IleDAix			19.2			7.3		20.3
Kristineberg1			4.9			5.2		7.0
LaRochelle			16.0			7.0		17.2
LeCrouesty			13.9			5.4		14.7
LesSablesDOlonne			12.4			5.5		13.2
Mando			8.5			12.3		13.6
Onsala			4.1			6.2		6.4
PortBloc			12.6			5.6		13.5
PortTudy			8.9			4.8		9.8
Ringhals			3.5			6.1		6.6
SaintNazaire			16.3			6.9		17.4
Santander			5.2			3.7		6.3
SjaellandsOdde			2.7			7.8		8.9
Smogen			4.8			6.0		6.9
Socoa			7.1			5.1		8.6
Stenungsund			5.1			6.6		7.2
Udbyhoej			8.2			8.0		11.9
Vidaa			8.5			11.5		14.2
Viken			3.0			7.0		7.2
A2			5.2			5.1		7.3
Appelzak			5.6			5.3		8.0
Blankenberge			6.7			5.6		8.5
Bol_Van_Heist	4.3	4.7	5.5	5.5	5.3	5.2	7.0	7.1	7.5
Nieuwpoort			8.5			5.5		10.1
Oostende			6.8			5.2		8.6
Scheur_Wielingen_Bo.	4.4	5.3	5.7	5.6	5.5	5.4	7.1	7.6	7.7
Wandelaar	4.9	4.4	5.3	5.4	5.3	5.2	7.0	6.6	7.1
Westhinder			6.6			4.9		8.1
Zeebrugge_Leopoldd.	4.8	4.6	5.8	6.2	6.0	5.8	7.8	7.6	8.2
BERGSDSWT	7.1	4.6	11.0	6.0	5.5	6.2	9.2	7.1	12.6
BROUWHVSGT08	4.6	5.0	6.1	6.2	6.1	6.1	7.6	7.8	8.5
CADZD	4.3	4.4	5.8	5.9	5.7	5.7	7.3	7.3	8.1
DELFZL	15.4	6.8	10.8	11.1	7.5	7.9	19.0	10.1	13.4
DENHDR	5.1	4.6	4.2	5.3	5.2	5.1	7.4	6.9	6.6

DENOVBTN	6.0	6.5	7.4	6.8	6.8	6.9	9.1	9.4	10.1
EEMSHVN	6.3	6.8	7.2	6.8	6.3	6.2	9.3	9.3	9.5
EURPFM	4.8	4.0	3.7	4.9	4.7	4.7	6.8	6.1	5.8
HANSWT	14.2	6.1	18.9	7.8	6.2	7.1	16.2	8.6	20.2
HARLGN	8.0	4.5	8.7	7.8	5.8	6.8	11.2	7.3	11.0
HARVT10	4.3	4.4	4.3	5.5	5.4	5.4	7.0	7.0	6.9
HOEKVHLD	4.8	5.0	4.4	5.8	5.3	5.8	7.5	7.3	7.3
HOLWD			31.0			14.6			34.3
HUIBGT	5.4	4.9	5.2	6.1	6.1	5.7	7.9	7.5	7.5
IJMDBTHVN	5.9	6.3	5.4	6.0	5.9	5.8	8.4	8.7	7.9
KORNWDZBTN	4.3	3.7	4.6	6.3	5.7	5.7	7.6	6.8	7.3
KRAMMSZWT		4.3	8.1		6.4	6.3		7.7	10.2
LAUWOG	9.4	6.5	14.2	7.5	6.8	7.5	12.0	9.4	16.0
LICHTELGRE	4.1	4.9	4.7	4.9	4.8	4.7	6.4	6.8	6.7
NES	8.8	5.9	15.4	7.7	6.0	7.6	11.7	8.4	17.2
OUDSD	4.3	4.8	4.6	4.9	4.7	4.7	6.5	6.7	6.6
ROOMPBNN	7.2	4.3	4.4	5.1	4.9	4.9	8.8	6.4	6.6
ROOMPBTN	3.9	4.4	3.8	5.4	5.2	5.0	6.6	6.8	6.3
SCHEVNGN	5.0	5.2	4.5	5.7	5.6	5.6	7.6	7.6	7.1
SCHIERMNOG	10.3	7.2	24.2	7.9	6.9	9.9	13.0	10.0	26.1
STAVNSE	5.8	3.9	5.5	5.5	5.2	5.4	7.9	6.4	7.7
TERNZN	7.9	5.6	6.7	6.5	6.0	6.2	10.3	8.2	9.1
TERSLNZE	4.3	4.1	4.4	5.8	5.8	5.6	7.2	7.0	7.1
TEXNZE	5.1	4.9	5.0	5.7	5.7	5.6	7.6	7.4	7.4
VLIELHVN	5.8	4.7	3.8	5.1	5.0	5.0	7.7	6.9	6.3
VLISSGN	5.2	4.8	6.3	5.9	5.5	5.6	7.9	7.3	8.4
WESTKPLE	3.8	4.4	6.3	5.3	5.2	5.1	6.6	6.8	8.1
WESTTSLG	4.5	3.6	4.8	5.5	5.0	5.0	7.1	6.1	7.0
WIERMGDN	4.8	4.1	4.8	5.7	5.7	5.5	7.4	6.9	7.2
F16	2.8	2.9	3.0	4.1	4.4	4.1	5.0	5.2	5.0
F3PFM			3.6			4.5			5.5
K13APFM	3.4	3.4	4.3	4.5	4.4	4.4	5.6	5.5	6.1
NORTHCMRT			5.0			4.4			6.5
Q1	4.7	4.2	4.2	4.6	4.6	4.6	6.6	6.2	6.3

E.1.2   High waters

Table E.2   Overview of the DCSM-FM model skill to represent skew surge heights (high waters), for three different event classes, in terms of bias (cm) and the RMSE (cm) for all shelf-wide tide gauge stations.

Station	**<99.0% skew surges**		**99.0% - 99.8% skew surges**		**>99.8% skew surges**		
	bias (cm)	RMSE (cm)	bias (cm)	RMSE (cm)	bias (cm)	std (cm)	RMSE (cm)
BAKE_A	0.4	7.9	4.1	14.2	5.2	12.5	13.5
BAKE_Z	1.3	6.8	10.9	15.9	-5.7	11.5	12.9
BHV_ALTER_LT	0.5	8.6	3.4	13.3	-17.4	14.1	22.4
BORKUM_Sudstran.	-0.2	5.6	-0.3	9.5	-24.6	11.7	27.2
BorkumFischerbalje	-0.1	5.6	3.3	9.8	-18.8	11.1	21.8
CUXHAVEN_STEU.	-0.3	8.9	17.5	23.8	3.5	12.3	12.7
DAGEBULL	0.6	7.0	7.6	16.0	0.0	15.8	15.8
DUKEGAT	-0.3	6.4	-2.6	16.4	-42.7	15.8	45.6
DWARSGAT	0.4	7.5	4.7	14.5	-11.9	10.3	15.8
EMSHORN	0.0	5.7	-3.2	11.7	-29.0	13.8	32.1
HELGOLAND_BIN.	-0.5	5.6	5.4	11.4	-6.3	9.0	11.0
HELGOLAND_SUD.	-1.5	5.8	1.9	12.5	-12.5	6.7	14.2
HOOKSIELPLATE	-0.7	7.1	6.0	14.0	-12.1	12.3	17.3
HORNUM	0.3	5.6	2.8	11.3	-12.5	10.1	16.1
KNOCK	0.3	6.7	3.1	13.6	-29.3	17.2	34.0
LANGEOOG	-0.4	7.0	-4.1	12.7	-35.3	12.1	37.3
LEUCHTTURM_AL.	-0.3	6.7	5.7	14.2	-0.7	11.2	11.2
LIST	0.1	7.2	7.7	12.6	0.1	15.7	15.7
MELLUMPLATE	-0.1	6.9	5.4	14.4	-10.5	8.6	13.5
MITTELGRUND	0.0	8.2	5.6	14.9	2.4	9.2	9.5
NORDERNEX_RIF.	0.3	5.8	-3.0	12.2	-30.3	14.8	33.7
PELLWORM_Anleg.	-0.5	7.3	15.0	19.6	11.0	11.9	16.2
ROBBENSUDSTEE.	0.2	8.0	5.9	14.9	-11.3	14.6	18.5
SCHARHORN	-0.2	7.2	6.8	16.8	-0.2	8.1	8.1
SCHILLIG	-0.1	6.6	7.0	14.2	-10.7	10.5	15.0
SPIEKEROOG	2.5	7.4	-0.3	13.6	-31.6	9.5	33.0
WANGEROOGE_N.	-1.5	7.1	2.7	12.3	0.9	8.5	8.6
WANGEROOGE_O.	-0.2	6.7	-2.8	13.4	-20.2	9.2	22.2
WANGEROOGE_W.	1.4	7.1	-5.4	15.9	-27.7	12.3	30.3
WHV_ALTER_VOR.	-0.6	8.1	7.1	17.6	-11.5	16.7	20.2
WHV_NEUER_VO.	-0.8	7.9	5.2	15.8	-13.5	15.0	20.2
WITTDUN	0.1	5.9	6.3	15.4	-0.5	11.0	11.0
ZEHNERLOCH	-0.8	7.8	8.3	15.1	14.3	18.7	23.6
ABDN	0.1	4.4	-4.5	7.5	-11.6	8.8	14.6
BANGR	0.5	4.5	-0.6	7.9	-2.4	3.9	4.6
BARMH	-0.7	5.8	-7.6	11.6	-2.5	2.0	3.2
CROMR	1.0	6.4	4.5	6.0	1.2	10.8	10.9
DEVPT	0.7	4.0	-2.8	6.6	0.6	6.1	6.2
DOVR	0.3	4.5	4.0	5.2	4.3	1.9	4.7
FISHGD	-1.3	4.3	-2.0	3.8	-4.2	4.5	6.1

HARWH	1.4	8.6	-4.8	11.1	9.6	8.7	13.0
HEYSHM	2.0	7.5	-2.8	10.4	-0.7	5.8	5.9
HINKLPT	0.1	6.1	0.7	10.7	-1.8	10.5	10.7
HOLHD	0.0	4.2	-1.0	4.3	3.9	4.3	5.8
ILFCBE	0.4	4.5	0.9	7.1	-3.5	7.1	7.9
IMMHM	6.1	9.1	5.7	16.3	-16.8	2.4	17.0
KINLBVE	-0.9	4.5	-1.4	7.2	4.5	4.9	6.6
LEITH	0.4	6.2	-5.4	10.6	-8.2	10.9	13.7
LERWK	-0.5	3.5	-1.6	5.4	-5.2	7.2	8.9
LIVPL	-1.7	6.1	-2.3	8.5	-8.0	20.4	21.9
LLANDNO	2.1	5.6	4.6	8.3	3.7	7.2	8.1
LOWST	-0.2	5.3	2.2	9.3	-5.5	17.8	18.7
MILFHVN	0.9	4.8	-2.0	7.7	-7.4	5.0	9.0
MILLPT	-0.1	6.3	1.8	12.4	0.2	10.1	10.1
MUMBS	0.3	4.5	0.1	9.8	-7.9	2.6	8.3
NEWHVN	-0.1	4.3	-2.5	6.6	0.4	12.4	12.4
NEWLN	-0.6	3.8	-1.2	5.5	-4.5	5.2	6.9
NORTHSS	-0.3	5.1	-4.8	9.7	-5.0	11.0	12.1
PORTERIN	-0.2	4.2	0.9	6.6	0.8	4.8	4.8
Portbury	3.7	10.1	0.2	13.1	-4.0	11.2	11.8
PORTPTK	0.7	4.3	-0.2	7.4	-7.8	4.2	8.9
PORTRH	0.0	4.6	3.6	7.6	0.7	4.3	4.4
PORTSMH	1.1	4.7	-2.6	6.4	3.1	7.0	7.7
StHelierJersey	0.1	4.6	0.0	7.6	3.4	9.2	9.8
STORNWY	-1.2	4.8	-0.9	6.9	-2.1	3.9	4.4
TOBMRY	0.1	4.3	2.0	8.0	1.9	8.5	8.7
ULLPL	0.5	4.9	-1.4	11.0	2.7	10.2	10.6
WEYMH	-0.8	3.5	-6.0	7.5	6.3	1.6	6.5
WHITBY	1.9	5.3	-5.6	10.0	-10.1	11.8	15.5
WICK	-1.5	4.5	-5.0	7.0	-12.6	8.5	15.2
WORKTN	0.0	5.6	6.4	13.1	13.1	10.1	16.5
Aalesund	-0.1	4.4	-0.3	6.7	-0.7	4.4	4.5
Aranmore	0.1	4.3	-2.0	8.1	0.0	3.3	3.3
Ballum	0.8	7.9	4.2	15.8	0.3	24.8	24.8
Ballycotton	-0.6	4.5	-4.8	7.1	-5.8	3.9	7.0
Ballyglass	0.0	4.3	-0.7	6.3	1.1	4.9	5.0
Bergen	0.0	4.3	1.7	6.3	1.7	3.7	4.0
BoulogneSurMer	-0.8	4.6	0.5	6.1	2.1	12.7	12.9
Brest	1.2	5.4	5.3	10.5	1.6	3.9	4.2
Calais	-0.7	5.1	-2.4	6.5	-2.7	5.6	6.2
Castletownbere	0.4	5.6	-1.9	6.3	-0.1	5.6	5.6
Cherbourg	-0.8	4.0	-8.8	9.9	-12.6	3.8	13.1
Dielette	0.2	4.5	-2.2	4.5	-10.3	4.6	11.3
Dieppe	-0.1	5.3	-3.0	8.5	-0.5	6.6	6.6
Dunkerque	-0.8	5.1	-1.4	7.2	-6.9	5.6	8.9
Dunmore	1.1	3.8	-0.5	3.7	4.3	0.3	4.3
Esbjerg	0.3	9.5	3.9	14.0	0.1	22.3	22.3

GalwayPort	0.1	8.9	-2.1	14.0	-8.4	15.6	17.7
Havneby	0.5	8.7	4.8	11.3	3.3	20.1	20.4
Heimsjoe	0.1	4.5	-4.0	7.5	-4.0	3.8	5.6
Helgeroa	-0.5	4.7	-3.6	7.4	-3.5	3.1	4.7
Hirtshals	-2.4	5.7	-2.0	8.7	-6.0	11.2	12.7
Howth	-0.1	4.0	1.1	5.7	-3.5	5.7	6.7
HvideSandeKyst	-2.8	10.0	-27.6	30.4	-24.1	6.4	24.9
Killybegs	0.2	4.8	-2.7	9.6	0.8	4.4	4.5
Kristiansund	-0.1	4.6	0.1	6.7	0.4	3.6	3.6
LeConquet	-0.5	3.9	-5.8	9.3	-2.1	5.4	5.8
LeHavre	-0.2	6.7	-28.1	32.0	-56.1	33.8	65.5
MalinHead	0.1	6.2	-0.5	6.3	0.0	4.5	4.5
Maloy	-0.5	4.3	-1.9	6.9	-3.3	7.7	8.4
Mausund	0.2	6.9	-16.4	17.9	-27.2	6.3	27.9
Oscarsborg	0.6	6.7	-5.9	10.0	3.9	5.8	7.0
Oslo	1.0	7.5	-3.0	10.4	0.9	7.5	7.6
Ribe	1.1	8.9	-7.4	15.4	-26.3	21.4	33.9
Roscoff	-0.3	3.8	-2.3	6.2	-2.2	6.1	6.5
SaintMalo	0.1	5.4	-5.4	9.5	-3.5	12.4	12.9
SkerriesHarbour	-1.0	4.6	5.7	7.0	-2.2	2.3	3.2
Stavanger	-0.3	5.2	-2.3	6.0	4.4	4.4	6.2
ThyboronKyst	-1.9	7.9	-5.9	11.5	-12.1	12.2	17.2
TorsmindeKyst	-1.4	6.1	-6.6	10.2	-9.4	10.5	14.1
Tregde	-0.7	5.7	-3.0	9.6	-2.9	4.6	5.4
Viker	-0.3	5.4	-4.8	8.3	-2.5	5.6	6.1
VLAKTVDRN	0.0	5.6	6.0	7.6	4.2	4.8	6.4
Aarhus	-0.9	6.0	-11.1	15.7	-9.4	5.2	10.7
Ballen	-0.8	5.6	-10.1	13.1	-24.8	10.5	26.9
BayonneBoucau	-0.6	6.0	-17.0	18.2	-24.5	9.1	26.1
Bilbao	0.0	3.6	-6.3	7.6	-3.1	3.3	4.5
Bogense	1.3	7.0	-8.8	13.0	-15.2	3.2	15.6
Brons	0.4	10.0	-7.6	21.3	-29.5	27.5	40.3
Concarneau	-1.7	4.9	-8.2	10.9	-4.5	10.2	11.1
Coruna	0.1	4.0	-5.5	6.4	-2.6	3.3	4.2
Ferrol	0.0	4.2	-6.7	7.4	-4.5	3.7	5.9
Fredericia	-2.1	9.0	-4.7	14.3	-8.4	4.8	9.7
Frederikshavn	-0.9	4.7	-7.2	10.3	-10.0	5.7	11.5
Gijon	0.1	3.5	-3.4	4.9	-1.2	3.8	4.0
Grena	-1.9	5.9	-13.1	13.8	-12.3	3.0	12.7
Hanstholm	-2.7	6.2	0.5	7.1	-10.9	9.2	14.3
Herbaudiere	-0.9	5.3	-9.4	13.5	-9.8	6.6	11.9
Hornbaek	-3.2	6.0	-8.6	12.2	-4.2	5.2	6.7
Hov	-2.3	6.3	-13.0	15.3	-18.4	9.0	20.4
IleDAix	-0.1	6.9	-4.5	13.0	-13.3	5.3	14.3
Kristineberg1	-0.5	5.3	-5.5	9.3	-0.3	1.7	1.7
LaRochelle	-0.4	6.8	-6.5	12.6	-12.5	6.7	14.2
LeCrouesty	-0.7	5.0	-4.7	10.2	-2.8	11.4	11.7

Deltares

LesSablesDOlonne	-2.7	5.5	-10.5	13.6	-5.5	9.3	10.8
Mando	0.9	9.2	0.5	16.2	-7.0	30.6	31.3
Onsala	-0.3	6.1	-1.7	8.3	4.7	2.7	5.4
PortBloc	-0.5	5.0	-7.5	11.2	-9.7	3.9	10.5
PortTudy	-0.7	4.5	-6.5	9.4	-3.7	7.8	8.6
Ringhals	-1.7	6.0	2.3	8.0	-3.8	3.3	5.1
SaintNazaire	-0.3	6.3	-1.0	15.9	-5.8	6.5	8.7
Santander	0.1	3.6	-4.2	5.4	-3.5	4.4	5.6
SjaellandsOdde	-7.0	8.6	-17.5	19.9	-10.2	10.1	14.3
Socoa	-0.7	3.9	-8.8	9.7	-4.4	4.7	6.4
Stenungsund	-0.2	6.3	-3.2	4.0	-1.1	0.0	1.1
Udbyhoej	-3.9	7.4	-13.7	19.2	-6.1	0.7	6.1
Vidaa	0.0	8.3	4.4	13.6	-6.6	18.8	20.0
Viken	-1.9	7.2	7.5	9.2	-0.3	1.2	1.2
A2	-0.6	5.1	1.8	9.2	-0.9	9.6	9.7
Appelzak	0.0	5.1	-3.7	12.5	-7.6	4.3	8.7
Blankenberge	-0.7	5.0	-6.6	18.8	-7.9	4.1	8.9
Bol_Van_Heist	-1.0	5.3	0.3	7.5	-2.6	9.2	9.6
Nieuwpoort	0.3	5.5	-1.3	6.9	-2.2	6.2	6.5
Oostende	-0.4	5.3	-1.1	8.5	-2.0	10.0	10.2
Scheur_Wielingen_.	-0.2	5.3	0.1	9.3	-3.7	10.4	11.1
Wandelaar	-0.2	5.2	0.7	8.1	-2.9	8.9	9.4
Westhinder	-0.3	5.0	0.4	6.3	1.7	5.9	6.1
Zeebrugge_Leopold.	-1.5	6.0	0.9	10.2	-5.1	11.5	12.6
BERGSDSWT	0.9	6.0	12.6	15.6	2.6	9.5	9.9
BROUWHVSGT08	-1.4	6.2	-5.3	13.8	-15.4	14.6	21.2
CADZD	0.0	5.5	1.5	8.2	0.4	7.9	7.9
DELFZL	-0.6	6.7	0.6	13.5	-36.5	17.5	40.4
DENHDR	-0.7	4.8	-5.7	9.0	-18.4	17.8	25.6
DENOVBTN	-0.8	5.2	-5.3	9.6	-20.8	22.5	30.6
EEMSHVN	-0.3	5.9	-3.2	11.7	-27.1	13.1	30.1
EURPFM	0.1	4.7	0.4	7.1	-2.4	8.8	9.2
HANSWT	0.0	6.7	9.8	14.4	8.7	8.3	12.1
HARLGN	0.1	5.7	-3.2	11.4	-18.1	18.4	25.8
HARVT10	-0.9	5.6	-0.7	10.7	-6.3	6.5	9.0
HOEKVHLD	-3.9	7.1	-2.6	13.2	-9.7	7.4	12.2
HOLWD	0.0	7.9	-7.5	17.0	-32.7	18.4	37.5
HUIBGT	-0.7	5.7	8.0	11.9	-4.1	7.7	8.7
IJMDBTHVN	-1.5	6.1	-4.6	12.9	-16.7	8.5	18.8
KORNWDZBTN	-0.5	5.3	-4.0	10.3	-22.9	21.1	31.2
KRAMMSZWT	-0.9	7.5	2.8	11.8	1.4	11.7	11.8
LAUWOG	0.6	6.5	-5.5	13.0	-30.8	14.8	34.1
LICHTELGRE	-0.5	4.9	0.0	7.8	-3.7	8.8	9.6
NES	0.5	5.7	-7.1	13.6	-26.8	13.9	30.2
OUDSD	-0.3	4.5	-2.6	7.2	-17.7	17.7	25.0
ROOMPBNN	-0.8	5.2	5.2	10.0	1.2	5.9	6.0
ROOMPBTN	-0.5	5.0	-0.6	9.7	-8.2	8.9	12.1

SCHEVNGN	-1.6	6.2	-3.8	10.5	-12.1	12.8	17.6
SCHIERMNOG	0.8	6.5	-4.5	12.7	-28.8	13.1	31.6
STAVNSE	0.1	5.8	8.1	12.3	0.6	8.4	8.4
TERNZN	1.0	6.0	1.9	10.1	3.6	10.4	11.0
TERSLNZE	-1.0	5.5	-5.1	11.9	-15.9	12.5	20.2
TEXNZE	-1.2	5.4	-5.9	13.9	-12.7	13.5	18.5
VLIELHVN	-0.2	4.6	-3.4	9.0	-24.0	9.0	25.6
VLISSGN	0.1	5.6	2.7	8.5	-0.4	10.1	10.1
WESTKPLE	0.5	5.1	3.0	7.2	-2.0	7.7	8.0
WESTTSLG	-0.3	4.7	-2.2	9.0	-24.1	7.6	25.3
WIERMGDN	-0.4	5.3	4.2	10.2	-12.7	5.5	13.8
F16	-0.4	4.2	-0.6	5.3	-11.8	5.2	12.9
F3PFM	-0.3	4.5	-3.3	6.7	-10.6	6.1	12.2
K13APFM	-0.1	4.3	0.3	6.6	-7.9	10.6	13.2
NORTHCMRT	0.0	4.4	-1.9	5.4	-2.3	7.5	7.8
Q1	-0.6	5.1	-1.8	10.1	-12.7	15.5	20.1

E.1.3   Low waters

Table E.3   Overview of the DCSM-FM model skill to represent skew surge heights (high waters), for three different event classes, in terms of bias (cm) and the RMSE (cm) for all shelf-wide tide gauge stations.

Station	<99.0% skew surges		99.0% - 99.8% skew surges		>99.8% skew surges		
	bias (cm)	RMSE (cm)	bias (cm)	RMSE (cm)	bias (cm)	std (cm)	RMSE (cm)
BAKE_A	1.6	7.9	10.8	17.2	1.7	8.2	8.4
BAKE_Z	1.9	7.6	7.2	14.7	3.3	18.1	18.4
BHV_ALTER_LT	1.2	9.0	-13.4	18.9	-41.7	22.8	47.6
BORKUM_Sudstran.	0.4	6.2	-10.7	15.0	-14.3	13.3	19.5
BorkumFischerbalje	0.1	6.0	-7.9	12.9	-12.0	12.4	17.2
CUXHAVEN_STEU.	-0.2	6.9	-4.6	15.6	-20.2	16.3	25.9
DAGEBULL	1.8	10.9	-25.2	27.9	-34.8	16.8	38.6
DUKEGAT	1.1	7.4	-11.1	15.1	-15.7	11.3	19.3
DWARSGAT	0.9	7.7	-11.0	16.2	-21.5	11.1	24.2
EMSHORN	0.6	6.7	-14.2	17.3	-22.0	12.6	25.4
HELGOLAND_BIN.	0.6	5.7	-1.7	10.9	-10.6	9.1	14.0
HELGOLAND_SUD.	0.2	5.9	4.8	10.1	-6.0	9.2	11.0
HOOKSIELPLATE	0.8	7.5	-8.1	15.8	-27.7	17.8	32.9
HORNUM	0.6	6.1	1.3	12.3	-7.9	8.4	11.6
KNOCK	0.7	7.7	-15.3	19.6	-22.3	13.0	25.8
LANGEOOG	-0.3	6.6	-14.9	19.1	-27.0	8.8	28.4
LEUCHTTURM_AL.	0.2	6.4	-2.1	11.5	-12.4	10.3	16.1
LIST	0.5	6.6	-12.5	16.2	-15.8	14.8	21.7
MELLUMPLATE	0.5	7.2	-5.5	12.6	-18.8	12.8	22.7
MITTELGRUND	-0.2	7.8	-2.4	15.6	-19.2	17.9	26.2

NORDERNEX_RIF.	0.2	5.9	-11.6	15.8	-20.5	9.7	22.7
PELLWORM_Anleg.	1.1	7.7	-17.1	22.6	-22.6	14.5	26.8
ROBBENSUDSTEE.	1.3	8.1	-9.9	15.6	-28.6	16.5	33.0
SCHARHORN	-0.1	7.0	-1.0	11.1	-15.6	14.5	21.3
SCHILLIG	0.5	7.1	-6.9	14.5	-25.1	16.3	29.9
SPIEKEROOG	0.5	6.2	-13.1	16.3	-30.3	11.6	32.4
WANGEROOGE_N.	0.0	6.7	3.7	10.6	-7.6	9.4	12.1
WANGEROOGE_O.	0.6	6.6	-13.2	17.1	-35.0	12.9	37.3
WANGEROOGE_W.	0.0	6.7	-14.3	18.7	-31.3	11.3	33.3
WHV_ALTER_VOR.	1.4	8.3	-6.6	16.0	-27.5	19.3	33.6
WHV_NEUER_VO.	1.4	8.3	-7.0	15.4	-28.2	18.9	33.9
WITTDUN	0.9	7.2	-11.2	16.7	-15.3	12.6	19.8
ZEHNERLOCH	-0.8	7.4	1.5	14.1	-17.9	14.7	23.1
ABDN	1.1	4.7	-0.8	6.5	-6.2	7.9	10.0
BANGR	1.2	4.5	1.0	7.3	2.3	5.8	6.2
BARMH	0.8	5.6	-0.4	5.8	-2.3	2.7	3.6
CROMR	1.6	6.5	2.2	8.0	1.0	4.3	4.4
DEVPT	-1.6	4.7	-4.6	7.9	-1.5	7.1	7.2
DOVR	0.3	4.0	-0.2	2.8	-2.2	5.7	6.1
FISHGD	-0.7	4.3	-1.1	6.6	4.3	6.8	8.0
HARWH	-0.4	6.3	-4.1	11.9	-5.4	9.6	11.0
HEYSHM	-0.4	6.1	3.9	14.8	-1.8	10.0	10.2
HINKLPT	2.1	7.4	-4.4	12.4	-11.9	11.2	16.3
HOLHD	0.6	4.1	2.6	7.4	1.2	5.1	5.3
ILFCBE	0.4	4.8	3.0	9.4	-5.8	4.3	7.2
IMMHM	4.6	7.9	-4.0	7.0	-2.8	2.6	3.8
KINLBVE	0.1	4.8	3.0	6.5	9.5	5.6	11.0
LEITH	-0.3	6.1	-5.5	9.5	-11.4	12.3	16.7
LERWK	0.8	3.8	0.7	5.0	-3.5	4.5	5.7
LIVPL	-2.7	7.7	-8.8	17.6	5.5	11.7	12.9
LLANDNO	0.6	5.1	3.4	7.6	0.0	8.0	8.0
LOWST	0.6	5.0	3.4	7.9	-1.2	6.9	7.0
MILFHVN	0.5	4.7	-1.5	5.7	-4.3	8.2	9.3
MILLPT	-0.2	6.1	3.2	7.2	-0.2	8.1	8.1
MUMBS	0.5	4.7	-5.9	11.0	-3.9	4.9	6.2
NEWHVN	0.6	3.9	2.4	8.2	-4.3	9.8	10.7
NEWLN	0.6	3.8	2.1	5.3	1.7	3.9	4.2
NORTHSS	0.2	4.8	-6.9	11.1	-8.0	8.4	11.6
PORTERIN	0.2	3.9	0.6	5.4	1.1	6.5	6.6
Portbury	6.6	16.6	-28.0	34.0	-33.0	25.1	41.5
PORTPTK	0.8	4.3	-1.1	6.0	-6.7	7.2	9.8
PORTRH	0.4	4.6	2.5	6.8	1.9	3.4	3.8
PORTSMH	-0.8	5.2	-8.4	15.5	-6.0	4.4	7.4
StHelierJersey	0.1	4.7	-1.5	8.8	-0.1	4.2	4.2
STORNWY	-0.2	4.8	-1.2	5.4	-3.3	6.7	7.5
TOBMRY	-0.1	4.5	-1.5	6.6	1.0	5.5	5.6
ULLPL	1.6	5.2	4.6	6.8	-0.8	8.6	8.6

WEYMH	0.6	3.9	2.2	3.2	5.7	5.2	7.7
WHITBY	2.6	5.7	-4.4	8.4	-11.7	10.2	15.5
WICK	-0.4	4.4	-3.2	6.0	-8.5	4.5	9.6
WORKTN	0.1	5.0	4.0	10.5	2.2	12.6	12.8
Aalesund	0.2	4.6	-0.5	6.1	2.8	8.3	8.8
Aranmore	0.0	4.3	-1.5	4.9	-4.8	5.9	7.6
Ballum	-2.9	19.8	44.4	48.0	35.8	15.1	38.9
Ballycotton	-0.7	4.3	-2.7	5.7	0.3	2.3	2.3
Ballyglass	-0.1	4.4	-0.1	4.6	-5.1	4.1	6.5
Bergen	-0.2	4.0	-0.2	4.6	-5.4	3.0	6.1
BoulogneSurMer	0.6	4.5	0.6	7.1	1.0	7.2	7.3
Brest	-0.2	5.4	-2.1	9.4	2.9	2.7	3.9
Calais	2.0	5.4	-2.1	7.5	-5.7	4.0	7.0
Castletownbere	0.1	5.6	-1.8	6.6	0.0	6.7	6.7
Cherbourg	2.4	4.9	-0.6	6.6	-0.2	4.9	5.0
Dielette	1.2	5.3	-10.0	12.1	-10.3	2.7	10.7
Dieppe	1.2	5.5	1.3	5.8	-3.2	4.6	5.6
Dunkerque	0.9	5.0	-5.6	11.2	-4.4	8.0	9.1
Esbjerg	0.3	10.5	-18.4	21.7	-16.4	10.5	19.4
GalwayPort	-0.4	9.2	-3.8	14.7	-5.5	21.6	22.3
Havneby	0.4	10.5	-20.1	22.9	-28.0	13.4	31.0
Heimsjoe	0.3	4.5	-2.7	6.1	-3.1	5.1	6.0
Helgeroa	0.3	4.4	-0.2	3.7	2.7	3.2	4.2
Hirtshals	2.3	5.5	4.6	9.8	6.8	8.9	11.2
Howth	-0.1	3.7	2.9	7.8	-2.6	5.7	6.3
HvideSandeKyst	2.5	10.6	-4.9	16.3	0.3	12.7	12.7
Killybegs	-0.2	5.0	-2.3	7.4	-5.0	7.7	9.2
Kristiansund	0.2	4.5	1.7	7.2	5.8	9.5	11.1
LeConquet	0.6	4.5	0.5	7.0	4.5	5.8	7.4
LeHavre	2.2	5.5	-2.1	6.9	1.1	11.4	11.5
MalinHead	0.0	5.8	-2.5	6.0	2.7	8.5	8.9
Maloy	0.5	4.4	-0.4	5.2	2.2	7.0	7.3
Mausund	0.6	6.8	-14.8	16.4	-19.8	9.3	21.9
Oscarsborg	-0.2	6.4	-7.3	9.4	-8.9	5.7	10.6
Oslo	-0.4	7.4	-9.0	11.7	-12.2	3.4	12.7
Ribe	-1.1	12.7	-7.1	15.3	-3.5	19.2	19.5
Roscoff	-0.1	4.2	-2.1	6.3	0.3	4.8	4.8
SaintMalo	0.5	5.6	-2.7	6.3	-5.3	10.6	11.9
SkerriesHarbour	-0.7	4.2	11.2	13.2	15.1	13.0	19.9
Stavanger	0.4	5.2	-2.2	7.1	0.5	4.4	4.4
ThyboronKyst	1.4	8.3	3.8	10.5	-2.0	1.5	2.5
TorsmindeKyst	1.4	6.6	8.7	11.1	3.1	7.4	8.1
Tregde	0.5	5.7	1.0	6.8	0.1	11.2	11.2
Viker	0.2	5.1	-3.0	5.6	-0.3	4.7	4.7
VLAKTVDRN	0.0	5.8	1.6	11.0	3.5	14.6	15.0
Aarhus	0.7	6.1	-0.1	7.4	3.7	3.9	5.4
Ballen	0.9	5.7	-2.4	6.9	0.1	1.3	1.3

BayonneBoucau	0.4	7.5	-13.7	15.2	-13.4	8.9	16.1
Bilbao	0.0	3.7	-4.7	6.7	-4.2	5.0	6.5
Bogense	2.3	7.3	-3.4	9.1	-10.6	6.9	12.7
Brons	-3.5	25.8	66.5	67.9	63.3	18.8	66.0
Concarneau	2.4	5.6	2.2	7.4	0.1	7.0	7.0
Coruna	0.0	4.2	-5.9	6.7	-3.2	5.0	6.0
Ferrol	0.0	4.2	-5.9	6.6	-3.1	3.1	4.4
Fredericia	-1.9	8.8	-12.3	18.5	2.6	1.4	2.9
Frederikshavn	0.8	4.7	-1.7	5.8	-6.3	9.4	11.3
Gijon	0.0	3.9	-3.5	4.7	-1.6	2.3	2.8
Grena	0.5	5.2	-7.0	7.6	-2.6	3.7	4.5
Hanstholm	2.4	6.6	9.3	10.9	17.3	11.8	21.0
Herbaudiere	1.3	5.5	0.9	6.4	-2.8	9.8	10.1
Hornbaek	0.5	5.0	0.1	7.5	-0.5	8.7	8.7
Hov	-0.6	5.7	-5.9	9.4	1.8	4.7	5.0
IleDAix	0.1	7.1	-4.4	10.0	-3.0	18.0	18.3
Kristineberg1	0.7	5.1	-0.5	7.1	1.6	4.8	5.1
LaRochelle	0.5	6.8	-4.0	9.3	-2.1	8.8	9.0
LeCrouesty	1.0	5.7	-0.3	7.8	1.8	11.5	11.7
LesSablesDOlonne	0.7	5.3	-2.5	7.8	-6.9	9.4	11.7
Mando	-4.0	18.2	5.7	13.2	12.8	12.3	17.8
Onsala	-1.1	5.9	-0.1	5.8	-8.3	2.2	8.6
PortBloc	-0.1	5.7	-9.0	11.5	-9.4	5.2	10.7
PortTudy	0.7	4.7	-0.4	5.3	1.3	8.2	8.3
Ringhals	-0.8	6.1	3.0	6.6	5.7	5.5	7.9
SaintNazaire	-1.0	6.8	-2.6	10.0	-6.0	15.7	16.9
Santander	0.0	3.6	-3.0	5.6	-7.4	10.6	12.9
SjaellandsOdde	-4.6	6.9	-4.7	8.1	-4.8	4.1	6.3
Socoa	1.2	6.7	-11.1	14.1	-21.0	13.8	25.1
Stenungsund	0.1	6.2	-1.0	2.0	0.4	5.7	5.7
Udbyhoej	-3.7	8.0	-10.8	12.5	-15.7	0.3	15.7
Vidaa	-2.7	18.6	15.8	20.8	12.2	12.7	17.6
Viken	-0.4	6.6	4.7	8.9	12.4	3.4	12.8
A2	0.1	5.1	-0.7	10.5	-9.8	12.8	16.1
Appelzak	0.1	5.4	-3.8	7.6	-11.0	0.3	11.0
Blankenberge	1.3	5.3	4.1	11.4	-12.6	14.6	19.3
Bol_Van_Heist	0.0	5.1	-1.2	10.1	-11.1	13.9	17.8
Nieuwpoort	0.2	5.2	-5.9	12.6	-2.6	7.7	8.1
Oostende	0.8	5.0	0.1	10.8	-9.4	10.2	13.9
Scheur_Wielingen_.	-0.5	5.3	-1.3	10.8	-16.5	11.4	20.1
Wandelaar	0.3	5.2	-2.9	10.9	-6.0	8.2	10.1
Westhinder	0.0	4.8	-2.4	9.1	-4.0	8.0	9.0
Zeebrugge_Leopold.	0.3	5.8	0.1	11.5	-9.1	12.2	15.2
BERGSDSWT	1.1	5.3	-5.9	14.1	-11.5	12.2	16.8
BROUWHVSGT08	-0.3	5.9	-2.1	9.9	-8.8	7.7	11.7
CADZD	-0.6	5.6	-0.1	9.8	-10.5	15.2	18.4
DELFZL	1.6	8.1	-15.0	19.5	-21.8	11.7	24.7

DENHDR	0.6	4.9	-1.5	8.8	-11.1	13.1	17.2
DENOVBTN	-0.4	8.7	3.9	11.2	-7.0	15.0	16.6
EEMSHVN	1.1	6.7	-10.6	15.2	-16.9	11.4	20.3
EURPFM	0.6	4.8	3.4	7.9	-3.8	8.4	9.2
HANSWT	-1.0	5.4	-7.9	15.5	-22.2	18.1	28.7
HARLGN	-0.1	8.1	-12.0	15.8	-28.6	20.8	35.4
HARVT10	0.3	5.4	4.3	9.2	2.2	14.1	14.3
HOEKVHLD	0.8	5.8	4.3	9.9	4.8	9.6	10.7
HOLWD	6.9	24.4	-68.4	71.5	-75.5	26.9	80.2
HUIBGT	0.1	5.9	4.1	9.3	0.9	11.7	11.7
IJMDBTHVN	1.8	6.4	3.3	9.0	-5.6	11.3	12.6
KORNWDZBTN	0.1	6.3	1.4	11.1	-11.3	17.8	21.1
KRAMMSZWT	0.9	5.4	-3.1	11.0	-17.4	16.0	23.7
LAUWOG	-0.1	6.4	-20.7	23.5	-30.7	21.8	37.7
LICHTELGRE	0.2	4.7	1.0	7.5	0.1	12.2	12.2
NES	-0.2	8.9	-28.4	30.5	-44.1	20.1	48.4
OUDSD	0.3	4.5	-3.2	8.6	-11.6	13.0	17.4
ROOMPBNN	-0.3	4.8	-2.8	9.7	-9.9	9.3	13.6
ROOMPBTN	0.2	4.8	-0.7	10.3	-10.4	12.4	16.1
SCHEVNGN	1.1	5.6	4.0	9.4	1.5	7.0	7.1
SCHIERMNOG	-1.6	10.0	-34.5	36.9	-41.8	21.3	46.9
STAVNSE	0.6	5.1	-5.2	10.8	-8.4	14.1	16.4
TERNZN	0.0	5.5	-2.4	9.7	-22.3	16.9	28.0
TERSLNZE	0.7	5.6	5.0	10.7	-6.1	10.7	12.3
TEXNZE	1.3	5.4	3.9	8.0	-9.7	10.2	14.1
VLIELHVN	0.4	5.3	-8.4	13.6	-27.8	12.7	30.6
VLISSGN	-0.2	5.3	-1.2	8.6	-16.8	15.1	22.6
WESTKPLE	-0.1	4.9	0.6	8.6	-11.1	12.7	16.9
WESTTSLG	0.4	5.5	-7.7	13.8	-22.3	17.8	28.5
WIERMGDN	0.1	5.7	4.5	10.8	0.7	14.0	14.0
F16	0.3	4.0	0.6	5.8	-3.1	5.3	6.1
F3PFM	0.4	4.4	-0.6	5.6	-3.5	6.4	7.3
K13APFM	0.4	4.1	-0.4	4.8	-4.3	10.9	11.7
NORTHCMRT	0.2	4.4	-1.0	3.6	-3.8	5.9	7.0
Q1	0.4	4.4	1.6	7.2	-5.6	10.2	11.7

Development of a sixth generation model for the NW European Shelf (DCSM-FM 0.5nm)

E.2 Dutch coastal waters

E.2.1 High waters

E.2.1.1 DCSMv6

Table E.4 Overview of the DCSMv6 model skill to represent skew surge heights (high waters), for three different event classes, in terms of bias (cm) and the RMSE (cm) for Dutch coastal stations

Station	<99.0% skew surges		99.0% - 99.8% skew surges		>99.8% skew surges		
	bias (cm)	RMSE (cm)	bias (cm)	RMSE (cm)	bias (cm)	std (cm)	RMSE (cm)
Wandelaar	-0.9	5.4	0.8	8.0	-2.8	8.5	8.9
Zeebrugge_Leopold.	-2.2	6.4	1.6	10.7	-3.8	11.6	12.2
Bol_Van_Heist	-1.6	5.6	0.4	7.9	-2.3	9.8	10.0
Scheur_Wielingen_.	-0.5	5.5	1.0	9.8	-3.9	10.8	11.5
CADZD	0.0	5.6	2.6	8.4	1.5	9.3	9.4
WESTKPLE	0.4	5.3	3.6	7.8	-1.4	8.5	8.6
EURPFM	0.3	4.9	0.9	6.7	-2.7	11.5	11.8
VLISSGN	-0.1	5.6	5.0	10.0	1.6	9.9	10.1
ROOMPBTN	-0.4	5.1	-1.7	9.3	-10.0	12.4	15.9
LICHTELGRE	-0.1	5.1	-0.3	7.1	-4.3	10.9	11.7
BROUWHVSGT08	-0.1	6.2	-5.3	13.3	-15.0	17.0	22.6
TERNZN	0.0	6.3	9.1	14.4	6.1	8.9	10.8
HARVT10	-0.8	5.7	-0.1	10.3	-6.9	8.1	10.6
HANSWT	1.5	8.0	15.2	18.5	6.2	10.8	12.5
ROOMPBNN	-1.6	5.5	1.0	10.4	-0.3	7.2	7.2
HOEKVHLD	-2.4	6.1	-1.4	12.7	-9.6	8.3	12.6
STAVNSE	-0.3	6.0	8.5	12.4	0.7	8.1	8.1
BERGSDSWT	3.1	6.7	10.1	13.4	1.8	12.7	12.9
KRAMMSZWT	-1.2	5.9	-3.2	11.1	-12.6	13.9	18.8
SCHEVNGN	-1.5	6.1	-3.2	14.2	-17.7	10.1	20.4
IJMDBTHVN	-0.9	5.3	-0.9	11.3	-12.3	13.2	18.1
Q1	-0.3	4.7	-2.2	8.8	-14.1	16.4	21.6
DENHDR	-1.2	5.5	-4.2	13.7	-12.3	13.3	18.1
TEXNZE	-0.1	4.4	1.7	7.2	-9.3	8.7	12.8
K13APFM	-0.4	4.2	-0.4	6.1	-12.4	3.5	12.9
F16	-0.1	4.8	1.3	8.0	-12.0	15.7	19.8
OUDSD	-0.4	5.3	-4.1	10.6	-17.8	20.8	27.4
DENOVBTN	-0.8	5.5	-0.9	12.4	-11.7	11.8	16.6
TERSLNZE	0.1	5.0	1.2	10.1	-17.7	10.1	20.4
VLIELHVN	0.6	5.3	-2.0	11.4	-22.4	10.0	24.6
WESTTSLG	-0.3	5.5	-0.2	11.1	-17.9	20.8	27.5
KORNWDZBTN	-0.6	5.5	7.4	12.4	-11.6	7.0	13.6
WIERMGDN	-0.6	5.9	10.4	14.3	-4.8	10.8	11.9
HUIBGT	0.0	5.8	-1.2	12.4	-15.0	20.8	25.7
HARLGN	0.2	5.9	-4.9	13.9	-25.2	13.9	28.8
NES	0.3	6.3	-6.8	14.4	-39.4	18.2	43.4

LAUWOG	0.5	6.2	-3.1	13.5	-34.0	16.5	37.8
SCHIERMNOG	-0.4	7.2	10.9	17.0	-12.4	14.6	19.2
BORKUM_Sudstran.	1.0	8.3	11.5	20.1	-22.9	22.0	31.7
Average (total)	-0.3	5.7	1.5	11.4	-10.3	12.2	17.4
Average (offshore)	-0.1	4.7	-0.1	7.3	-9.1	11.6	15.6
Average (coast)	-0.6	5.7	1.1	11.1	-7.6	11.2	14.6
Average (SWD)	0.0	6.0	5.1	11.9	-0.5	10.1	11.3
Average (Wad. S.)	0.0	6.1	0.8	13.7	-21.5	15.6	27.0

E.2.1.2 DCSMv6-ZUNOv4

Table E.5   Overview of the DCSMv6-ZUNOv4 model skill to represent skew surge heights (high waters), for three different event classes, in terms of bias (cm) and the RMSE (cm) for Dutch coastal stations

Station	<99.0% skew surges		99.0% - 99.8% skew surges		>99.8% skew surges		
	bias (cm)	RMSE (cm)	bias (cm)	RMSE (cm)	bias (cm)	std (cm)	RMSE (cm)
Wandelaar	-0.9	5.2	0.0	7.9	-5.3	9.0	10.4
Zeebrugge_Leopold.	-2.0	6.1	0.3	10.1	-6.8	11.9	13.7
Bol_Van_Heist	-1.6	5.5	-0.7	8.2	-4.3	10.2	11.1
Scheur_Wielingen_.	-0.6	5.4	0.0	9.5	-5.9	10.9	12.5
CADZD	-0.3	5.5	0.8	8.3	-1.0	9.1	9.2
WESTKPLE	-0.2	5.1	1.4	7.6	-3.8	9.2	10.0
EURPFM	0.3	4.7	0.7	6.1	-4.9	11.5	12.5
VLISSGN	-0.3	5.3	1.5	8.7	-3.4	10.9	11.4
ROOMPBTN	0.3	5.1	-2.5	9.4	-10.8	13.7	17.4
LICHTELGRE	0.0	4.9	-1.2	7.3	-7.6	11.0	13.4
BROUWHVSGT08	0.1	6.1	-6.9	14.3	-17.3	17.2	24.4
TERNZN	-0.2	5.6	0.2	10.0	-2.8	11.7	12.1
HARVT10	-0.1	5.6	-1.7	10.3	-9.6	8.0	12.5
HANSWT	0.8	5.7	1.5	10.3	-5.8	11.9	13.2
ROOMPBNN	-0.4	4.8	0.8	9.4	-3.4	5.1	6.1
HOEKVHLD	-1.2	5.6	-3.7	11.9	-10.7	9.0	13.9
STAVNSE	0.1	5.3	5.5	10.6	-1.5	9.5	9.6
BERGSDSWT	0.2	5.5	6.6	11.4	-0.5	11.4	11.4
KRAMMSZWT	2.0	8.1	3.1	11.3	-3.5	7.9	8.7
SCHEVNGN	-1.0	5.8	-4.3	11.8	-14.5	14.1	20.2
IJMDBTHVN	-0.8	5.9	-4.6	15.0	-19.3	10.2	21.8
Q1	-0.8	4.8	-1.3	10.6	-11.8	12.6	17.3
DENHDR	-0.5	4.6	-4.9	9.5	-17.0	15.4	22.9
TEXNZE	-1.4	5.5	-4.6	14.3	-13.0	12.8	18.2
K13APFM	-0.2	4.2	1.7	7.2	-9.6	8.5	12.8
F16	-0.3	4.4	0.7	6.5	-11.0	3.5	11.6
OUDSD	-0.2	4.5	-2.5	8.9	-17.8	15.8	23.8
DENOVBTN	-0.4	5.2	-4.6	10.1	-18.5	20.7	27.8
TERSLNZE	-0.8	5.5	-1.8	12.4	-13.1	11.5	17.5
VLIELHVN	-0.1	4.8	-2.5	11.2	-25.9	9.7	27.6

WESTTSLG	-0.1	4.7	-3.1	11.2	-27.0	8.2	28.2
KORNWDZBTN	-0.4	5.2	-3.9	11.7	-22.5	19.7	29.9
WIERMGDN	-0.5	5.3	5.2	11.4	-13.9	6.4	15.3
HUIBGT	-0.7	5.8	9.6	13.7	-4.2	10.1	10.9
HARLGN	-0.3	5.4	-4.5	13.0	-19.2	18.9	26.9
NES	-0.3	5.5	-10.5	16.8	-31.3	14.0	34.3
LAUWOG	-0.4	6.4	-2.6	12.9	-29.0	16.9	33.6
SCHIERMNOG	-0.5	6.5	-0.9	13.5	-28.0	14.8	31.7
BORKUM_Sudstran.	-0.2	5.8	1.7	10.4	-22.6	13.2	26.2
BorkumFischerbalje	0.1	5.8	4.6	11.1	-18.8	12.7	22.7
EMSHORN	-0.1	6.2	1.9	11.7	-26.2	14.2	29.8
EEMSHVN	-0.2	6.4	2.0	11.5	-23.8	14.2	27.7
DUKEGAT	-0.5	7.1	2.6	15.7	-40.3	17.5	44.0
DELFZL	1.3	7.1	2.9	13.4	-35.4	20.8	41.1
KNOCK	0.6	7.0	5.3	14.6	-27.3	20.2	34.0
Average (total)	-0.3	5.6	-0.3	11.0	-14.4	12.4	19.8
Average (offshore)	-0.2	4.6	0.1	7.5	-9.0	9.4	13.5
Average (coast)	-0.6	5.5	-0.9	10.9	-9.8	11.1	15.3
Average (SWD)	0.2	5.8	3.0	10.2	-2.5	9.4	9.9
Average (Wad.S.)	-0.1	5.8	-0.9	12.4	-25.8	15.7	30.6

E.2.2   Low waters

E.2.2.1   DCSMv6

Table E.6   Overview of the DCSMv6 model skill to represent skew surge heights (low waters), for three different event classes, in terms of bias (cm) and the RMSE (cm) for Dutch coastal stations

Station	**<99.0% skew surges**		**99.0% - 99.8% skew surges**		**>99.8% skew surges**		
	bias (cm)	RMSE (cm)	bias (cm)	RMSE (cm)	bias (cm)	std (cm)	RMSE (cm)
Wandelaar	0.3	5.4	-2.4	11.4	-6.6	7.1	9.7
Zeebrugge_Leopold.	0.4	6.2	0.3	11.9	-8.7	12.4	15.1
Bol_Van_Heist	0.1	5.4	-0.7	11.4	-11.7	13.5	17.9
Scheur_Wielingen_.	-0.3	5.6	0.7	12.3	-16.0	11.3	19.6
CADZD	-0.3	6.0	2.1	11.6	-9.1	13.7	16.5
WESTKPLE	0.0	5.2	0.8	9.7	-12.3	11.0	16.5
EURPFM	0.8	5.0	4.4	8.9	-3.3	8.3	9.0
VLISSGN	0.2	5.5	0.1	10.3	-16.1	14.0	21.3
ROOMPBTN	0.3	5.2	-2.3	12.2	-12.0	11.3	16.4
LICHTELGRE	0.3	4.9	0.3	8.2	-1.4	9.5	9.5
BROUWHVSGT08	-0.7	6.2	-2.2	12.4	-7.7	8.1	11.2
TERNZN	0.3	5.8	-1.1	10.7	-22.1	16.0	27.2
HARVT10	0.3	5.4	2.8	9.1	3.0	13.2	13.5
HANSWT	-0.8	5.7	-4.7	14.6	-24.8	16.1	29.6

ROOMPBNN	0.4	5.0	1.3	10.1	-7.6	5.8	9.6
HOEKVHLD	0.5	5.8	3.7	10.0	3.7	11.4	12.0
STAVNSE	0.1	5.4	-3.1	10.9	-7.2	10.8	12.9
BERGSDSWT	0.2	5.4	0.2	13.5	-2.9	11.8	12.1
KRAMMSZWT	0.8	5.5	3.6	9.6	4.8	7.9	9.3
SCHEVNGN	1.5	5.9	2.2	9.6	-1.9	11.1	11.3
IJMDBTHVN	0.4	4.4	2.9	7.4	-4.2	10.3	11.1
Q1	0.5	5.0	-2.4	8.4	-11.8	12.1	16.9
DENHDR	1.3	5.4	4.8	8.6	-8.6	9.7	12.9
TEXNZE	0.2	4.2	0.9	5.9	-6.0	10.7	12.3
K13APFM	0.4	4.2	1.4	6.6	-2.8	5.9	6.5
F16	0.3	4.8	-3.7	8.2	-13.5	11.2	17.5
OUDSD	-0.7	8.6	0.6	9.7	-9.7	17.2	19.7
DENOVBTN	0.6	5.8	7.6	11.9	-2.4	10.8	11.0
TERSLNZE	0.4	5.2	-5.6	11.5	-19.6	12.2	23.1
VLIELHVN	0.2	6.0	-10.9	16.3	-26.0	16.0	30.5
WESTTSLG	-0.3	6.8	1.5	11.4	-10.9	17.3	20.4
KORNWDZBTN	0.4	5.8	5.5	11.4	5.4	14.2	15.2
WIERMGDN	0.0	6.1	5.7	11.0	5.7	10.9	12.3
HUIBGT	-0.2	9.0	-11.4	17.0	-27.3	20.0	33.8
HARLGN	-1.1	8.5	-20.7	25.0	-30.5	21.9	37.6
NES	0.1	6.8	-18.8	23.1	-27.3	21.7	34.9
LAUWOG	-0.6	6.8	-17.3	21.7	-21.9	18.3	28.5
SCHIERMNOG	0.8	7.4	-7.8	14.8	-6.9	13.8	15.5
BORKUM_Sudstran.	1.7	9.5	-19.0	25.6	-17.9	15.6	23.7
Average (total)	0.2	5.9	-2.1	12.2	-10.1	12.7	17.5
Average (offshore)	0.5	4.8	0.0	8.0	-6.5	9.4	11.9
Average (coast)	0.2	5.7	-0.1	11.0	-9.1	11.9	16.4
Average (SWD)	0.4	5.4	0.2	10.9	-8.5	11.0	15.4
Average (Wad. S.)	0.1	7.2	-7.9	17.1	-14.8	16.7	23.7

E.2.2.2 DCSMv6-ZUNOv4

Table E.7   Overview of the DCSMv6-ZUNOv4 model skill to represent skew surge heights (low waters), for three different event classes, in terms of bias (cm) and the RMSE (cm) for Dutch coastal stations

Station	<99.0% skew surges		99.0% - 99.8% skew surges		>99.8% skew surges		
	bias (cm)	RMSE (cm)	bias (cm)	RMSE (cm)	bias (cm)	std (cm)	RMSE (cm)
Wandelaar	0.2	5.3	-3.5	11.8	-7.0	6.5	9.6
Zeebrugge_Leopold.	0.3	5.9	-1.2	11.9	-10.1	12.0	15.7
Bol_Van_Heist	0.0	5.3	-1.7	11.9	-12.2	13.0	17.8
Scheur_Wielingen_.	-0.2	5.5	-0.1	12.6	-15.6	10.8	19.0
CADZD	-0.2	5.9	0.8	11.3	-9.7	13.9	16.9
WESTKPLE	0.1	5.2	1.4	9.9	-11.9	10.9	16.1
EURPFM	0.7	4.9	4.0	8.7	-4.6	7.6	8.9

Deltares

VLISSGN	-0.2	5.5	-0.1	10.3	-15.4	14.5	21.1
ROOMPBTN	0.2	5.2	-1.1	11.7	-10.3	10.9	15.0
LICHTELGRE	0.3	4.8	-0.7	7.6	-3.7	9.6	10.2
BROUWHVSGT08	-0.3	6.0	-2.2	12.0	-8.4	8.4	11.8
TERNZN	-0.2	5.8	-0.2	10.7	-17.9	16.5	24.4
HARVT10	0.4	5.4	2.3	8.7	0.8	12.9	12.9
HANSWT	-0.2	5.5	-2.0	13.2	-15.1	17.6	23.2
ROOMPBNN	0.1	4.9	1.4	9.9	-6.7	5.8	8.9
HOEKVHLD	1.4	6.0	4.4	9.4	3.3	11.8	12.2
STAVNSE	0.2	5.2	0.7	10.6	-2.5	11.7	12.0
BERGSDSWT	-0.1	5.3	2.4	13.8	-0.2	12.1	12.1
KRAMMSZWT	0.6	5.6	2.2	11.4	-11.5	13.3	17.5
SCHEVNGN	1.0	5.6	5.0	10.0	6.0	8.1	10.1
IJMDBTHVN	1.4	5.8	3.0	9.7	-1.9	10.7	10.8
Q1	0.4	4.4	2.2	7.2	-4.8	10.4	11.4
DENHDR	0.7	4.9	-1.4	8.9	-10.8	12.7	16.7
TEXNZE	1.6	5.5	4.4	8.3	-8.9	9.9	13.4
K13APFM	0.2	4.1	1.4	5.6	-5.2	10.0	11.3
F16	0.4	4.3	2.4	6.7	-1.2	5.3	5.4
OUDSD	0.4	4.7	-1.5	7.7	-10.6	11.9	15.9
DENOVBTN	-0.4	9.2	5.6	11.4	-1.6	15.5	15.5
TERSLNZE	0.6	5.7	7.5	12.1	-3.4	10.0	10.6
VLIELHVN	0.3	5.0	-4.2	12.1	-21.5	12.9	25.0
WESTTSLG	0.3	5.3	-6.7	13.8	-21.5	15.6	26.6
KORNWDZBTN	-0.6	6.5	4.4	11.6	-7.5	15.9	17.5
WIERMGDN	0.3	5.9	7.4	11.9	5.4	14.2	15.2
HUIBGT	0.4	6.2	7.8	12.3	8.3	10.9	13.7
HARLGN	-0.5	6.0	-1.6	11.1	-18.0	16.4	24.4
NES	0.1	6.1	-11.0	15.3	-23.2	16.7	28.5
LAUWOG	0.0	6.5	-5.1	13.9	-7.4	22.2	23.4
SCHIERMNOG	0.1	6.3	-7.3	14.7	-9.3	20.1	22.1
BORKUM_Sudstran.	0.4	6.2	-6.3	13.4	-7.5	12.5	14.6
BorkumFischerbalje	-0.2	6.2	-3.0	11.7	-8.3	11.4	14.1
EMSHORN	0.5	6.7	-7.0	13.2	-13.0	12.1	17.7
EEMSHVN	1.0	6.9	-2.7	12.4	-6.9	10.1	12.2
DUKEGAT	1.1	7.7	-0.7	11.9	-2.2	10.3	10.6
DELFZL	1.3	8.5	-3.4	14.5	-4.6	8.0	9.2
KNOCK	0.2	8.1	-4.5	14.7	-5.4	10.4	11.7
Average (total)	0.3	5.8	-0.2	11.2	-7.6	12.1	15.4
Average (offshore)	0.4	4.5	1.8	7.2	-3.9	8.6	9.5
Average (coast)	0.4	5.6	1.7	11.0	-5.6	11.4	14.5
Average (SWD)	0.1	5.4	1.1	11.1	-9.0	12.3	16.0
Average (Wad. S.)	0.2	6.6	-3.4	12.7	-10.5	13.9	18.1

Development of a sixth generation model for the NW European Shelf (DCSM-FM 0.5nm)